

T-2857

HYDROPROCESSING OF COAL-DERIVED ASPHALTENES

ARTHUR LAKES LIBRARY
COLORADO SCHOOL of MINES
GOLDEN, COLORADO 80401

by

Michael K. Maholland

ProQuest Number: 10782555

All rights reserved

INFORMATION TO ALL USERS

The quality of this reproduction is dependent upon the quality of the copy submitted.

In the unlikely event that the author did not send a complete manuscript and there are missing pages, these will be noted. Also, if material had to be removed, a note will indicate the deletion.



ProQuest 10782555

Published by ProQuest LLC (2018). Copyright of the Dissertation is held by the Author.

All rights reserved.

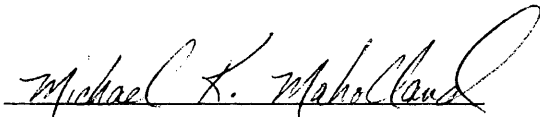
This work is protected against unauthorized copying under Title 17, United States Code
Microform Edition © ProQuest LLC.

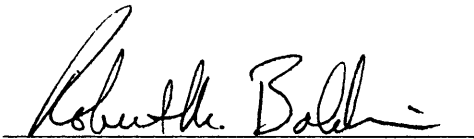
ProQuest LLC.
789 East Eisenhower Parkway
P.O. Box 1346
Ann Arbor, MI 48106 – 1346

T-2857

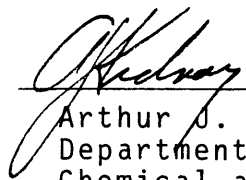
A thesis submitted to the Faculty and the Board of Trustees of the Colorado School of Mines in partial fulfillment of the requirements for the degree of Master of Science (Chemical and Petroleum-Refining Engineering).

Golden, Colorado
Date 12/1/83

Signed: 
Michael K. Maholland

Approved: 
Robert M. Baldwin
Thesis Advisor

Golden, Colorado
Date 12/2/83


Arthur J. Kidnay
Department Head
Chemical and Petroleum-
Refining Engineering

T-2857

DEDICATION

To my wife Linda

ABSTRACT

Asphaltenes derived from Wilsonville SRC-I have been thermally and catalytically hydrogenated in a 1-liter batch stirred autoclave reactor. Rates of the thermal conversion to oils were measured at 355^o, 375^o and 400^oC. An activation energy for the temperature range 375^o to 400^oC has been calculated. Rates of catalytic conversion to oils were measured for the mineral matter additives H₂S and pyrite, and for metal supported commercial hydroprocessing catalysts containing Co-Mo, Ni-Mo, and Ni-W. Compositional changes in the residual asphaltenes were measured by elemental analysis and molecular weight determinations to elucidate the effects of catalyst properties on the hydrogenation, hydrodesulfurization and hydrodenitrogenation reactions. Proton and ¹³C nmr spectra were used to calculate the average structural parameters of the feed and residual asphaltenes. Hypothetical structures for coal-derived asphaltenes are presented.

TABLE OF CONTENTS

	<u>Page</u>
TITLE PAGE.....	i
LETTER OF SUBMITTAL.....	ii
DEDICATION.....	iii
ABSTRACT.....	iv
TABLE OF CONTENTS.....	v
TABLE OF FIGURES.....	vii
TABLE OF TABLES.....	x
ACKNOWLEDGEMENTS.....	xiii
INTRODUCTION.....	1
LITERATURE SURVEY.....	4
Characterization of Coal Hydrogenation Products.....	4
Comparison of Coal and Petroleum Asphaltenes.....	11
Physical, Chemical and Structural Characterization of Coal-Derived Asphaltenes.....	13
Asphaltene Hydroprocessing: Kinetics, Mechanisms and Catalysts.....	24
EQUIPMENT.....	32
EXPERIMENTAL DESIGN.....	36
Reaction Conditions.....	36
Catalyst Selection.....	41
Reagents.....	43
EXPERIMENTAL PROCEDURE.....	44
Asphaltene Separation and Recovery.....	44
Pyrite Separation.....	47
Catalyst Presulfiding.....	48
Asphaltene Mixture Preparation.....	49
Run Procedure - Catalytic.....	50
Run Procedure - Noncatalytic.....	52
Shutdown Procedure.....	52
Material Balance.....	53

ANALYTICAL METHODS.....	55
Product Fractionation by Solvent	
Separation Analysis.....	55
Product Analysis.....	58
RESULTS.....	60
DISCUSSION.....	65
Material Balance and Gas Production.....	65
Tetralin/Asphaltene Interactions.....	65
Kinetic Model Development.....	67
Conversion Analysis.....	77
Elemental and Structural Analysis of Residual Asphaltenes.....	103
CONCLUSIONS.....	128
RECOMMENDATIONS FOR FURTHER STUDY.....	133
REFERENCES.....	135
APPENDIX A. FEED COAL/SRC-I ANALYSIS.....	142
APPENDIX B. EXPERIMENTAL RUN RESULTS.....	145
APPENDIX C. ASPHALTENE STRUCTURAL RESULTS.....	160
APPENDIX D. CATALYST PROPERTIES.....	166
APPENDIX E. SAMPLE CALCULATIONS.....	172

TABLE OF FIGURES

<u>Figure</u>	<u>Page</u>
1. Selective Solvent Fractionation Process.....	5
2. Typical ^1H nmr Spectra of Asphaltenes.....	21
3. Typical ^{13}C nmr Spectra of Asphaltenes.....	21
4. Hypothetical Structures of Coal-Derived Asphaltenes.....	23
5. Rates of Asphaltene Hydrogenation.....	26
6. Temperature Dependence of Asphaltene Hydrogenation.....	26
7. Mechanism of Asphaltene Conversion.....	27
8. Experimental Apparatus.....	33
9. Asphaltene Separation Scheme.....	46
10. Product Fractionation by Solvent Separation Analysis.....	56
11. Run Temperature and Pressure Profile.....	61
12. Sample Output: C, H, N Analysis.....	63
13. Sample Output: Gas Analysis.....	64
14. Shock Effects of Injection.....	69
15. Peel-Back Method Analysis: Overall Reaction.....	72
16. Peel-Back Method Analysis: Isolated Reaction of the Reactive Asphaltene Fraction.....	73
17. Comparison of Kinetic Rate Constants for Run 11.....	76

18. Conversion Results of Thermal Hydroprocessing of Coal-Derived Asphaltenes.....	79
19. Arrhenius Plot of Thermal Hydroprocessing Results.....	80
20. Conversion to THF Soluble Materials.....	83
21. Oil Yield.....	83
22. Conversion Results Using Pyrite and H ₂ S Additives.....	85
23. Conversion Results Using Commercial Hydroprocessing Catalysts.....	88
24. Effect of Presulfiding HDS-9A Catalyst on Asphaltene Conversion.....	95
25. Activity of Presulfided HDN-30 Catalyst After H ₂ S Purge by H ₂	96
26. Fractional Conversion to Oils at 400 ^o C Using HDN-30 Catalyst. Combined Results of Runs 14 and 18 Are Used.....	98
27. Fractional Conversion to Oils at 425 ^o C Using HDN-30 Catalyst.....	101
28. Percent Sulfur in Residual Asphaltenes For 3 Run Conditions.....	107
29. Percent Nitrogen in Residual Asphaltenes For 3 Run Conditions.....	108
30. Atomic H/C Ratio of Residual Asphaltenes For 3 Run Conditions.....	109

31. Typical ^1H nmr of Residual Asphaltene.....	111
32. Typical Proton Decoupled ^{13}C CP/MAS nmr of Residual Asphaltene.....	112
33. Comparison of Aromaticities as Determined by ^{13}C and ^1H NMR.....	120
34. Hypothetical Average Asphaltene Structure I.....	125
35. Hypothetical Average Asphaltene Structure II.....	126

TABLE OF TABLES

<u>Table</u>	<u>Page</u>
1. Results with Methods A, B and C.....	7
2. Comparison of Methods of Asphaltene Analysis in an SRC Sample.....	7
3. SESC Fractionation Procedure Developed by Mobil.....	9
4. Comparisons of Properties Between Coal- and Petroleum-Derived Asphaltenes.....	12
5. Ultimate Analyses and Molecular Weights of Asphaltenes and Their Acidic and Basic Components.....	14
6. Elemental Analysis and Molecular Weights of Asphaltenes.....	15
7. Elemental Analysis of Products A, B and C and of Their Group Components.....	16
8. Definitions of Structural Parameters.....	20
9. Rate Constants for Anthraxylon Hydrogenation.....	25
10. New Hydrogenation Catalytic Systems.....	31
11. Reaction Conditions.....	40
12. Fresh Catalyst Properties.....	42
13. Pyrite Properties.....	43
14. List of Reagents.....	43
15. SRC-I Ultimate Analysis.....	44

16. Presulfiding Conditions.....	49
17. Feed Asphaltene Analysis.....	66
18. Comparison of Kinetic Rate Constants For Run 11.....	77
19. Thermal Hydroprocessing Rate Parameters.....	78
20. Pyrite and H ₂ S Rate Parameters.....	84
21. Commercial Catalyst Hydroprocessing Rate Parameters.....	89
22. Recovered Catalyst Properties.....	92
23. Elemental Analysis of HDN-30 Catalyst After 180 Minutes of Reaction at 400 ^o C.....	100
24. Elemental Analysis of HDN-30 Catalyst After 180 Minutes of Reaction at 425 ^o C.....	103
25. Elemental Analysis of Residual Asphaltenes Following Thermal Hydroprocessing.....	104
26. Elemental Analysis of Residual Asphaltene Following H ₂ S and Pyrite Catalytic Hydroprocessing.....	104
27. Elemental Analysis of Residual Asphaltenes Following Commercial Catalyst Hydroprocessing.....	105
28. Assignments of Proton and Carbon Bands of NMR Spectra of Asphaltenes.....	114
29. Definitions of Structural Parameters.....	116
30. Calculated H/C Aliphatic Ratio.....	118

31. Aromaticities of Asphaltenes as Determined by ^{13}C nmr and ^1H nmr.....	119
32. Average Molecular Properties of Asphaltenes.....	122

ACKNOWLEDGMENTS

I am extremely grateful for the guidance and patience which my thesis advisor, Dr. Robert Baldwin, provided during the course of this study. Thanks are also extended to Professor Scott Cowley and to Dr. Marvin Johnson of Phillips Petroleum Company, who together assisted me in the interpretation of the results of the catalytic phase of this study. I would like to thank the Colorado State University Regional NMR Center, funded by National Science Foundation Grant No. CHE 78-18581, for running the ^{13}C nmr spectra. Finally, I would like to acknowledge the financial support provided to me in the form of a fellowship from the Phillips Petroleum Company and from a grant from the Department of Energy under contract DE-AC22-79ET14881.

INTRODUCTION

The direct liquefaction of coal, regardless of the process used, generates reaction products consisting of oils, asphaltenes and preasphaltenes. The asphaltene and preasphaltene fractions are the result of incomplete conversion in the coal-to-oil reaction and represent undesirable, yet stable, intermediates. These three fractions (oils, asphaltenes and preasphaltenes) are operationally defined according to their solvent solubility. Consequently, each fraction is comprised of a wide variety of organic compounds.

Asphaltenes are generally accepted to be condensed, polynuclear aromatic substances with heteroatoms such as sulfur, nitrogen and oxygen. They are a major concern in coal liquefaction both because they constitute a major portion of the intermediate fraction and because they are highly resistant to further processing.

Presently envisioned coal liquefaction processes consist of initial thermal dissolution of the organic coal matrix, producing an asphaltene-rich stream, followed by residue separation and catalytic upgrading of the dissolved products. Several advantages are apparent from such a process. Undesirable thermal reactions such as coking and gas production could be minimized by maintaining short residence times in the first reactor. In the second reactor,

after residue separation, a suitable hydroprocessing catalyst could be utilized to upgrade the asphaltene-rich stream to oils by increasing the H/C ratio and by removing heteroatoms. This reactor could be operated at lower temperatures taking advantage of catalyst selectivity while reducing coking and gas production.

The presence of the asphaltene intermediate makes it apparent that a detailed investigation of the physical and chemical properties of asphaltenes is necessary in order to determine more about the coal-to-oil mechanism. That the asphaltene structure may well reflect the basic structure of coal has been previously noted. Therefore, a study of asphaltene reactivity would be helpful in elucidating the reaction mechanism of coal itself. Also, as stated above, asphaltenes are undesirable liquefaction products. Knowledge of conditions for minimizing or eliminating this fraction would again help to improve the overall coal hydrogenation process.

The primary objective of the research undertaken in this thesis was to investigate the hydrogenation of coal-derived asphaltenes using a variety of commercial hydroprocessing catalysts and to compare these results to those obtained under thermal conditions. Particular interest was in following the changes of the heteroatom (N, S, O) content and the atomic hydrogen-to-carbon ratio of the

hydroprocessed asphaltenes. These two parameters, along with the degree of overall conversion, were the principal factors considered in evaluating the effectiveness of a catalyst for asphaltene hydroprocessing.

An ancillary goal of this research was to evaluate and compare the activities of hydrogen sulfide and coal-derived pyrite for asphaltene hydrogenation to the thermal and commercial catalyst activities. Previous work suggests that H_2S and pyrite act as catalysts in coal liquefaction. However, it is unknown whether they act to catalyze the primary dissolution reactions to form the intermediate species, preasphaltenes and asphaltenes, or whether they are able to effect the more difficult, intermediate-to-oil, secondary reactions.

Finally, it was desired to determine the average structural parameters of both the feed and residual asphaltenes. With a knowledge of these parameters hypothetical asphaltene structures may be proposed.

LITERATURE SURVEY

Characterization of Coal Hydrogenation Products

The dissolution of coal in a hydrogen-donating solvent is primarily attributed to the breaking of non-valence bonds and weak carbon-heteroatom bonds. The liquid produced contains organic compounds with a diverse range of molecular weights and chemical structures. A common means of characterizing these coal liquids is by selective solvent fractionation. A typical selective solvent fractionation process is presented in Figure 1.

The four fractions generated by this extraction process are classified as oils, asphaltenes, preasphaltenes, and insoluble organic matter plus mineral matter. Specifically, oils are defined as being soluble in straight-chained or cyclic, saturated hydrocarbons. Usually n-pentane is used, however researchers have also used n-hexane, n-heptane and cyclohexane [1,2]. Asphaltenes are compounds insoluble in the above solvents but soluble in non-polar aromatics. Until recently benzene was commonly used as the non-polar aromatic solvent. However, due to health hazards associated with exposure to benzene, many laboratories have since switched to toluene. Preasphaltenes, also referred to as asphaltols because of their high -OH group content [3], are defined as compounds insoluble in non-

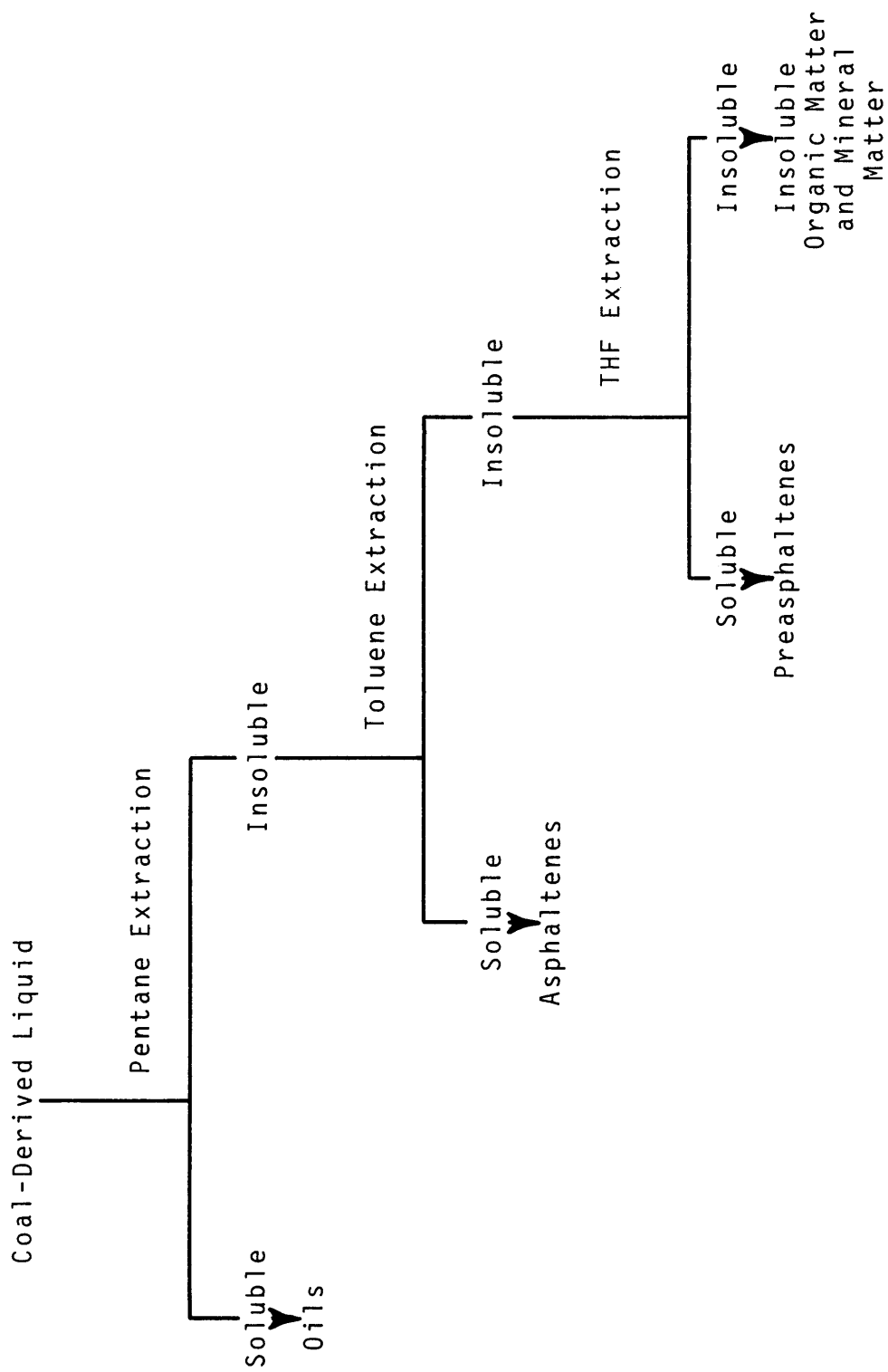


Figure 1. Selective Solvent Fractionation Process

polar aromatics but soluble in polar aromatics such as tetrahydrofuran (THF) or pyridine. Materials insoluble in the above polar aromatic solvents are considered to be insoluble organic matter and mineral matter.

The above definitions are rather nebulous in that they separate coal liquids by solubility into fractions, each of which obviously includes a large number of chemically distinct organic compounds. In the asphaltene fraction, insolubility in n-pentane can be caused by high molecular weight, high polarity, hydrogen bonding, acid-base complexing, or a combination of two or more of these parameters [1]. Corbett & Petrossi [4] have shown that, for petroleum asphaltenes, the yield of paraffin insolubles changes with the carbon number of the precipitating solvent. For paraffinic solvents smaller than n-heptane a marked increase in the amount of precipitate occurs, increasing the asphaltene yield. Schweighardt [5] reports that asphaltene yields may vary as much as fifty percent by simply changing the laboratory technique. Work reported by Schultz and Mima [6,7] details five solvent separation methods currently in use for the determination of asphaltenes in a coal-derived liquid. Results listed in Tables 1 and 2 show that between the five processes there exist significant variations in determination of the asphaltene product. In four of the five separation processes studied, the yield of asphaltenes

appeared to be reproducible, however the isolated end products were not necessarily equivalent.

Table 1. - Results with Methods A, B, and C [6].

Method	% Insolubles + 1S	% Asphaltenes + 1S	% Oils + 1S
A	5.2 \pm 0.3	26.9 \pm 0.7	67.9 \pm 0.7 (by difference)
B	7.6 \pm 0.5	23.8 \pm 0.7	67.2 \pm 0.9
C	4.6 \pm 0.5	22.0 \pm 2.0	70 \pm 3.0

Table 2. - Comparison of Methods of Asphaltene Analysis of an SRC-I Sample [7].

Method	% Insolubles + 1S	% Asphaltenes + 1S	% Oils + 1S
A	37 \pm 3	52 \pm 3	12.0 \pm 2.0
B	58 \pm 5	43 \pm 6	1.5 \pm 0.6
C	-----See Text -----		
D	64 \pm 3	27 \pm 4	14.0 \pm 2.0
E	49 \pm 2	34 \pm 2	22.0 \pm 0.8

The above studies clearly illustrate the need for a standardized method of separating and defining coal-derived asphaltenes. As of today no such standardized method has found general acceptance.

The use of solvent extraction to separate coal liquids provides very little fundamental chemical information. The

solubility of a substance is a function not only of its molecular weight, carbon-hydrogen skeleton and chemical functionality, but depends also on interactions with other substances which can act as co-solvents [8]. It is possible for a given compound to act as an oil or as an asphaltene depending on the presence or absence of other substances. Additionally, a single compound may distribute itself between two fractions even if the extractions are carefully performed.

Farcasiu and co-workers at Mobil Research & Development Corporation [3,8,9] have developed a method of direct fractionation of whole coal liquids in order to circumvent the above problems and to obtain a better chemical understanding of coal liquids. The method, sequential elution with specific solvents chromatography (SESC), utilizes liquid chromatography with a silica gel stationary phase to isolate chemically distinct fractions. Table 3 shows the elution procedure and the major compound classes which are eluted with each solvent. As can be seen there is an overlap between the classically defined fractions (oils, asphaltenes and preasphaltenes) and the SESC eluted fractions.

Table 3. SESC Fractionation Procedure Developed by Mobil [3]

<u>Classical Description</u>	<u>Frac-tion</u>	<u>Elution Solvent</u>	<u>Major Compounds</u>
Oils (1-3)	1	Hexane	Saturates
	2	Hexane/15% Benzene	Aromatics
	3	Chloroform	Polar aromatics; non-basic N, O, S-heterocyclics
Asphaltenes (3-5)	4	Chloroform/10% Et ₂ O	Simple phenols
	5	Et ₂ O/3% EtOH	Basic Nitrogen heterocyclics
	6	MeOH	Highly-functional molecules (10 wt % heteroatoms)
	7	CHCl ₃ /3% EtOH	Polyphenols
	8	THF	Increasing O content and increasing basicity of nitrogen
	9	Pyridine	
	10		Non-eluted, unknown materials
Multifunctional Cpds. (5 thru 9)			

The SESC process differs primarily from that of selective solvent fractionation in that it separates coal liquids by chemical class rather than by polarity. Oils, by the SESC procedure, are saturated and aromatic hydrocarbons with some non-polar heterocycles. Asphaltenes are primarily monofunctional compounds such as mono-phenols and mono-basic nitrogen compounds. Preasphaltenes (or asphaltols)

are polyfunctional compounds differing widely in the extent of functionality [9]. The main utility of SESC is that it separates coal liquids into functionally similar fractions. This can simplify the characterization of the chemistry and structure of coal liquids.

Other researchers [10,11] have developed similar chromatographic fractionation techniques for the separation of coal liquids. While one method has as much merit as the other, the acceptance of a standardized method of separation may ultimately be determined by the speed, ease and reproducibility with which the process can be carried out.

There has been some recent work on further fractionation of coal-derived asphaltenes. Sternberg, et al. [12], have separated asphaltenes into acidic and basic subfractions by passing dry HCl gas through an asphaltene-toluene solution. The basic component precipitates as an HCl adduct while the acidic component remains in solution. This result indicates that asphaltenes consist of hydrogen bonded complexes and is compatible with the solubility characteristics of the asphaltenes. In moderately polar aromatic solvents, such as toluene, the asphaltenes are soluble because the acidic and basic components are separately solvated. In non-polar solvents, such as pentane, hydrogen bonding occurs between the acid-base subfractions. As a result the asphaltenes precipitate from solution as large

hydrogen-bonded acid-base complexes.

More recently, Scheppele, et al. [13] have developed a chromatographic separation of asphaltenes into acidic, neutral and basic subfractions. Their primary goal in doing so was to obtain detailed molecular information about asphaltenes through mass spectrometric and infrared analysis of each of these subfractions. The implications of instrumental analysis on asphaltene structural determination will be discussed in more detail in the section on structural characterization.

Comparison of Coal and Petroleum Asphaltenes

The original definition of asphaltenes is based on the solution properties of petroleum residua in various solvents. In recent years this definition has been extended to apply to fractions derived from other carbonaceous sources such as coal. Other than the separation procedure, few similarities exist between coal- and petroleum-derived asphaltenes. The asphaltenes differ not only in their origin and mode of generation, but also in their chemical composition and physical behavior [2,14,15].

In Table 4 a comparison is made between asphaltenes derived from bituminous coal liquids and those derived from petroleum crudes.

Table 4. Comparisons of Properties Between Petroleum- and Coal-Derived Asphaltenes.

<u>Property</u>	<u>Coal</u>	<u>Asphaltenes</u>	<u>Petroleum</u>
Solubility (Benzene Sol/Pentane Insol)	Yes	Yes	
Number Average Molecular Weight	400-800	2,000-10,000	
Weight Percent Carbon	84-89	80-86	
Weight Percent Hydrogen	5.8-7.3	7.7-9.3	
Weight Percent Oxygen	2-4	1-2.7	
Weight Percent Nitrogen	1-3	.3-.5	
Weight Percent Sulfur	.1-.8	3-9.3	
% Ash by Low or High Temperature	.1	2	
Aromaticity, F_a , by ^{13}C NMR	.6-.7	.4-.55	
Forms of Oxygen	OH, -O-	OH, -C=O, -O-	
Forms of Nitrogen	-N=, NH	NH, NH_2 , -N=	
Metals	Iron, 100-300 ppm Titanium, 50-20 ppm	Vanadium, 100-400 ppm Nickel, 50-150 ppm	

In comparison to petroleum asphaltene, coal-derived asphaltene are lower in molecular weight and H/C ratio, but higher in aromaticity (f_a) and heteroatom content. In addition, the nature of the heteroatom functional groups are also quite dissimilar. Yen [15] has summarized the major differences between coal- and petroleum-derived asphaltene. This summary is listed below.

1. The aromaticity of petroleum-derived asphaltene ($f_a=0.2-0.5$) is lower than that of coal-derived asphaltene ($f_a=0.6-0.7$).
2. The aromatic ring systems within petroleum-derived asphaltene are much more condensed (peri) ($H_{aru}/C_{ar}=0.3-0.5$) than that of coal-derived asphaltene (kata) ($H_{aru}/C_{ar}=0.5-0.7$).
3. The substituents of the petroleum-derived asphaltene are longer ($n=4-6$) than those of coal-derived asphaltene ($n=1$).
4. The aromatic system of petroleum-derived asphaltene is extensively substituted (70-80%), whereas the coal-derived asphaltene is sparingly substituted (35-45%).
5. The molecular weight of petroleum-derived asphaltene is ca. 10 times higher than that of the coal-derived asphaltene.
6. Petroleum-derived asphaltene is less reactive to physical or chemical agents than that of coal-derived asphaltene.
7. Petroleum-derived asphaltene is more highly associated ($Me=5-7$) than that of coal-derived asphaltene ($Me=2-4$). This will be reflected in the ease of processing.
8. Petroleum-derived asphaltene is less polar than the coal-derived asphaltene.

Physical, Chemical and Structural Characterization of Coal-Derived Asphaltene

Asphaltene are considered to be the principle inter-

mediate in the coal liquefaction mechanism and are primary precursors of oils [16-18]. Their presence in coal liquids are undesirable because they are responsible for high viscosity [19-22], solvent incompatibility, and processing difficulties [16]. Still, asphaltenes are important because they convey the extent of conversion which takes place during coal hydrogenation. It has therefore become increasingly desirable to determine the chemical composition and structural details of the asphaltene fraction.

Typical elemental analyses of the asphaltene fraction are given in Tables 5-7 for work done by Sternberg et al. [12], Taylor and Li [23], and Marzec et al. [24]. While the numerical values of the elements vary in each study due to differences in parent coals and processing histories [25,26], the differences are usually less than 1% indicating good compositional similarity.

Table 5. Ultimate Analyses and Molecular Weights of Asphaltenes and Their Acidic and Basic Components [12].

Material	Composition (%)						Molecular weight
	C	H	O	N	S	Cl	
Asphaltene (415°C)	85.91	6.85	4.11	1.67	1.46		686
Acidic component	85.72	7.18	3.86	0.99	0.88	1.37	
Basic component (as HCl adduct)	81.27	6.39	4.63	2.12	1.05	4.54	
Basic component (calc. HCl-free)	85.25	6.57	4.86	2.22	1.10		
Asphaltene (450°C)	87.43	6.52	3.52	2.16	0.37		417
Acidic component	87.40	7.04	3.39	0.99	0.51	0.67	550
Basic component (as HCl adduct)	83.35	5.78	3.48	2.72	0.53	4.14	
Basic component (calc. HCl-free)	87.06	5.91	3.64	2.84	0.55		368

Table 6. Elemental Analysis and Molecular Weights of Asphaltenes [23].

CLP		C	H	O	N	S	Cl	MW
	Asphaltene	87.65	5.65	3.95	1.96	0.81		530
44-56	Acid component	87.3	6.05	3.4	0.85	1.02	*	380
	Base (HCl-free)	88.3	6.15	2.9	2.16	0.32	0.27	600
	Asphaltene	86.2	5.95	3.6	1.34	0.93		505
50-17	Acid component	87.5	6.2	3.4	0.83	1.03	1.06	390
	Base (HCl-free)	87.45	5.85	3.15	2.49	0.84	0.20	680

* Not determined

Table 7. Elemental Analysis of Products A, B and C
And of Their Group Components [24].

	(wt. %)					
	C	H	N	S	O*	
Product A (residuum, b.p. above 220°C)	90.3	8.1	0.4	0.6	0.6	0.6
Hydrocarbon concentrate	89.8	8.0	0.2	0.6	1.4	1.4
Preasphaltenes	86.5	4.8	2.9	0.5	5.3	5.3
Asphaltenes	88.4	5.9	2.1	0.7	2.9	2.9
Basic fraction separated from asphaltenes	89.0	6.5	3.5	0.2	0.8	0.8
Acidic fraction separated from asphaltenes	88.4	6.7	1.0	0.6	3.3	3.3
Product B (residuum, b.p. above 220°C)	89.8	8.4	0.5	0.3	1.0	1.0
Hydrocarbon concentrate	89.9	8.1	0.3	0.3	1.4	1.4
Preasphaltenes	85.1	4.9	2.6	0.6	6.8	6.8
Asphaltenes	87.6	6.1	2.2	0.7	3.4	3.4
Basic fraction separated from asphaltenes	88.6	6.5	3.6	0.2	1.1	1.1
Acidic fraction separated from asphaltenes	86.8	6.9	1.0	0.6	4.7	4.7
Product C (residuum, b.p. above 220°C)	89.0	7.0	0.5	0.8	2.7	2.7
Hydrocarbon concentrate	89.9	7.3	0.3	0.6	1.9	1.9
Preasphaltenes	83.9	5.5	2.8	0.9	6.9	6.9
Asphaltenes	87.4	5.0	2.2	0.8	4.6	4.6
Basic fraction separated from asphaltenes	89.9	5.1	3.6	0.2	1.2	1.2
Acidic fraction separated from asphaltenes	80.3	6.1	0.8	0.5	12.3	12.3

* By difference

Of particular interest in these tables is the heteroatom content of the acidic and basic components of the asphaltenes. Sternberg et al. [12] have determined that in the acidic component, oxygen is present as phenolic hydroxyl and nitrogen present as acidic nitrogen as in pyrrole. The oxygen in the basic component is present as ring or ether oxygen, and the nitrogen present as ring nitrogen as in pyridine. Marzec et al. [24] have applied a number of instrumental techniques (FIMS, IR, TLC, $^1\text{H-NMR}$, HRMS) in order to elucidate the heterocompounds present in asphaltenes. A summary of their primary results for the basic and acidic fractions is listed below.

Basic fraction:

1. The fraction consists of substances with various molecular weights (from 100 to 660) and the highest content of compounds is in the 300-400 amu range. Their average molecular weight is 360.
2. The fraction represents a mixture of compounds containing at least one nitrogen atom with a lone pair of electrons in a molecule, i.e. it is mainly a mixture of pyridine derivatives (phenylpyridine, quinoline, dihydroquinoline, phenylquinoline, acridine, tetrahydroacridine, benzoacridine, dibenzoacridine) and possibly amines.
3. The number of aromatic rings condensed with the pyridine and/or the aniline rings ranges from 1 to 5. Some more highly condensed systems may be present.
4. Compounds with more than five saturated carbon atoms have not been found.
5. Diazo compounds of carboline, naphthophenazone, naphthylphenazine and diazodibenzopyrene series were found.

6. A few compounds C_xH_yON were detected in which oxygen is most probably in a furan ring or an ether bond.
7. Sulphur compounds were not detected.
8. An average molecule contains two methyl groups.

Acidic fraction:

9. The fractions contain substances within the 100-650 amu range; substances of 400-500 amu range prevail. The average molecular weight is 400 amu. They are a mixture of O-compounds, N-compounds and O,N-compounds. A small number of sulphur compounds was also identified.
10. Nitrogen present in this fraction is most probably in pyrrole rings associated with 1 to 5 aromatic rings.
11. Diazo compounds are represented by benzimidazole, acenaphthydrine and carboline series.
12. Oxygen is bound in phenol groups, but ether and ketone structures cannot be excluded.
13. The number of aromatic rings condensed with phenolic structures does not exceed 4.
14. Compounds with two oxygen atoms in a molecule were found: they are derivatives of hydroxyacetophenone, hydroxybenzofuran, hydroxyindanofuran and/or biphenyl, and also dihydroxy anthracene and/or phenanthrene.
15. The acidic/neutral fraction contains oxaza compounds of $C_xH_yON_2$ and $C_xH_yO_2N$ types.
16. Sulfur is represented by thiophene derivatives.
17. An average molecule contains 2.5 methyl groups.

Also shown in Tables 5 and 6 are molecular weight values for the whole asphaltene, the acidic component, and the basic component. Again, here, as in elemental analysis, asphaltene molecular weight appears to be a function of both the parent coal and the processing history. Generally this molecular weight falls between 300 and 600, but much higher values have been observed.

In order to determine the gross skeletal structure of

coal-derived asphaltenes, the carbon and hydrogen environments must be established. This can be accomplished by proton and carbon nuclear magnetic resonance spectroscopy. High resolution ^1H nmr spectroscopy was first used by Brown and Ladner for structural characterization of coal pyrolysis products [27]. Other workers have since extended this type of analysis to coal extracts [28,29], and coal hydrogenation products [30-35]. The advent of ^{13}C nmr has enabled direct elucidation of the aromatic fraction, f_a . Retcofsky, et al. [36] have compared f_a values from ^{13}C nmr and those estimated from ^1H nmr by the Brown and Ladner equation, and found good agreement for coal-derived materials. Some of the structural parameters which may be calculated are: C_{al} , number of aliphatic carbon atoms; f_a , aromaticity; σ , degree of alkyl substitution; CL, average alkyl chain length; dC, degree of condensation; and $(\text{H/C})_{al}$, the aliphatic hydrogen-to-carbon ratio. These parameters are given by the equations listed in Table 8. Representative ^1H nmr and ^{13}C nmr are given in Figures 2 and 3. The appropriate absorption peaks for the various parameters are indicated.

Table 8. Definitions of Structural Parameters [29].

STRUCTURAL PARAMETER	DEFINITION
No. of aliphatic carbon atoms, C_a	$\frac{H_{\alpha,2}}{a} + \frac{H_{\alpha}}{b} + \frac{H_{\beta}}{c} + \frac{H_{\gamma}}{d}$
Aromaticity, f_a	$\frac{C - C_{a1}}{C}$
Degree of alkyl substitution,	$\frac{H_{\alpha}}{b}$ $H_{AR,OH} + \frac{H_{\alpha}}{b}$
Average alkyl chain length, CL	$\frac{C_{a1} - H_{\alpha,2}}{H_{\alpha}} \frac{1}{b}$
Degree of condensation, dC	$\frac{H_{AR,OH} + \frac{H_{\alpha}}{b} + 2(\frac{H_{\alpha,2}}{a} + \text{non-phenolic O+N+S})}{(C - C_{a1}) + (\frac{H_{\alpha,2}}{a} + \text{non-phenolic O+N+S})}$
Aliphatic $\frac{H}{C}$ ratio	$\frac{H}{C} \times \frac{\text{aliphatic hydrogen}}{H} \times \frac{\text{aliphatic carbon}}{C}$ (from 1H NMR) (from ^{13}C NMR)

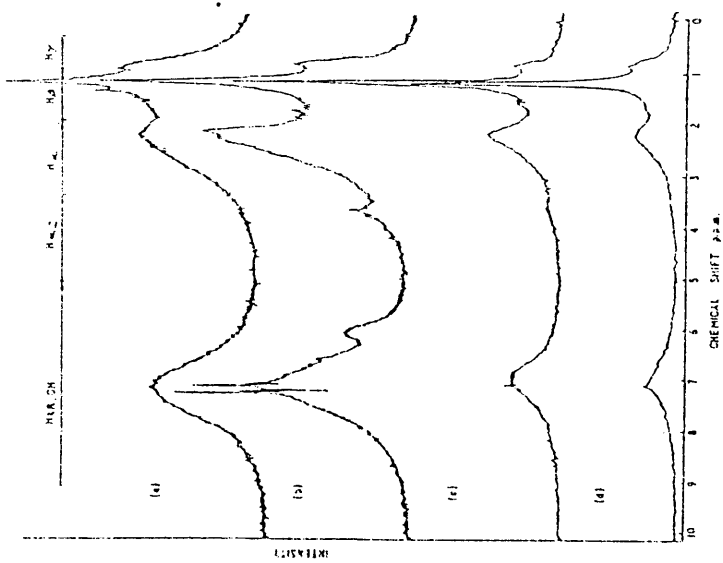


Figure 2 [29]. Typical ¹H nmr spectra of Asphaltene.

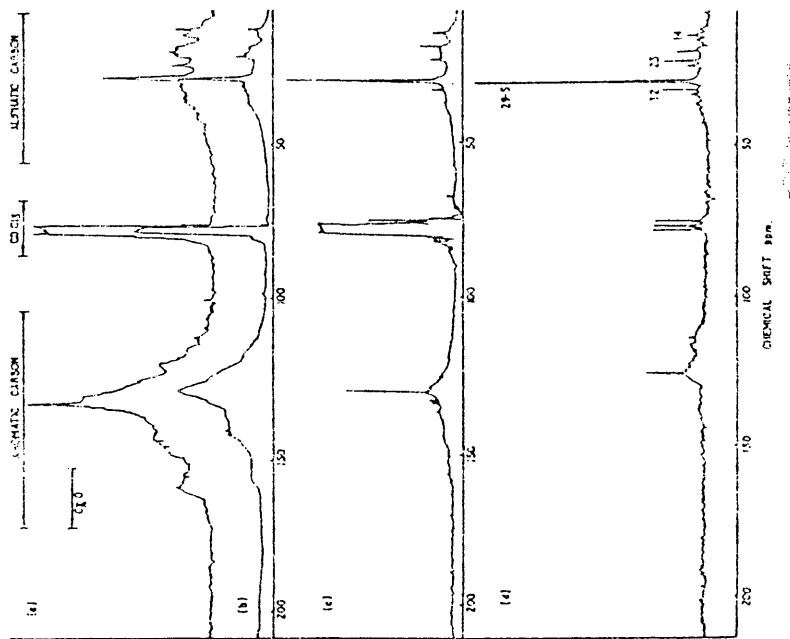


Figure 3 [29]. Typical ¹³C nmr spectra of Asphaltene.

Additional analytical and chemical techniques have been applied in the structural determination of coal-derived asphaltenes. Schwager and Yen have been instrumental in characterizing asphaltenes by these methods. Results of their work is summarized below [37].

Nuclear-magnetic-resonance structural-parameter calculations suggest that the asphaltene components are made up of cata-systems of small ring number (3-5), with 30-50% of the available aromatic edge atoms occupied by substituents, and joined together by naphthenic, methylenic or etheric bridges. N.M.R. analysis of silylated asphaltenes indicates that the fraction of total oxygen present as OH ranges from 0.59 to 0.83, and that the major hydroxyl components are simple phenols. (Minor Components may be benzylic, alcoholic, or hindered phenolic-type compounds). Methylation of chromatographic fractions followed by infrared N-H analysis indicates that the fraction of total nitrogen present as NH ranges from 0.53 to 0.74.

The macrostructure of asphaltene crystallites has been studied by X-ray diffraction. An average of about four condensed aromatic sheets is assumed to be stacked on top of each other with sheets parallel, and with aliphatic chains or naphthenic rings protruding from the edges.

The results of these macro- and micro-structural parameters have allowed insight into the molecular structure of asphaltenes. Ladner, et al. [29], Yen [38], and Bartle, et al. [39] have each proposed "average" structures for coal-derived asphaltenes. Three of these structures are shown in Figure 4. In spite of variations in molecular

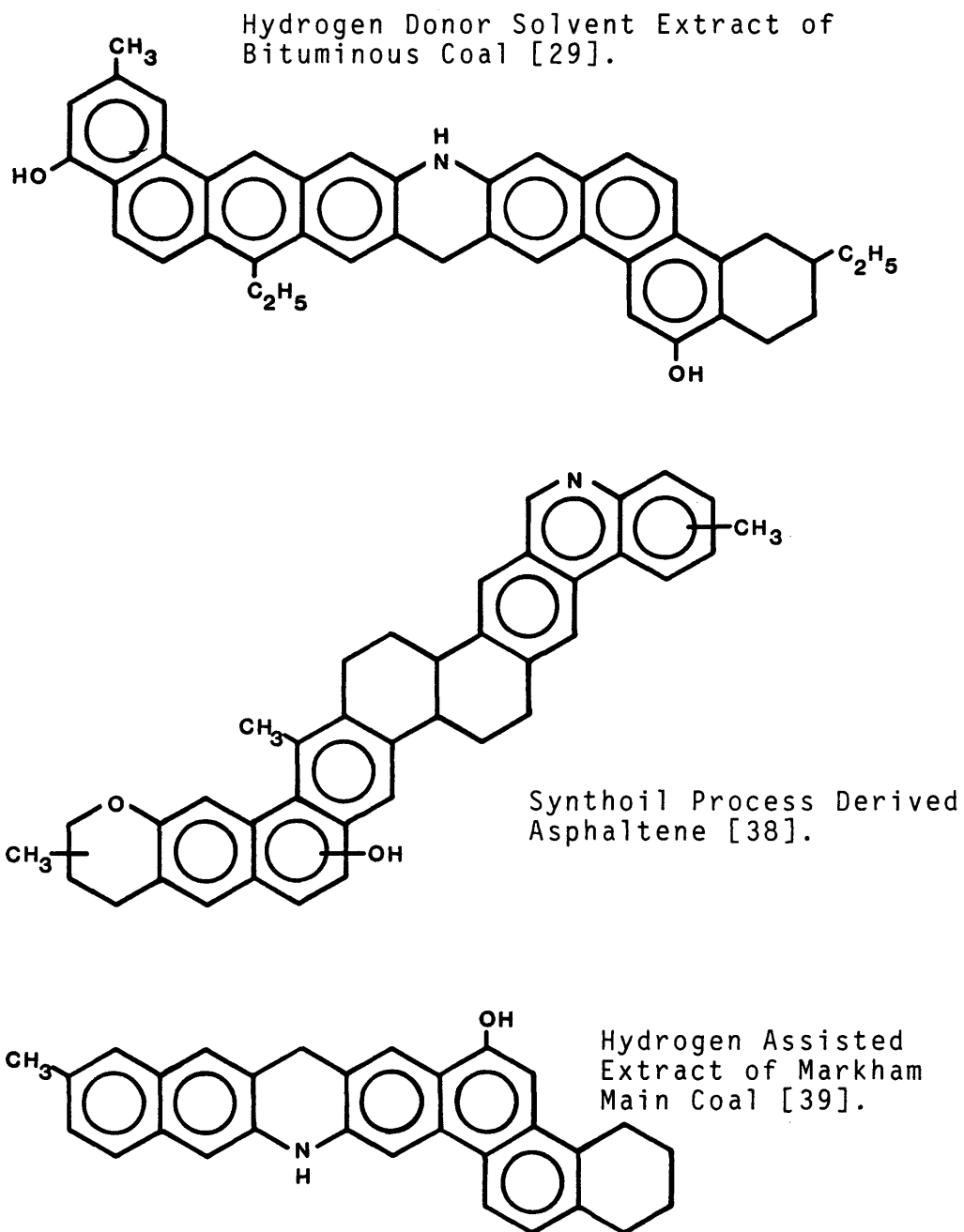
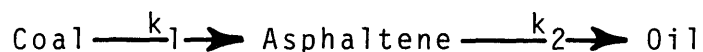


Figure 4. Hypothetical Structures of
Coal-Derived Asphaltenes.

weight, different parent coals and processing conditions, the proposed structures are very similar.

Asphaltene Hydroprocessing:
Kinetics, Mechanisms, and Catalysts

The overall hydrogenation of coal proceeds via the formation of asphaltenes as an intermediate. The conversion of coal to asphaltene is a relatively rapid reaction involving cleavage of the coal structure primarily through the elimination of oxygen. The asphaltene-to-oil reaction is relatively slow involving the rupture of carbon-carbon bonds and necessitating more severe reaction conditions. Weller and co-workers at the U.S. Bureau of Mines investigated coal hydrogenation in the late 1940's and early 1950's. They suggested the conversion of coal-to-oil proceeds via the following reaction sequence [40]:



with both reactions proceeding via first order kinetics. Values of k_1 and k_2 are shown in Table 9. At 400°C k_1 is 25 times larger than k_2 . This suggests the desirability of performing coal hydrogenation in two separate stages. The first stage would be designed to take the coal through the primary reaction step under conditions required to minimize gas formation. The second stage would then process the primary products under more severe conditions, optimized

for asphaltene conversion.

Table 9. Rate Constants for Anthraxylon Hydrogenation [40].

Temp. (°C)	k_1 (min. ⁻¹)	k_2 (min. ⁻¹)
400	0.027	0.00107
420	0.060	0.00503
430	0.126	0.00895
440	0.129	0.01282

Weller et al. have studied asphaltene hydrogenolysis for an asphaltene feed derived from Bruceton coal [18]. The reactor charge in each experiment was 50 grams of asphaltene, 0.5 grams of stannous sulfide, 0.25 grams of ammonium chloride, and 1250 or 2500 psig hydrogen initial pressure. They found the conversion to be first order with respect to the residual asphaltene as is shown in Figure 5. The large temperature dependence of the rate constant was shown not to follow the simple Arrhenius relation:

$$k = k_0 e^{-Ea/RT}$$

over the temperature range studied, Figure 6. They reasoned that since the asphaltene fraction is a chemically heterogeneous grouping of organic molecules, it comprises a composite reaction system, and thus should not be expected to have an activation energy which is invariant with

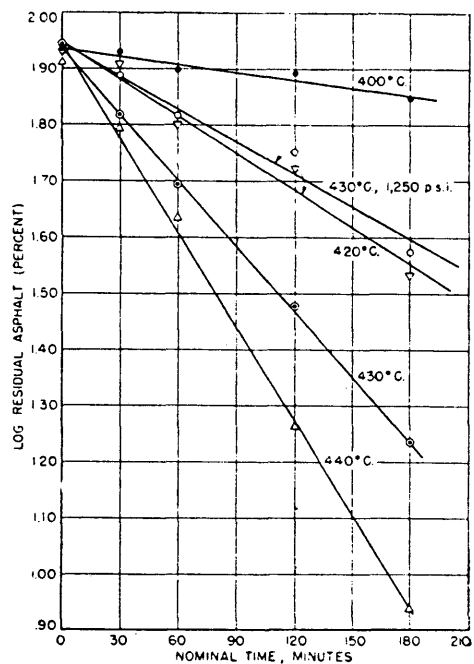


Figure 5. Rates of Asphaltene Hydrogenation [18].

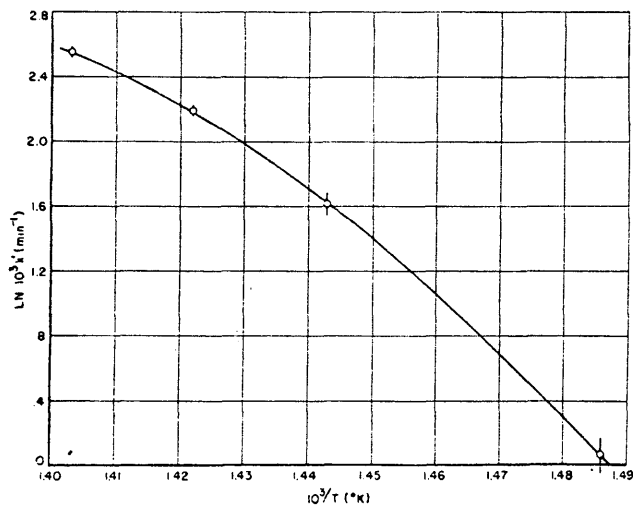


Figure 6. Temperature Dependence of Asphaltene Hydrogenation [18].

temperature.

Weller et al. [17] further investigated the asphaltene-to-oil reaction and suggested a mechanism to explain the results:

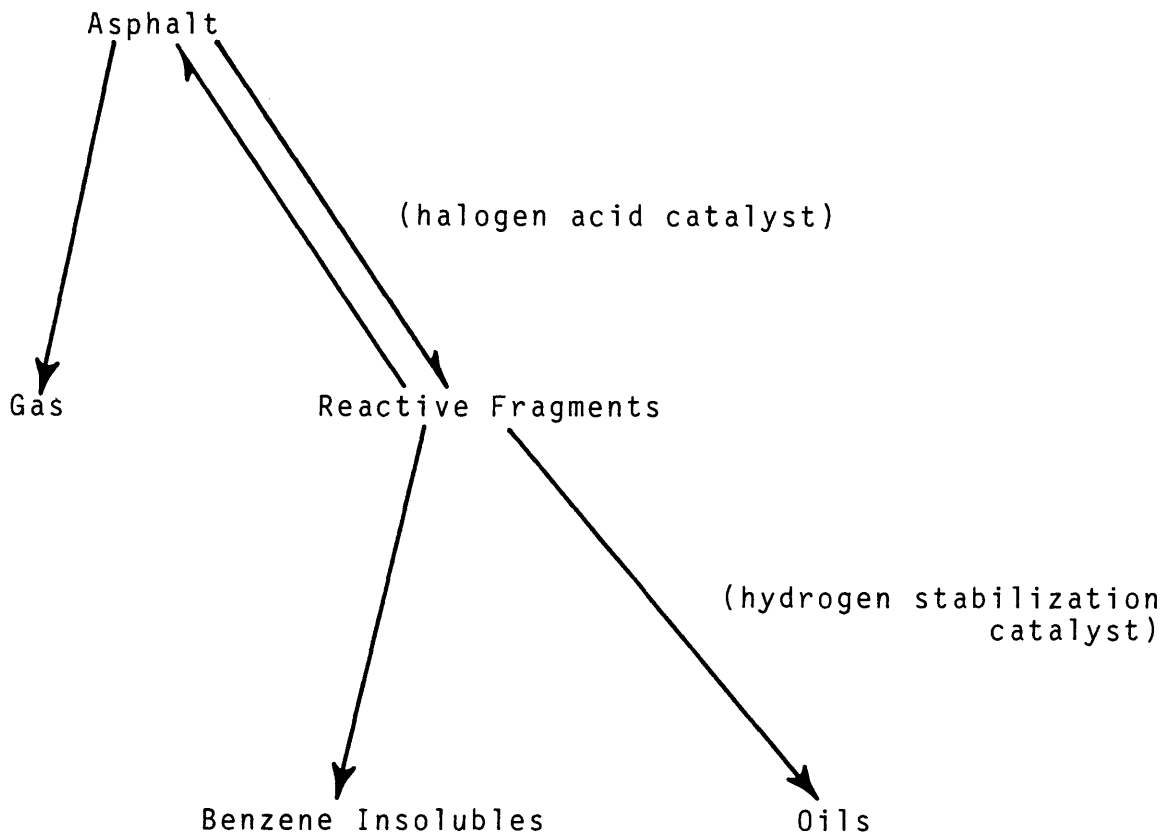
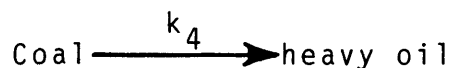


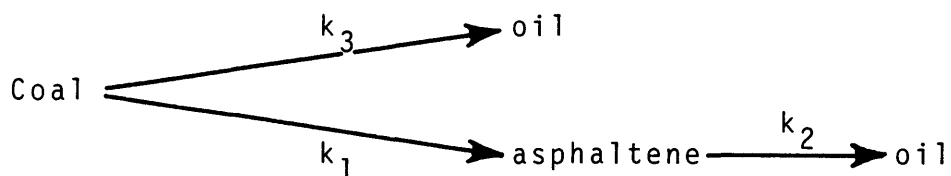
Figure 7. Mechanism of Asphaltene Conversion [17].

Here, asphaltenes are catalytically split by halogen acids (eg. HCl) to form reactive fragments. The fragments may recombine to form asphaltenes; they may polymerize further to form benzene insoluble products; or they may be stabilized by hydrogen to form oils. The hydrogen stabilization reaction is catalyzed by metals such as tin. The product distribution was found to be dependent on the presence of the splitting catalyst, the hydrogenation catalyst, and on hydrogen pressure.

Liebenberg and Potgieter [41] were unable to fit their data of the uncatalyzed hydrogenation of coal to the simple series mechanism suggested by Weller and co-workers. As a result, they proposed a more elaborate series-parallel mechanism as a fit to the data.

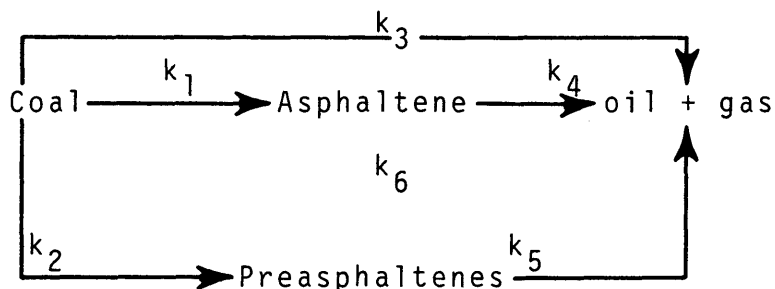


Yoshida, et al. [42] obtained a reasonably good fit for Taiheiyo and Oyubari coals with the following mechanism:



They used sulfur-promoted red-mud as a catalyst and maintained reactor temperature at 400°C. The hydrogenolysis of both coal and asphaltenes was found to obey first order kinetics. Values of k_2 were determined to be $4.9 \times 10^{-3} \text{ min}^{-1}$ and $4.4 \times 10^{-3} \text{ min}^{-1}$ for the Taiheiyo and Oyubari asphaltenes respectively.

Shalabi et al. [42] found that a better fit to the data could be obtained if preasphaltenes were incorporated into the mechanism. They proposed the mechanism:



At 400°, k_4 , the rate constant for the conversion of asphaltene to oil + gas, was $2.79 \times 10^{-3} \text{ min}^{-1} \pm 0.00257$.

Few researchers have investigated the hydrotreatment of asphaltenes without interference from other components (coal, preasphaltenes, oils) in the starting material. Recently however, Kanda et al. [44], and Yoshida et al. [45], in independent studies, have used separated asphaltenes as starting material in order to investigate the structural changes taking place in the asphaltene-to-oil reaction. From these studies it was concluded that the

asphaltenes remaining after hydrotreatment were more aromatic, contained fewer polar functional groups, and were of lower average molecular weight than those present before hydrotreating. Most of the conversion of asphaltenes to oils was suggested to involve the saturation of aromatic rings with hydrogen to form naphthenic rings without changes in the polymerization degree of the structural unit.

Dickey [46] studied the thermal hydrogenation of coal-derived asphaltenes in a continuous stirred-tank reactor. The maximum conversion of asphaltenes-to-oils was 20.8% at conditions of 400°C, 1500 psig, and 60-minute space time. Based on these results, processing asphaltenes to extinction would require a prohibitively long residence time or more severe hydrotreating conditions than commonly used in current coal liquefaction processes.

A more promising approach would be the use of new and novel catalytic systems. Kawa et al. [47] performed an extensive evaluation of the effectiveness of various pelleted catalysts for the hydrogenation and hydrodesulfurization (HDS) of a high-volatile bituminous coal. They found that a commercial, silica-promoted Co-Mo on alumina catalyst (Harshaw 0402T) was the most effective, both for hydrogenation and HDS.

Some of the more promising catalyst systems for coal hydrogenation have been summarized by Mills [48] and are

listed below in Table 10. For the most part they have not been developed into economical processes, however, further research work is in progress. Although most of these catalysts have not been tested on asphaltene feeds, their successful use in hydrotreating coal and petroleum feedstocks indicate that such utilization is possible.

Table 10. New Hydrogenation Catalytic Systems [48].

- "Nascent" - active hydrogen generated in situ
- Complexes of transition metals
- Massive amounts of halide catalysts
- Organic hydrogen donor solvents
- Alkali metals
 - (a) With H₂
 - (b) With amines
 - (c) Electrocatalytic
- Reductive Alkylation
- Miscellaneous

EQUIPMENT

All experimental runs were carried out in a one-liter stirred batch autoclave reactor. The reactor was equipped with a sample injection system, an on-line liquid products sampling system, a gas sampling system, and a temperature and pressure monitoring system. The composite reactor system, shown in Figure 8, was most recently used by Furlong and is described in his dissertation [49].

The reactor and line system was enclosed behind a $\frac{1}{4}$ " thick heat-tempered steel explosion barrier. Injection and product sampling as well as control of reaction variables was carried out remotely, external to the cage assembly.

Reactor and Stirrer Assembly

The reactor was a one-liter stainless steel (type 316) vessel manufactured by Autoclave engineers. The vessel was rated to 10,000 psi and included a line containing a rupture disk which led to a knock-out vessel and vent. The internals of the reactor included a thermowell, sample dip-tube, baffle and cooling coils. The reactor was also equipped with a MagneDrive stirrer which was controlled externally by a Reliance Electric drive unit. The stirrer speed was monitored by a magnetic detector ring and tachometer system.

Injection System

To facilitate injection of reactants into the reactor,

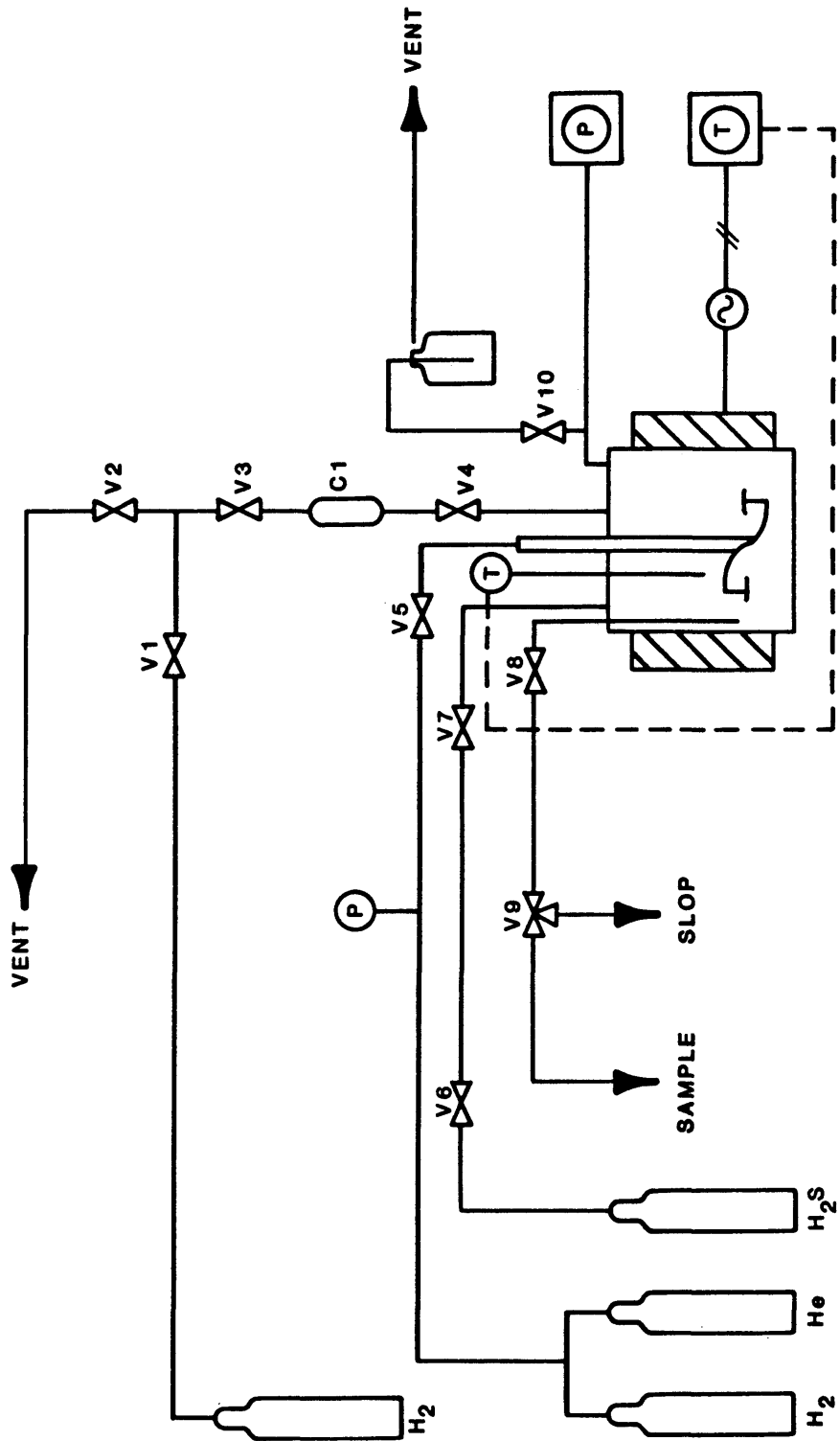


Figure 8. Experimental Apparatus.

a high pressure gas-forced sample injection system was used. A 150 ml. Hoke gas cylinder, C1, was attached by 1/8" stainless steel tubing to valve V4. The top of this vessel was attached by 1/4" steel tubing to valve V3 and from there to the high pressure hydrogen supply and vent system.

Sampling Systems

Liquid product was sampled during a run for analysis through 1/8" stainless steel tubing and the double valve system V8 and V9. The sample line was enlarged to 1/4" steel tubing downstream of V8 in order to allow for increased sample volume. Gas samples were taken in 500 ml valved gas sample bottles with 1/4" quick-connect fittings.

Temperature and Pressure Monitoring System

Temperature of the reactor was controlled by a 2.1 kW, 110 volt, A.C. resistance heater and a thermocouple in a submerged well connected to a Leeds and Northrup Electro-max 111 controller. Power to the heating jacket was regulated via a Leeds and Northrup Model 1106 SCR. The heating jacket was raised and lowered remotely by a GCA Precision Scientific power jack. A Thermo Electric digital temperature indicator and a Honeywell Electronik 111 chart recorder provided both an accurate temperature readout and a permanent record of the run temperature profiles.

Pressure was monitored by a Viatran pressure trans-

ducer and Viatran digital pressure indicator. A second Honeywell strip chart recorder was used to record pressure profiles during operation.

EXPERIMENTAL DESIGN

This study of the hydroprocessing of coal-derived asphaltenes has been separated into four principle phases. Each phase consisted of taking product samples at specified conditions and reaction times for kinetic model development and asphaltene structural analysis. The four phases of study are:

Phase I - Thermal Hydroprocessing

Phase II - Pyrite and H₂S Catalytic Hydroprocessing

Phase III - Commercial Catalyst Hydroprocessing

Phase IV - Effects of Processing Conditions

Reaction Conditions

Temperature

Since it was desired to obtain kinetic information from this study, it was necessary to select a reaction temperature which was high enough to allow adequate conversion of reactants yet low enough so that the reaction would not proceed too rapidly, even with added catalyst. Since most donor-solvent coal liquefaction processes normally operate between 350⁰-450⁰C, temperatures in that range were considered valid. The choice of tetralin as the solvent precluded operation at the upper end of this temperature range because the critical point of tetralin is 446⁰C. It was decided to try three different temperatures for the thermal (non-catalytic) runs and to utilize the

results of these to determine the best temperature at which to make the catalytic runs. For the thermal runs reaction temperatures of 21⁰, 355⁰, 375⁰ and 400⁰C were chosen. The catalytic runs were all made at 400⁰C.

Pressure

A total reaction pressure of 1500 psig was employed for all runs in this study. This provided sufficient hydrogen for the various hydroprocessing reactions as well as allowing direct comparison with the previous asphaltene study [46].

Solvent

Tetralin was chosen as the solvent for this study because of its hydrogen donating ability and other desirable solvent properties. Additionally, a large data base is available for tetralin in the literature and its decomposition products are quantifiable by gas chromatographic analysis [50,51].

Reaction Mass and Solvent/Asphaltene Ratio

The selection of a particular reaction mass and solvent/asphaltene ratio was made on the basis of several tradeoffs. Three interacting factors had primary influence on the choice of these two parameters. First, because samples were withdrawn from the reactor at specified intervals, the reaction mass varied throughout the run. It was therefore desired to begin with a large initial reaction

mass so as to minimize the fractional loss and thus be able to model the system as a constant volume batch reactor. Second, a large gas space above the liquid reactants was necessary in order to maintain sufficient hydrogen so that hydrogen starvation would be avoided. A large gas space would also minimize the pressure drop encountered when a sample was withdrawn. Third, it was desired to have as low a solvent/asphaltene ratio as possible so that for a given sample a large amount of product could be isolated for the necessary analytical tests.

The appropriate reaction mass and solvent/asphaltene ratio were determined after making several trial runs. The final conditions determined to be optimum for this study were a total reaction mass of 417 grams and a solvent/asphaltene ratio of 6/1. Sample masses were 5.0 ± 0.5 grams. At these conditions, five samples, with a line flush just prior to each, amounted to a loss of 50 grams of reactor material prior to taking the final sample. This represents a loss of 12 weight percent of the reactor material. That this loss does not have a significant effect on the kinetics of the reaction was verified by experiment. This factor is considered in more detail in the Discussion section.

Catalyst Mass and Particle Size

In order to observe a true catalytic effect it was

desired to keep the total catalyst mass to 5 weight percent of the original asphaltene. This required a catalyst mass of 3 grams. By grinding the catalyst pellets to -200 mesh (0.074 mm and smaller) mass transfer effects were assumed to be minimized. Also with -200 mesh particles, plugging of the 1/8" OD sample dip tube was avoided.

Stirrer Speed, Sample Size and Sample Times

The stirrer speed was maintained at 1500 rpm during operation to facilitate good mixing and solvent-asphaltene contact at all times.

The amount of product which was withdrawn from the reactor could be controlled by adjusting the length of the 1/4" OD sample tube. An appropriate mass of sample was determined to be 5 grams.

It was desired to obtain short reaction time kinetic data as well as data which approached equilibrium. For these reasons, samples were withdrawn from the reactor at 2, 5, 10, 15, 30 and 60 minutes following injection.

A summary of the final reaction conditions used in this study is given in Table 11.

Table 11. Reaction Conditions

Reactor: 1 liter semi-batch autoclave

Temperature - non-catalytic: 21^o, 355^o, 375^o, 400^oC

 catalytic: 400^oC

Pressure: 1500 psig total

Solvent: Tetralin (1, 2, 3, 4-Tetrahydronaphthalene)

Reaction mass - Asphaltene: 60 grams

 Catalyst: 3 grams

 Total: 417 grams

Solvent/Asphaltene: 6/1

Catalyst size: -200 mesh (0.074 mm)

Stirrer Speed: 1500 rpm

Sample size: 5 grams

Sample times: 2, 5, 10, 15, 30 and 60 minutes after injection

Catalyst Selection

Catalysts were selected on the basis of good hydroprocessing (ie. hydrogenation, hydrocracking, hydrodesulfurization, hydrodenitrogenation, and hydrodeoxygenation) ability in feedstocks comparable to coal-derived asphaltenes. In addition to the appropriate chemical properties, physical properties of the catalysts such as large pore diameters were sought in order to facilitate diffusion of the asphaltene molecules to the reactive sites. Four of the catalysts employed were from commercial suppliers and had the chemical and physical properties shown in Table 12. A fifth catalyst, coal-derived pyrite, was also included in order to determine its effectiveness as a hydroprocessing catalyst and to compare its activity to the commercial catalysts. The properties of the pyrite are shown in Table 13.

Table 12. Fresh Catalyst Properties*

CATALYST	METAL COMPOSITION (WT%)	SUPPORT	SURFACE AREA (m ² /g)	PORE VOLUME (cc/g)	PORE DIAMETER (A)
AMERICAN CYANAMID AERO HDS-20A	16.2% MoO ₃ 5.0% CoO	Al ₂ O ₃	230	0.70	122
AMERICAN CYANAMID AERO HDS-9A	18.4% MoO ₃ 3.1% NiO	Al ₂ O ₃	200	0.65	130
AMERICAN CYANAMID HDN-30	20.5% MoO ₃ 5.0% NiO	Al ₂ O ₃	160	0.59	148
HARSHAW Ni-4303E	19.0% W ₂ O ₃ 6.0% NiO	Al ₂ O ₃	152	0.62	163

* 0.074 mm catalyst particles

Table 13. Pyrite Properties

Pyrite	62%
Marcasite	38%
Surface Area	1.9 m ² /gram

Reagents

Table 14 lists the reagents used in the course of this work. Pentane, toluene and acetone were also used as recovered from the rotary evaporator.

Table 14. List of Reagents

3500 psi grade helium gas
3500 psi grade hydrogen gas
Pure grade (99% minimum) n-Pentane
Technical grade (99.5% minimum) Toluene
Industrial grade Tetrahydrofuran (THF)
Purified grade (99% minimum) Tetralin
Technical grade (99.5% minimum) Acetone

EXPERIMENTAL PROCEDURE

Asphaltene Separation and Recovery

The asphaltenes used in this study were separated from SRC-I obtained from the Catalytic, Inc. SRC pilot plant in Wilsonville, Alabama. The SRC was produced from Kentucky 9 coal from the Lafayette mine during February, 1980. The run number from which this material was obtained is 201. Analyses of the feed coal and the solvent refined coal as performed by Catalytic, Inc. are tabulated in Appendix A. Ultimate analysis of the SRC-I as performed at Catalytic, Inc. and at the CSM Coal Hydrogenation Laboratory are given in Table 15.

Table 15. SRC-I Ultimate Analysis

Component	wt %	
	Catalytic, Inc. Laboratories	CSM Laboratory
C	87.38	86.76
H	5.40	6.01
N	1.30	1.92
S	1.26	1.07
Ash	0.26	0.14
O*	4.40	4.10

* Oxygen determined by difference

Further details regarding the run conditions and the processing history of this SRC is available from reference 52.

The procedure used in this study for separation of asphaltenes from SRC-I represents a modification of that which was used previously in this laboratory by Dickey [46]. This scheme is shown in Figure 9 and is detailed in the following discussion.

A 30 gram sample of SRC-I was placed into a 62 mm x 180 mm Whatman cellulose, single-thickness extraction thimble. The thimble was fitted into a 500 ml Soxhlet extractor and 600 ml of toluene was placed in the 1 liter round bottom flask. The system was allowed to reflux for an 8-12 hour period. After this period the system was shut down, cooled and another 30 grams of SRC-I was added to the thimble and allowed to reflux. At the end of the second reflux period, the liquid was removed and fresh toluene was added. The process was repeated twice more until a total of 120 grams of SRC-I had been extracted. By placing small 30 gram samples in the extractors, problems with asphaltene swelling and agglomeration were avoided. Also, by replacing the extraction solvent after 24 hours of operation excessive polymerization and decomposition of the extract was avoided.

The toluene extract which contained oils, asphaltenes

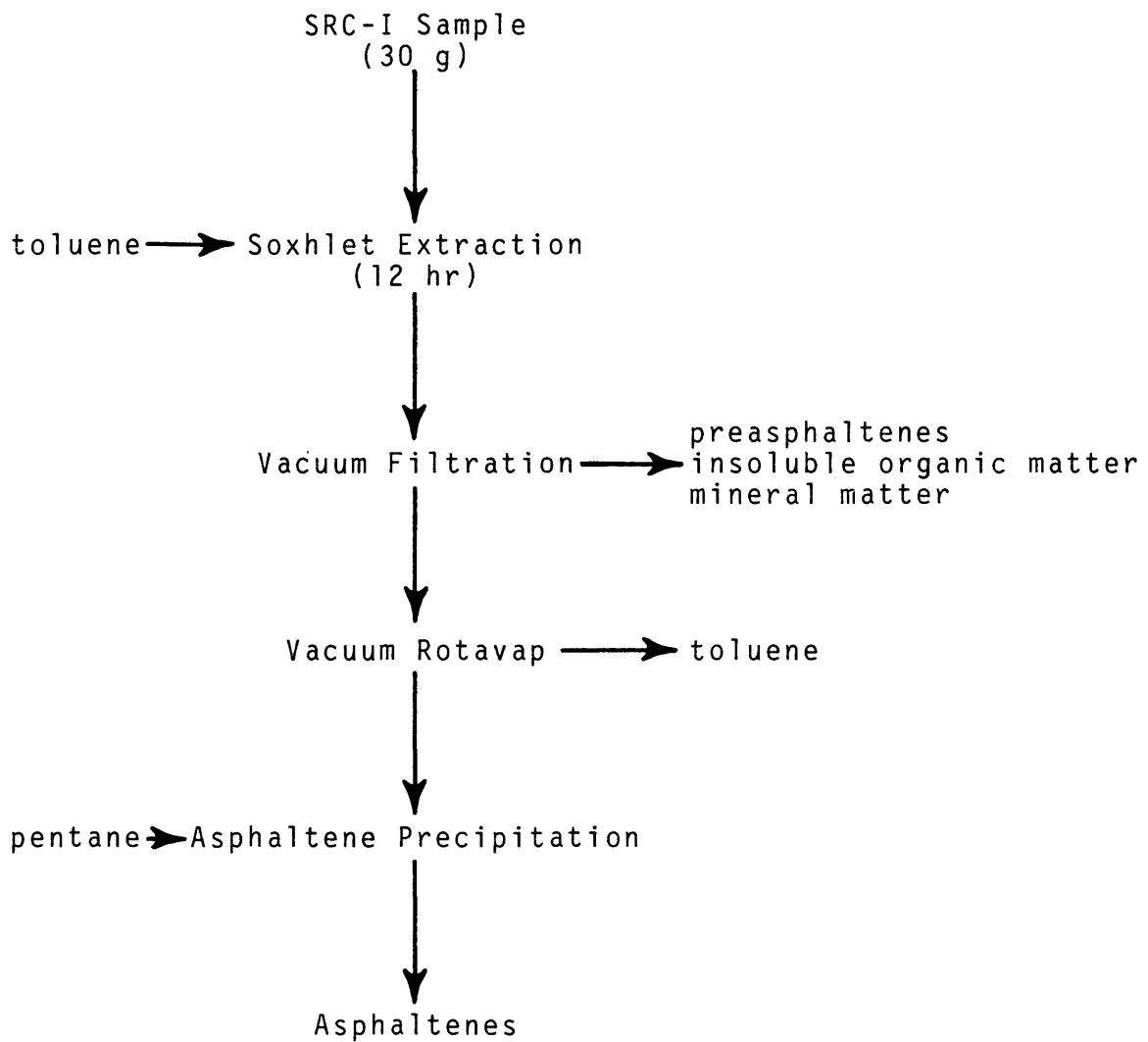


Figure 9. Asphaltene Separation Scheme

and some insolubles (which presumably had been carried through the thimble or formed in the boiling flask during extraction) was vacuum filtered through Whatman No. 42 ashless filter paper. The resulting filtrate was free of insolubles. The filtrate was concentrated in the asphaltene and oil fraction to a thick liquor by removal of the toluene by rotary evaporation at 70°C under vacuum. The liquor was transferred to 4-195 ml centrifuge tubes. Normal pentane (150 ml) was then added to each tube and the tubes placed into an 80 watt ultrasonic bath and sonicated for 5 minutes. The tubes were then transferred to an IEC explosion-proof centrifuge and centrifuged at 2600 rpm for 4 minutes. The pentane and pentane-soluble oils were decanted from the precipitated asphaltenes. This process was repeated and additional three times until the pentane, after sonication and centrifugation, remained relatively clear and colorless.

This procedure led to the separation and recovery of approximately 2000 grams of a relatively pure asphaltene fraction which was used as feedstock for this study.

Pyrite Separation

The pyrite used in this study was separated from a high pyrite coal received from the Colonial mine in Madisonville, Kentucky. The coal was ground using a jaw mill and shatter box and the pyrite separated out using a shaker

table. X-ray diffraction and Mössbauer Spectroscopy verified that the separated portion was in fact pyrite. A more detailed description of the separation process has been presented by Eaton [53].

Catalyst Presulfiding

Prior to initiation of reaction with asphaltenes, the commercial hydroprocessing catalysts were presulfided in a 10% H₂S in H₂ gas mixture according to the following sequential procedure.

1. Ground (-200 mesh) catalyst was dried in an oven at 110⁰C for 24 hours.
2. The dried catalyst was cooled in a dessicator, weighed to 3.0 ± 0.2 grams and loaded in the reactor along with 278 ± 2 grams of tetralin.
3. The reactor head assembly was attached and the lubricated head bolts torqued down to 150 ft-lb_f in 25 ft-lb_f increments.
4. The appropriate instrument connections, valve lines, valve handle extenders, heating jacket and sample injection cylinder, were attached. The cage fan was then actuated.
5. The system was leak checked with helium up the operating pressure of 1500 psig and the reactor head re-torqued as necessary.

6. The helium was slowly vented through valve V10. 400 psig of 10% H₂S/H₂ was charged through valves V6 and V7.
7. Cooling water to the stirrer was started and the Magne-drive stirrer was set at 1500 rpm.
8. The heater was turned on and the system brought to the presulfiding conditions outlined in Table 16.

Table 16. Presulfiding Conditions

Temperature	400°C
Pressure (cold)	400 psig
H ₂ S/H ₂ Concentration	10 mol %
Time	3 hours
Agitator Speed	1500 rpm

Asphaltene Mixture Preparation

During the catalyst presulfiding period the injection mixture of tetralin and asphaltene was prepared.

1. 75 grams of tetralin was added to 60 grams of asphaltene in a tared 400 ml beaker equipped with a magnetic stirring bar. The mixture was stirred rapidly on a magnetic stirrer to insure homogeneity.
2. A 3 inch No. 17 syringe needle was inserted into the opened top fitting of C1 and the syringe carefully filled with the tetralin/asphaltene mixture. The mixture was then forced into C1 through the needle with a

rubber pipet bulb connected by a glass tube to a rubber stopper inserted in the top of the plungerless syringe. The syringe was refilled until all of the mixture had been transferred into C1.

3. The syringe, needle, stirring bar and beaker were reweighed to determine the amount of "uncharged mixture".
4. The top of C1 was then attached to the hydrogen supply system and all fittings were pressure checked.

Run Procedure - Catalytic

1. At the end of the presulfiding period the temperature controller was set to 415⁰C.
2. As the reactor temperature approached 415⁰C the H₂ supply regulator was set at 1500 psig and the line between V1 and V3 flushed twice with hydrogen.
3. When the temperature reached 415⁰C the sample was injected by sequentially opening valves V1, V3 and V4.
4. When the reactor pressure jumped to 1500 psig the mixture had been injected and the stopwatch was started to indicate the run time.
5. The temperature controller was reset in order to maintain the desired reactor temperature. (usually 400⁰C).
6. Valves V4, V3 and V1 and the hydrogen supply valve were closed.

7. At one minute and fifty seconds into the run the sample line was flushed by opening valve V8 briefly and reclosing. One side of V9 was opened and the fluid was allowed to drain into a tared vessel labeled "slop". Valve V9 was closed.
8. At two minutes valve V8 was again opened briefly and closed. The other side of valve V9 was opened and the product sample allowed to drain into a clean, oven-dried, tared centrifuge tube labeled "2".
9. Valve V9 was closed and the line out of V9 was removed, flushed with acetone into a "wash" flask, blown dry with compressed air, and replaced.
10. Steps 7, 8 and 9 were repeated at 5, 10, 15, 30 and 60 minutes into the run. The samples were collected in tubes labeled "5", "10", "15", "30" and "60", respectively. In order to insure adequate material for analysis, two additional samples, labeled "60+1" and "60+2", were taken immediately following the 60 minute sample.
11. Each tube plus sample was weighed to the nearest 0.1 milligram on the two-pan analytical balance.
12. The "slop" vessel was reweighed.

Run Procedure - Non-Catalytic

The previous discussion applies to all of the catalytic runs. For the runs where no heterogeneous catalyst was added, the following modifications to the procedure were made.

1. The catalyst presulfiding procedure was omitted.
2. 278 grams of tetralin was charged to the reactor. The reactor was sealed and the appropriate fittings and instrument connections attached. The system was pressure tested to the desired operating pressure.
3. The tetralin/asphaltene mixture was loaded into the sample cylinder, C1, prior to heatup.
4. Cooling water to the stirrer was started, the Magne-drive stirrer was set at 1500 rpm, and the cage fan turned on.
5. Heating began by setting the temperature controller to 15^oC above the desired operating temperature.
6. When the reactor temperature reached 15^oC above the desired operating temperature, the tetralin/asphaltene mixture was injected and the run proceeded as before.

Shutdown Procedure

1. Following the 60 minute samples the temperature controller was shut off.

2. The heating jacket was lowered and the reactor cooling fan actuated.
3. The temperature of the system was monitored down to 30°C at which time a gas sample was taken.

Material Balance

The contents which remained in the reactor following a run were accounted for by material balance according to the following procedure:

1. The reactor was depressurized by slowly opening valve V10.
2. Injection cylinder, C1, was disconnected and reweighed. The difference between this weight and the initial cylinder weight was termed "uninjected mixture".
3. The valve handle extenders, rupture disk vent line, gas inlet system and water cooling lines were disconnected from the reactor unit.
4. The head bolts were loosened and removed.
5. The stirrer assembly was carefully lifted out and flushed with acetone into the "wash" flask. The head gasket and baffle were removed and rinsed with acetone into the "wash" flask.
6. Valve V9 was opened and the sample line was flushed with acetone into the "wash" flask.
7. The reactor body was unbolted from its mounting. Its

contents were carefully poured into a tared flask labeled "reactor" and reweighed. Remaining material was rinsed thoroughly with acetone and poured into the "wash" flask.

8. Acetone was stripped from the material in the "wash" flask by rotary evaporation at 70°C. When no further acetone was recovered, the flask was cooled and weighed to complete the material balance.

ANALYTICAL METHODS

Product Fractionation by Solvent Separation Analysis

The conversion of asphaltenes to oils was determined by performing a solvent fractionation on the reaction products. This procedure, outlined in Figure 10, is discussed in detail below.

1. 150 ml of N-pentane was added to each of the weighed samples.
2. The samples were sonicated in an ultrasonic bath for 5 minutes.
3. The sonicated samples were then centrifuged at 2600 rpm for 4 minutes.
4. The liquid was decanted into 500 ml Erlenmeyer flasks and labeled with the appropriate sample time.
5. Steps 1 through 4 were repeated two additional times until the liquid, following sonication and centrifugation, was clear and colorless.
6. After the last wash the tubes were placed in a dessicator and allowed to dry overnight.
7. The dried samples were weighed to the nearest 0.1 milligram to determine the weight of the pentane insolubles.
8. The samples were then extracted, sonicated and centrifuged three times with 150 ml each of toluene. The

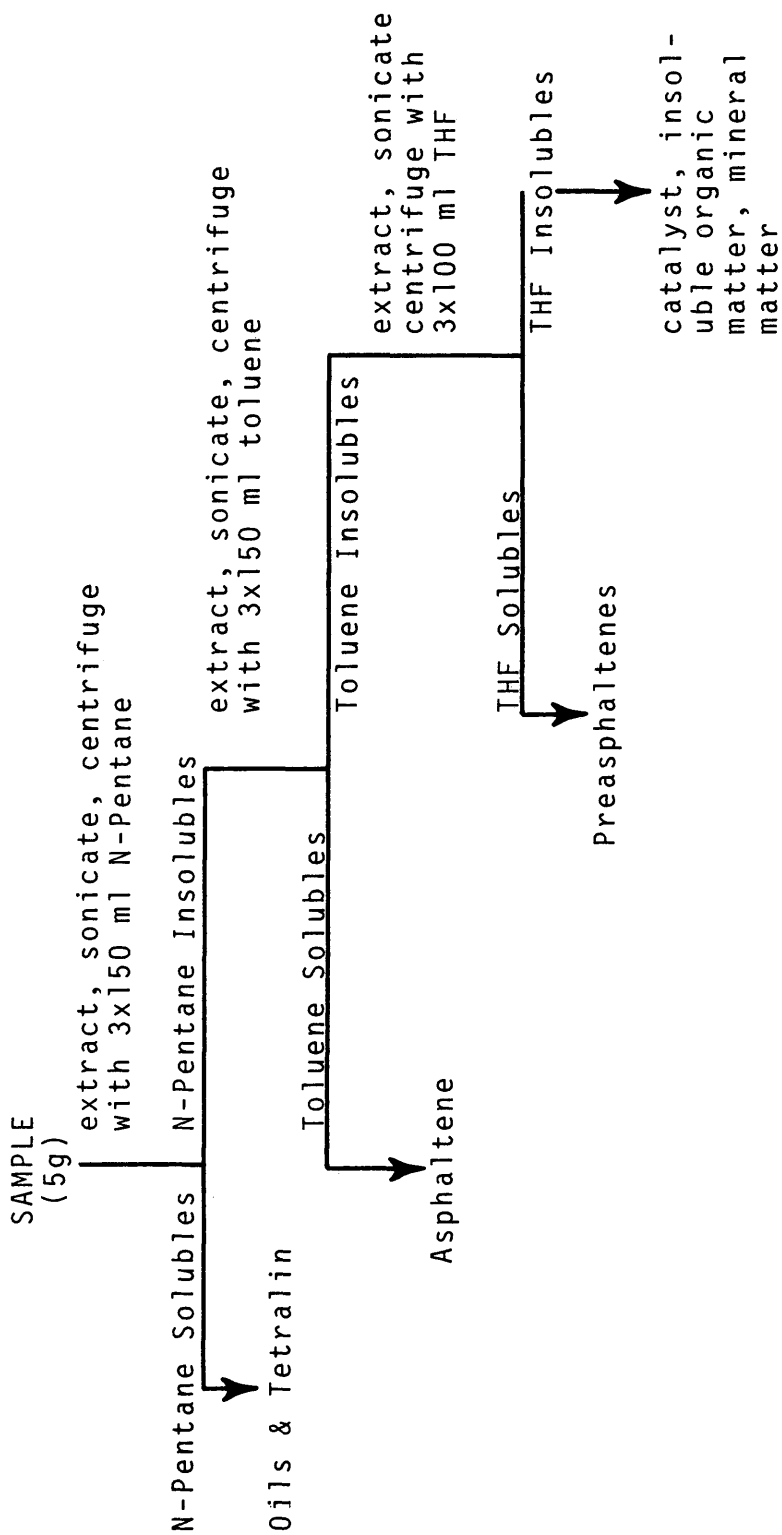


Figure 10. Product Fractionation by Solvent Separation Analysis

extract was decanted into 500 ml flasks which were designated with the appropriate sample time. This procedure was repeated twice more until the extract remained clear and colorless. The tubes were placed into a drying oven at 110°C overnight.

9. The tubes were cooled and weighed yielding toluene insolubles. They were then extracted, sonicated and centrifuged a final three times with 100 ml each of THF. The THF extract was decanted into labeled 500 ml flasks and the tubes oven-dried at 110°C overnight.
10. The samples were cooled and weighed a final time yielding THF insolubles.

The oil, asphaltene and preasphaltene fractions were recovered from the pentane, toluene and THF extracts, respectively, by the following procedure:

11. The pentane was evaporated from the sample by rotary evaporation at 50°C, 1atm. The pentane was recovered and reused. The oils were placed into 20 cc vials labeled with the run number and sample time and stored under refrigeration.
12. The toluene soluble fraction was concentrated to a thick liquor by rotary evaporation at 70°C under vacuum. The concentrate was poured into 4 centrifuge tubes and

each washed, sonicated, centrifuged and decanted with 3x100 ml n-pentane. The precipitated asphaltenes were then placed in a dessicator and allowed to dry.

13. The THF extract was rotary evaporated at 70°C, 1atm. The amount of this fraction was negligible so that recovery and analysis of the THF solubles (preasphaltenes) was not possible.

Product Analysis

Elemental analysis was performed on the SRC-I, the feed asphaltene, all of the isolated product asphaltene samples, and on the recovered catalysts. The carbon, hydrogen and nitrogen analysis was performed on a Carlo-Erba Model 1104 Elemental Analyzer with a Hewlett-Packard 3380A Peak Integrator. Sulfur was determined using a Leco Induction Furnace and Semi-Automatic Titrator. Oxygen was determined by difference in all cases.

The reaction gases were analyzed using a Carle Model 111H Gas Chromatograph with a Hewlett-Packard 3390A Peak Integrator. The chromatograph was equipped with a thermal conductivity detector.

Molecular weight determinations were performed by Huffman Laboratories, Wheat Ridge, Colorado. A four-point vapor pressure osmometry test was used with pyridine as the solvent at 80°C. The results were extrapolated to zero concentration to estimate the number average molecular

weight of each sample.

^1H nmr were recorded on a Varian EM-360A spectrometer. Deuteriochloroform was used as solvent and TMS as the internal standard.

^{13}C CP/MAS nmr were recorded at the Regional NMR Center, Colorado State University, on a Nicolet NT-150 spectrometer. Spectra were referenced to TMS.

Catalyst surface area determinations were made on an AccuSorb 2100E Physical Adsorption Analyzer using the four-point BET gas adsorption method. Pore volumes were measured at Coors Spectro-Chemical Laboratory, Golden, Colorado using mercury porosimetry at 15,000 psia (ASTM C-699).

RESULTS

Results of Experimental Runs

A temperature and pressure profile of a typical run is shown in Figure 11. Heatup to the injection temperature was usually accomplished within 1 hour. Following injection, the reaction temperature quickly stabilized and the desired temperature was attained just prior to taking the 2 minute sample. It was possible to maintain the reaction temperature to within $\pm 1^{\circ}\text{C}$ of the desired temperature by use of the temperature controller and the water cooling system. Pressure was maintained at 1500 ± 40 psig.

A total of 19 experimental runs were made during the course of this study. Of these, the first 5 were shakedown runs, made in order to determine proper system operation and optimum run conditions. Four of the remaining 14 runs were made under conditions of no added catalyst. Each of these runs were made at a different temperature so as to investigate the thermal reactivity of the asphaltenes. Of the 10 remaining runs, 6 involved a catalyst screening study. These runs were made in order to determine the most effective catalyst and catalyst properties for asphaltene hydroprocessing. The final 4 runs involved varying the reaction parameters so as to study their effect on asphaltene hydroprocessing and to attempt to determine an optimum set of run conditions. The results of the 14 runs which

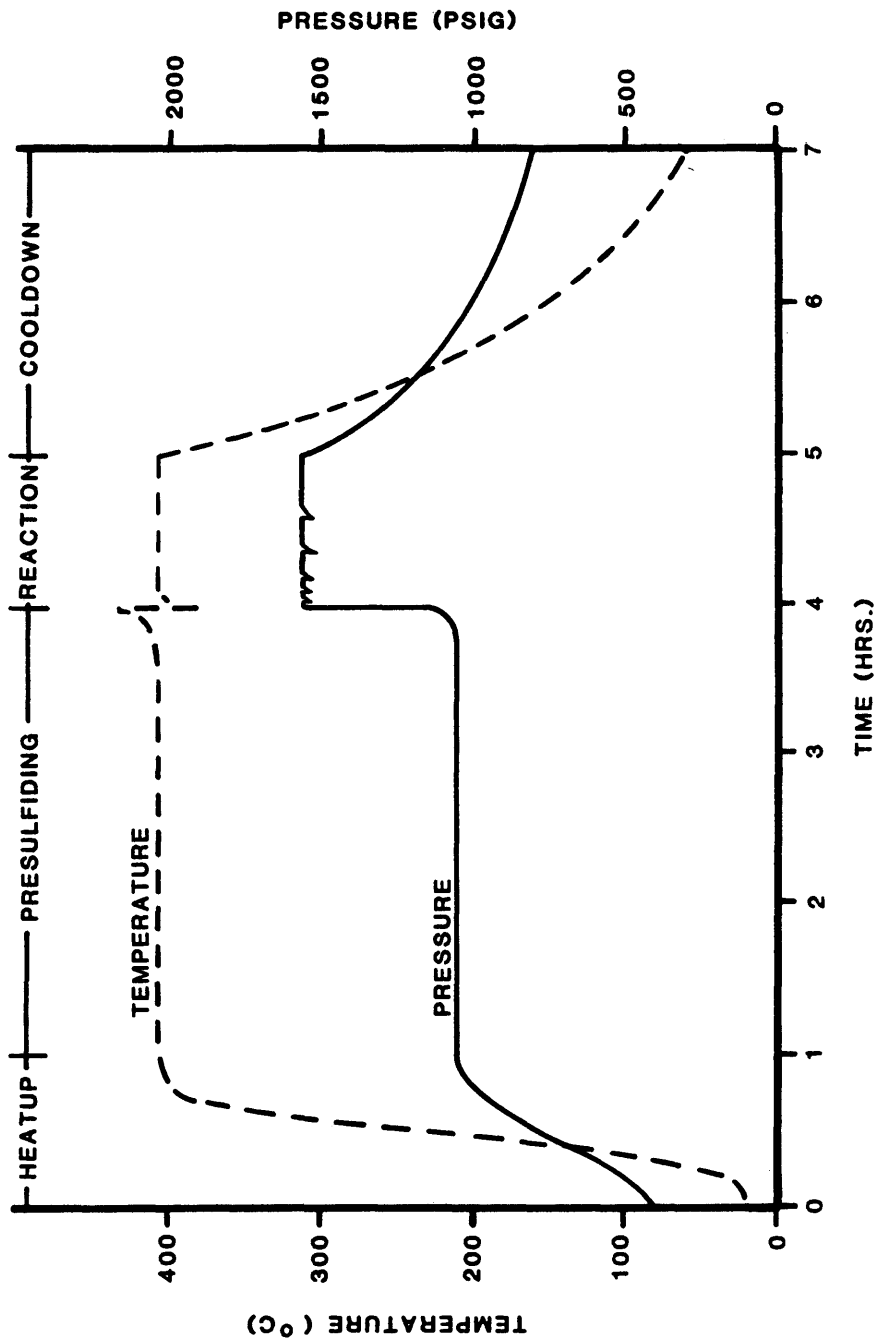


Figure 11. Run Temperature and Pressure Profile.

generated useful data are summarized in Appendix B.

Results of Elemental Analysis

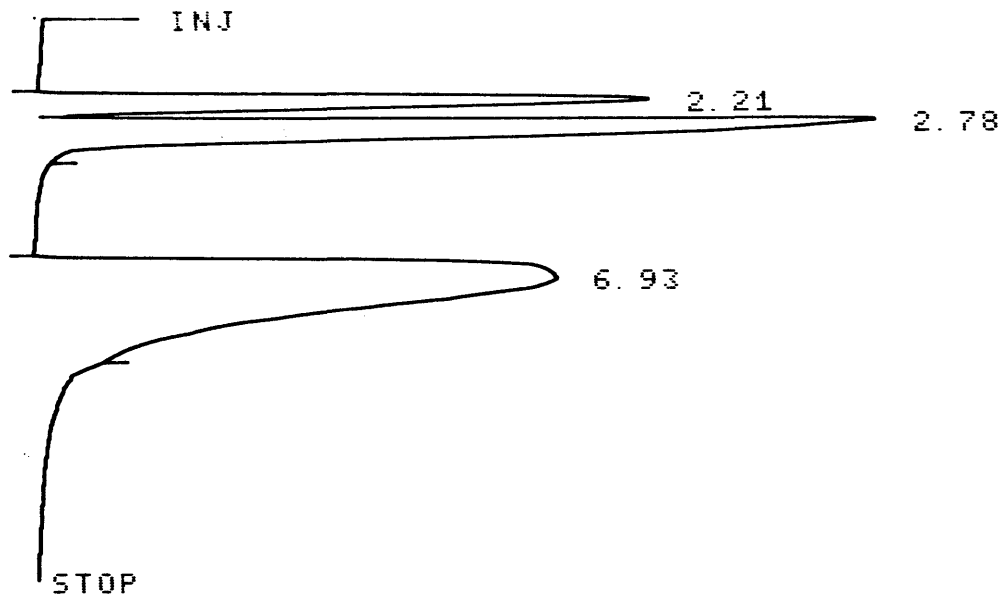
The feed and residual asphaltene samples were subjected to elemental analysis. Carbon, hydrogen and nitrogen were determined using a Carlo-Erba Elemental Analyzer. Sulfur was measured with the Leco Induction furnace system. A typical output from the Carlo-Erba Elemental Analyzer is given in Figure 12. Numerical results of all elemental analyses are tabulated in Appendix B.

Results of Gas Chromatography

Product gases for each experimental run were analyzed by gas chromatography and these results are reported in Appendix B. A typical output of the Carle GC system is given in Figure 13.

Results of ^1H nmr and ^{13}C nmr

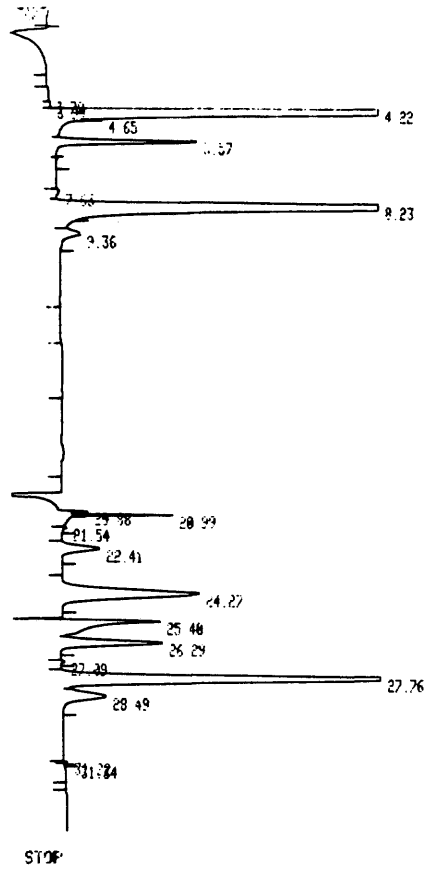
Typical ^1H nmr and ^{13}C nmr spectra for the feed and residual asphaltenes appear later in the Discussion section. A listing of the various hydrogen and carbon types of the feed and residual asphaltenes is given in Appendix C.



RT	TYPE	AREA	AREA %
2.21		135945	9.783
2.78	M	964521	69.41
6.93		289145	20.81

HP 3380A
 DLY OFF STOP 15 REJECT OFF
 MV/M .30 ATTN LOG

Figure 12. Sample Output: C, H, N Analysis.



RUN # 5 NOV/02/92 13:46:30

RT	AREA	TYPE	CAL#	AMOUNT
3.79	12875	PV		0.000
3.99	11023	VH		0.000
4.22	1.7504E+07	SHB	1R	97.100
4.65	5147	DTBB		0.000
5.57	253210	TBP	2R	0.005
7.63	7628	BP	4R	0.002
8.23	3127100	PB	5R	1.551
9.36	42676	BB	6R	0.012
20.99	658100	PV		0.000
20.99	53128	VB		0.000
21.54	1667	BB		0.000
22.41	110610	PB	7R	0.055
24.27	508110	BB	9R	0.244
25.40	522600	BV		0.000
26.29	369950	VB		0.000
27.09	3315	BB		0.000
27.76	1358400	BV	10R	0.842
28.49	183850	VB	11R	0.102
31.22	1331	BP		0.000
31.34	3577	PB		0.000

TOTAL AREA= 2.4819E+07
 MUL FACTOR= 1.0000E+00

Figure 13. Sample Output: Gas Analysis.

DISCUSSION

Material Balance and Gas Production

Material balances based on total recovered mass for each of the 14 reported runs are given in Appendix B. The average material recovery was 98.9%. This verifies both the adequacy of the experimental technique and the assumption of negligible gas production. Gas production, which typically amounted to less than 1% of the reaction product, was limited primarily to methane and ethane for the thermal runs. For the catalytic runs the primary gases produced were methane, ethane and propane.

Tetralin/Asphaltene Interactions

The asphaltenes isolated by the procedure outlined in Figure 9 were completely soluble in tetralin at the 6/1 solvent-to-feed ratio employed in this study. However, treatment of this solution with pentane failed to reprecipitate 30.16% of the original asphaltenes. This fraction, which was reproducible to within 0.35%, represents those asphaltene molecules which associate so strongly with tetralin that n-pentane fails to break apart the association interaction. Table 17 gives an indication of the types of asphaltene molecules which are lost to this solvent interaction effect. The asphaltenes reprecipitated from the 6/1 tetralin-to-asphaltene solution have a lower H/C ratio; are higher in the heteroatoms sulfur, nitrogen and oxygen;

Table 17. Feed Asphaltene Analysis

SAMPLE	FEED ASPHALTENE	REPRECIPITATED FEED ASPHALTENE (reprecipitated from 6/1 tetralin/asphaltene solution)
<u>Ultimate Analysis (wt.%)</u>		
C	86.40	85.53
H	6.48	6.05
N	1.69	1.88
S	1.04	1.09
O (a)	4.38	5.45
H/C	0.900	0.849
<u>Solvent Fractionation Analysis (wt.%)</u>		
Oil	3.83	0.0
Asphaltene	92.70	97.91
Preasphaltene	3.36	1.99
Insolubles	0.11	0.10
<u>Molecular^(b) Weight</u>		
	473.0	554.0
<u>Aromaticity^(c) (f'_a)</u>		
	.719	.747

^aOxygen determined by difference

^bMolecular weights determined by VPO with pyridine at 80°C

^cAromaticity determined by ¹H nmr

have substantially higher molecular weights; and have a higher aromatic fraction (f_a). These results indicate that the lower molecular weight asphaltene molecules, which are less aromatic and contain few heteroatoms, are those which fail to reprecipitate.

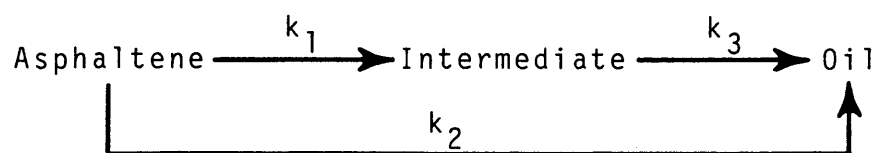
The reprecipitated asphaltenes listed in Table 17 are devoid of oils and have a purity of approximately 98%. These asphaltenes form the basis for comparisons of conversion, heteroatom removal, etc. and are referred to hereafter as "reprecipitated feed asphaltenes". Because of the consistent value of the reprecipitated asphaltene fraction it was decided to use the original asphaltene feedstock and correct the overall conversion by the 30.16% factor. This eliminated the need for reprecipitation of the entire asphaltene feedstock.

Kinetic Model Development

The high pressure gas-forced injection of the concentrated asphaltene/tetralin mixture into the preheated reactor vessel allowed precise definition of zero reaction time, and avoided complications which are consequences of long heat-up periods. However, the data indicate that there exists both a mechanical (pressure) and thermal shock effect associated with the injection. At ambient temperature (21°C) the mechanical shock effect of injection accounts for approximately a 2% conversion to oils as is

shown by the lower curve in Figure 14. The force of injection is great enough to break apart some of the more labile moieties of the asphaltene molecule, thereby resulting in a conversion to oils. The upper curve in Figure 14 shows that at preheat temperatures of 415°C (run temperature 400°C) a thermal shock effect acts in concert with the mechanical shock effect so as to enhance the initial conversion to oils. As a result, the conversion from time zero (injection), to the first sample at 2 minutes is a composite of the mechanical and thermal shock of injection as well as chemical reaction.

The shock effects of injection complicated the kinetic modeling of the system to the extent that simple zero, first or second order models did not give accurate representations of the data. More complex models such as the following series-parallel mechanism:



could not be used because of the lack of detection of an intermediate species.

Since these kinetic models failed to simulate the reaction system, a new approach was tried. The feed asphaltene was conceptually separated into two fractions:

- (1) a reactive asphaltene fraction

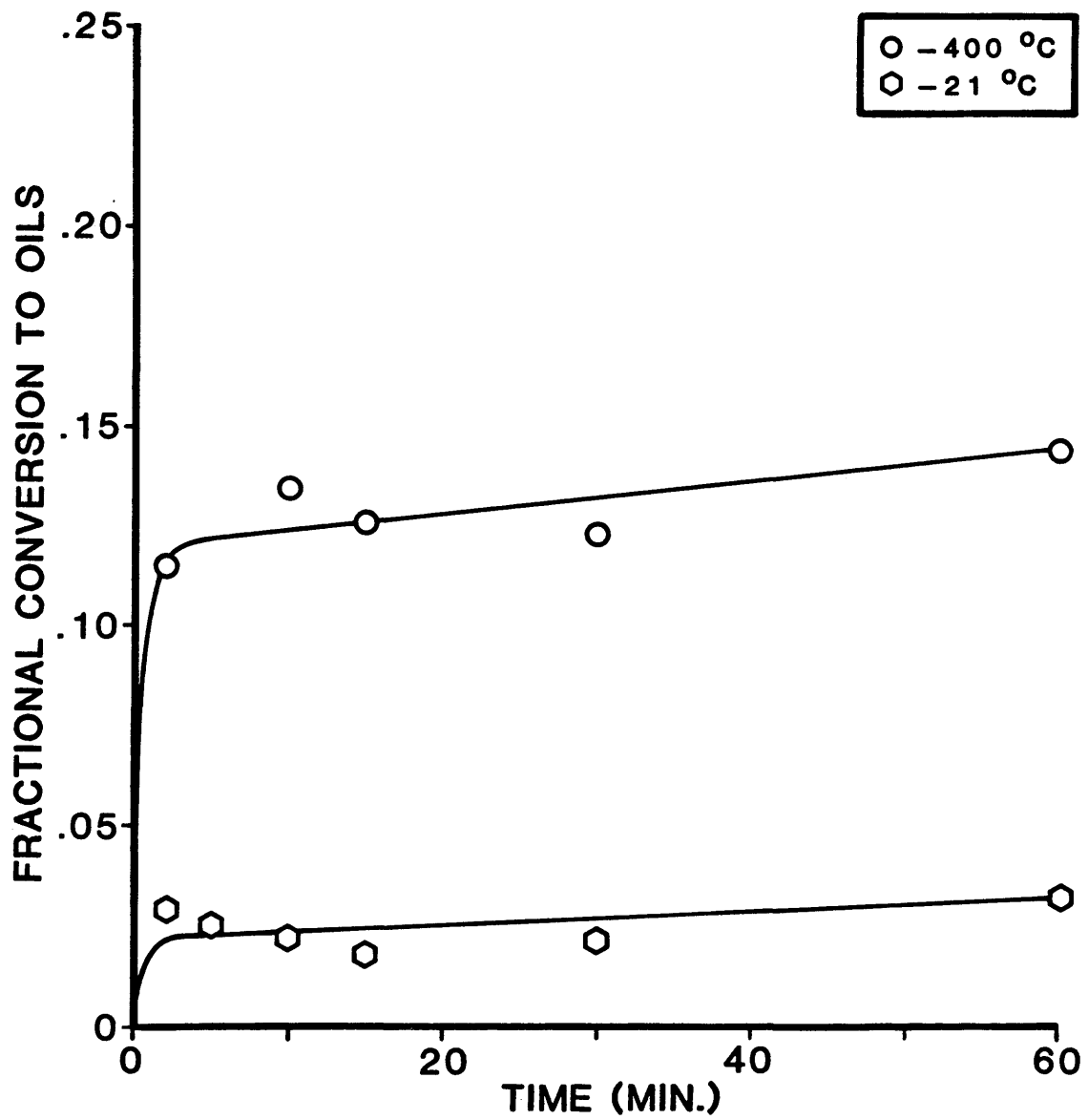


Figure 14. Shock Effects of Injection.

(2) an unreactive asphaltene fraction.

Assuming that the overall rate of asphaltene hydroprocessing is the sum of two first order rate expressions representing these two fractions, the overall rate equation may be written as follows:

$$r_A = \alpha_1 k_1 C_A + \alpha_2 k_2 C_A \quad (1)$$

where: r_A = rate of asphaltene production
 α_1 = fraction of reactive asphaltene
 k_1 = rate constant associated with reactive asphaltene hydroprocessing
 α_2 = fraction of unreactive asphaltene
 k_2 = rate constant associated with unreactive asphaltene hydroprocessing
 C_A = molar concentration of asphaltene

For a batch reactor the material balance is:

$$\frac{dN_A}{dt} = -r_A V \quad (2)$$

where: N_A = moles of asphaltene

Substituting the rate equation into the material balance the following equation results:

$$\frac{-dN_A}{dt} = \alpha_1 k_1 N_A + \alpha_2 k_2 N_A \quad (3)$$

The moles of asphaltene at any time can be rewritten as:

$$N_A = N_{A_0} (0.7 - X_A) \quad (4)$$

where: N_{A_0} = moles of feed asphaltene

X_A = fractional conversion of asphaltene

The factor 0.7 arises because only 70% of the feed asphaltene is recoverable. Substituting equation (4) into equation (3) the rate equation becomes:

$$\frac{dX_A}{dt} = \alpha_1 k_1 (.7 - X_A) + \alpha_2 k_2 (.7 - X_A) \quad (5)$$

Upon integration of (5) and substitution of the limits:

$$X_A(0) = 0$$

$$X_A(t) = X_A$$

the integrated form of the rate equation is obtained:

$$\frac{0.7 - X_A}{0.7} = \alpha_1 e^{-k_1 t} + \alpha_2 e^{-k_2 t} \quad (6)$$

Equation (6) contains 4 unknown parameters, α_1 , k_1 , α_2 and k_2 , and can be solved by using the Peel-Back Method of kinetic analysis.

The Peel-Back Method assumes that given a response function written in the form of equation (6), that all faster reactions are completed at long times. This allows the slow reactions to be uncoupled from the fast reactions and each analyzed separately. For this method to be valid however, there must be a distinct break in the curve when the response function is plotted vs. time on a semi-logarithmic graph. Figures 15 and 16 from run 11 illustrate

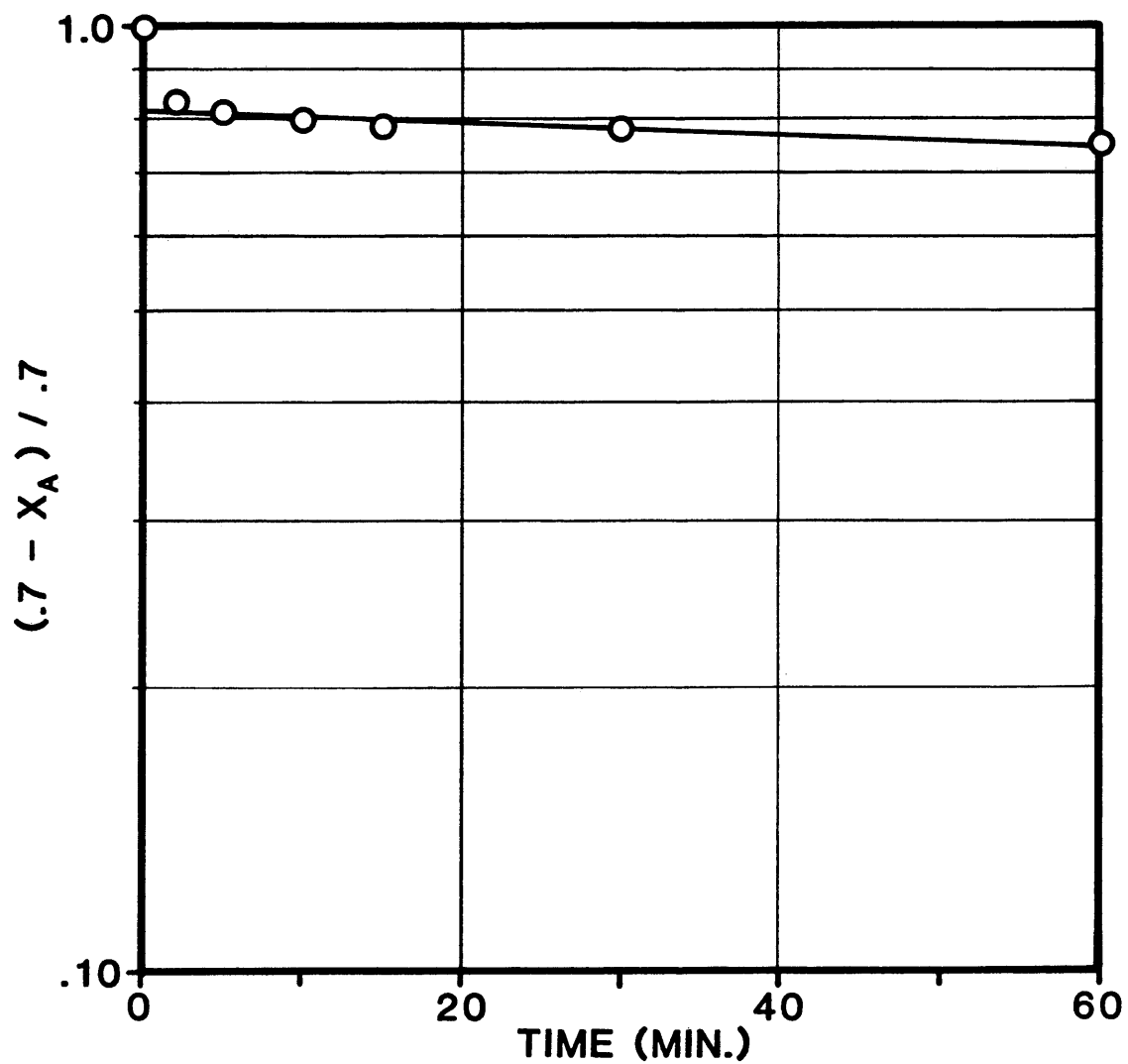


Figure 15. Peel-Back Method Analysis; Overall Reaction. Points represent overall reaction data. The line represents the isolated reaction of the unreactive asphaltene fraction.

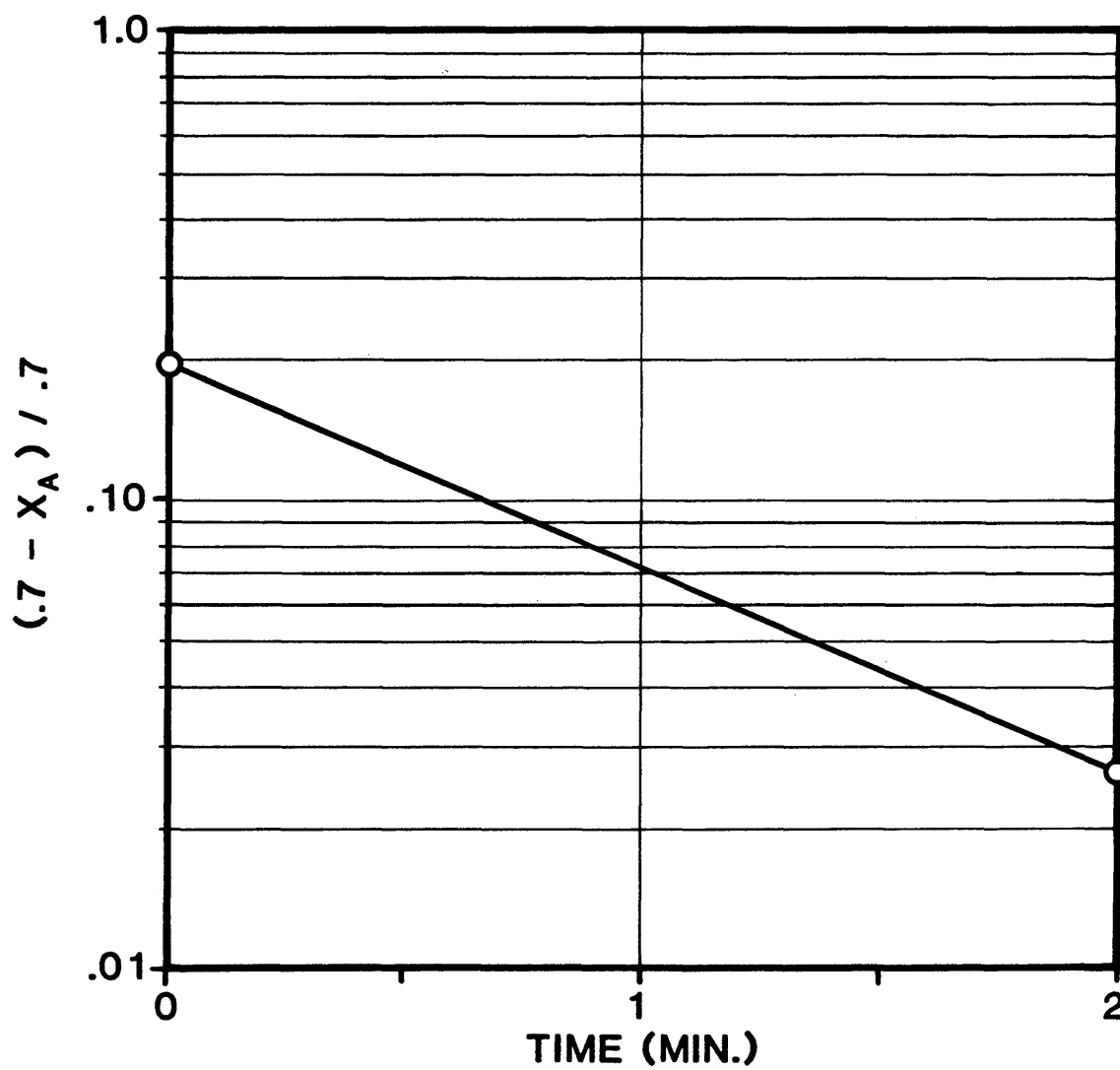


Figure 16. Peel-Back Method Analysis: Isolated Reaction of The Reactive Asphaltene Fraction.

the method. The response function $(0.7 - X_A)/0.7$ is plotted on the logarithmic ordinate while time is plotted along the abscissa. The data show that a definite break occurs at the 2 minute point. This indicates that the fast reaction, which involves the reactive asphaltene fraction, is complete by 2 minutes. This portion of the reaction accounts for the conversion by both mechanical and thermal shock effects as well as by chemical reaction. At the 2 minute point and beyond the data points are linear and involve chemical reaction of the unreactive asphaltene fraction only. By drawing a best-fit linear regression line through the data points at 2 through 60 minutes and extending this line to the zero time axis, the parameter α_2 , the fraction of unreactive asphaltene at time zero, is obtained. Since the response function has been normalized to 1.0, the fraction of reactive asphaltene at time zero is simply:

$$\alpha_1 = 1 - \alpha_2$$

The rate constant, k_2 , may now be determined. For a first-order reaction, the half-life is given by the equation:

$$t_{\frac{1}{2}} = \frac{\ln 2}{k}$$

Upon rearranging and solving for k the equation becomes:

$$k = \frac{\ln 2}{t_{\frac{1}{2}}}$$

By determining the time at which the concentration of the asphaltenes become half of their initial value, the rate constant may be determined. Because the rate of conversion of the unreactive asphaltenes was extremely slow, the half-life had to be extrapolated by using the equation of the best-fit line through the data points of the slow reaction.

The rate constant for the fast reaction, k_1 , is determined by subtracting the response function of the slow reaction from the overall response function. This procedure gives the response function for the fast reaction and is plotted in Figure 16 for run 11. The reactive asphaltene rate constant is then calculated by the same procedure as for the unreactive asphaltene fraction. Sample calculations using this procedure for Run 11 are given in Appendix E.

The rate constants k_1 and k_2 determined by this method represent a first cut to the optimized values of k_1 and k_2 . In order to optimize the kinetic model to the data, the values of k_1 and k_2 were systematically varied until the sum of squared residuals (SSR) were minimized. Table 18 and Figure 17 compare the values of k_1 and k_2 for Run 11 as determined directly from the Peel-Back method, and as determined by minimizing the sum of squared residuals. As expected, the optimized rate constant parameters

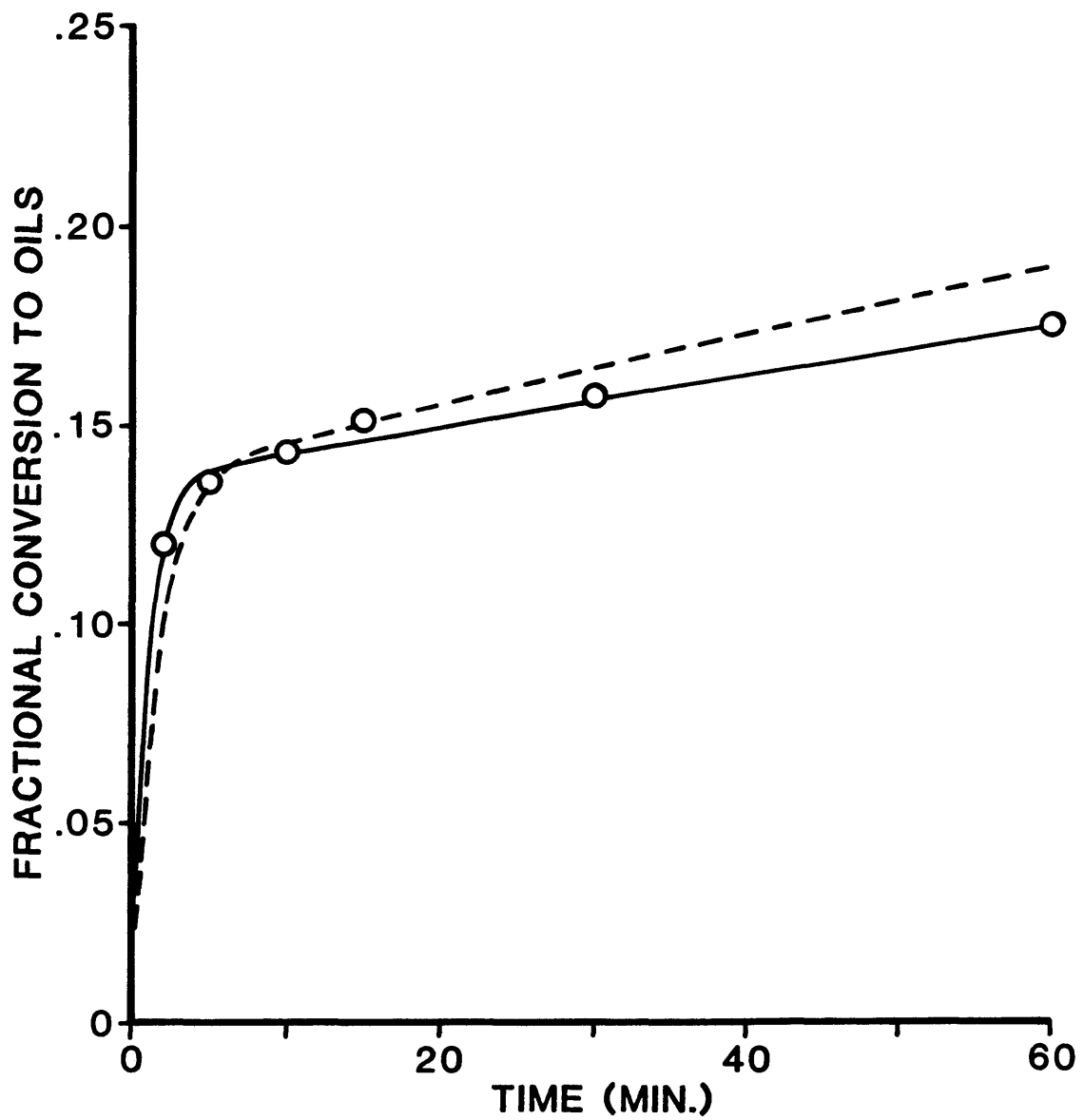


Figure 17. Comparison of Kinetic Rate Constants for run 11. Dashed line obtained directly from Peel-Back Method. Solid line obtained by minimizing SSR of parameters.

give a better fit throughout the entire range than does the directly determined rate constants.

Table 18. Comparison of Kinetic Rate Constants for Run 11.

	<u>Determined Directly from Peel-Back Method</u>	<u>Determined by Minimizing SSR</u>
k_1 (min. ⁻¹)	0.601	1.01
k_2 (min. ⁻¹)	1.63×10^{-3}	1.18×10^{-3}

Conversion Analysis

Conversion results for each of the 4 phases of study are discussed in this section. Each of the runs were modeled according to the Peel-Back Method of kinetic analysis. Optimized values of the rate constants are reported.

Phase I - Thermal Hydroprocessing

Values of α_1 , α_2 , k_1 and k_2 are reported in Table 19 for the thermal runs. The parameters α_1 and α_2 are the fractions of reactive and unreactive asphaltenes respectively. The rate constant k_1 represents that portion of the overall reaction where the reactive asphaltene fraction is converted to oils. This occurs within the first 2 minutes following injection. Beyond 2 minutes only the unreactive asphaltene fraction remains and the rate constant k_2 applies.

Table 19. Thermal Hydroprocessing Rate Parameters.

Run No.	Temp ($^{\circ}\text{C}$)	α_1	α_2	k_1 (min. $^{-1}$)	k_2 (min. $^{-1}$)
6	21	.032	.968	1.80	1.70×10^{-4}
7	355	.010	.900	1.12	3.60×10^{-4}
8	375	.010	.900	0.88	4.40×10^{-4}
9	400	.171	.829	1.53	7.20×10^{-4}

Figure 18 shows the fit of the kinetic model to the data at each of the thermal processing conditions. In each case the conversion to oils is extremely rapid within the first 2 minutes. Beyond 2 minutes, the conversion slowly increases over the remaining period of the reaction. The difference between the conversion at 355°C and 375°C is small, compared to the difference between 375° and 400°C . This indicates that temperatures in the range of 375°C and below are too mild to effect any significant changes upon the asphaltene molecule, and thus represents a lower limit to thermal asphaltene hydroprocessing.

The rate constant k_2 represents the chemical reaction of the unreactive asphaltenes and shows a noticeable temperature dependence. Figure 19 illustrates this dependence with a plot of $\ln k_2$ vs. $1/T$. As can be seen the fit of the points to the linear regression line is not as good as would be expected for a chemically pure compound. This may be due to random sampling errors and construction of error limits on the points would verify the linearity of the

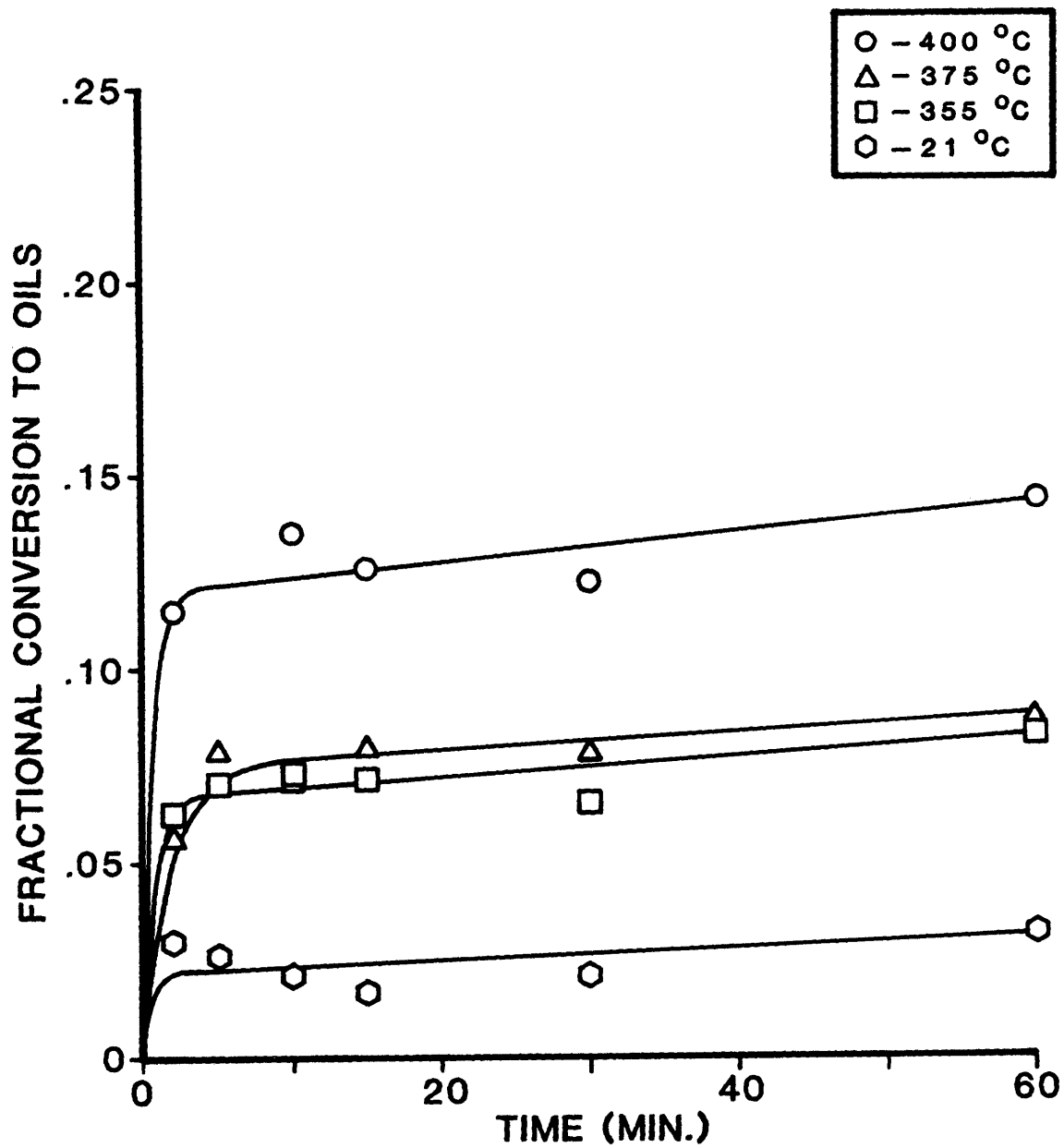


Figure 18. Conversion Results of Thermal Hydroprocessing of Coal-Derived Asphaltenes.

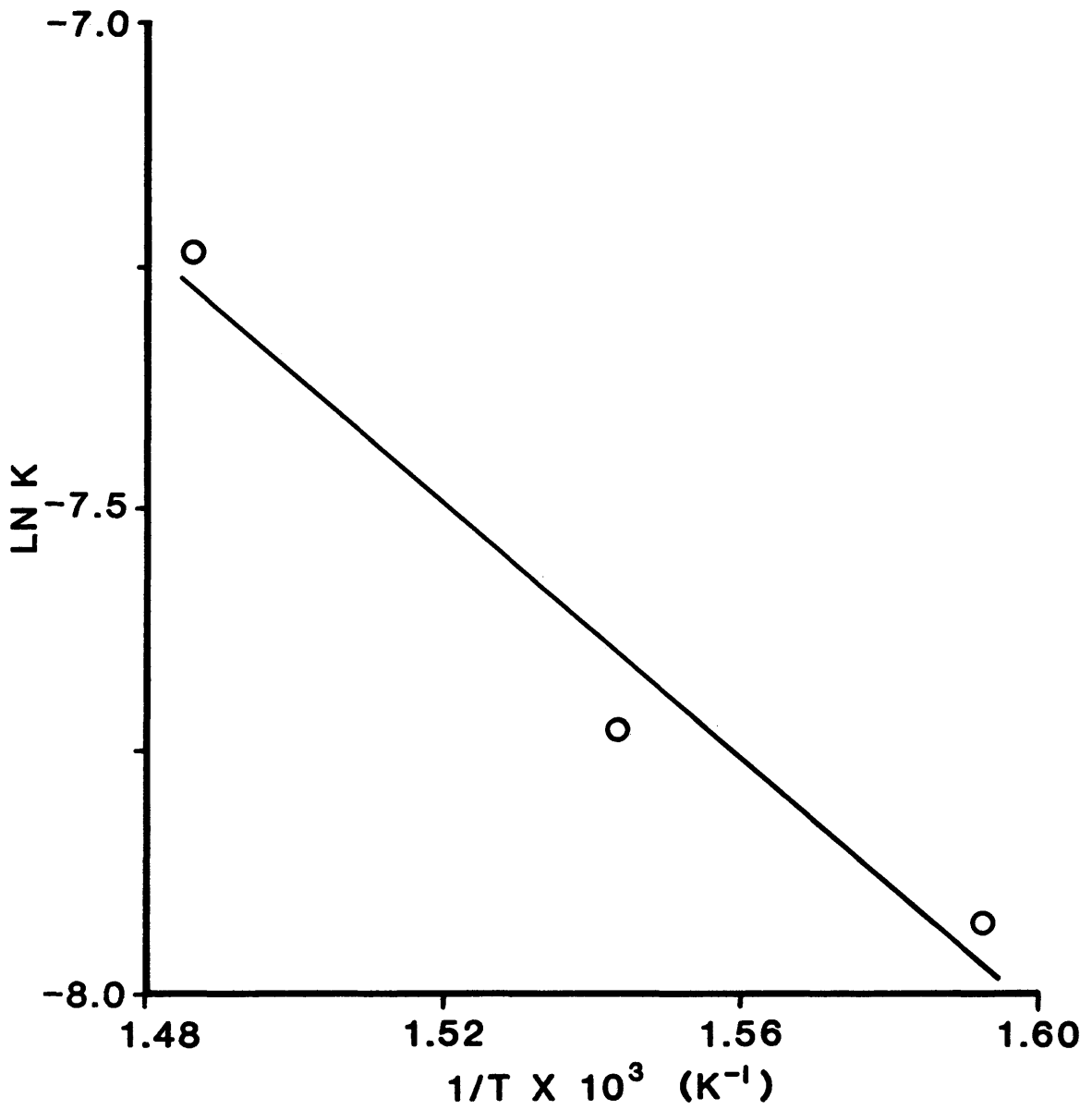


Figure 19. Arrhenius Plot of Thermal Hydroprocessing Results.

results. However, it is also possible that the points do not fit a straight line because asphaltenes are comprised of a large number of chemically heterogeneous compounds whose activation energies for the various hydroprocessing reactions differ considerably.

Assuming that the Arrhenius equation holds reasonably well over a narrow range of temperature, it was applied to the results at 375^o and 400^oC. For this temperature range an activation energy of 17.1 kcal·gmole⁻¹ was calculated. Although this value is lower than normal for a homogeneous reaction, it again indicates that the thermal processing conditions are so mild that only the most labile moieties of the asphaltene molecule are reacting to any significant extent.

Phase II - Pyrite and H₂S Catalytic Hydroprocessing

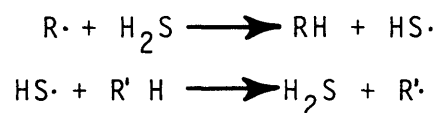
It has been known for some time that the presence of pyrite plays a significant catalytic role in the conversion of coal to liquid products. The general belief is that pyrite is rapidly reduced under coal liquefaction conditions to pyrrhotite, a non-stoichiometric iron sulfide compound. The reaction may be written as follows:



This suggests that pyrrhotite is the active catalyst and functions by catalyzing the reaction which transforms gaseous molecular hydrogen to donor hydrogen in the solvent

[54]. However, because of the low surface area of pyrite ($<2\text{m}^2\cdot\text{g}^{-1}$) it is difficult to see how it can function efficiently as a hydrogenation catalyst.

An alternative interpretation of the catalytic activity of pyrite is that the active catalyst is actually H_2S which is produced in situ by the reduction of pyrite. It has been established that H_2S is an effective hydrogen transfer catalyst for free radical reactions [55]. The catalysis occurs by replacing the slow hydrogen transfer step with two faster steps:



Since the early stages of coal liquefaction are thought to proceed via free radicals, the above mechanism may well be in effect.

A recent study by Baldwin and Vinciguerra [56] was designed to test the catalytic activities of pyrite, H_2S , and pyrite/ H_2S mixtures towards coal liquefaction. Their results, Figures 20 and 21, show that with respect to conversion to THF soluble materials, both pyrite and H_2S show catalytic properties at the 10 minute reaction time. At the 60 minute reaction time H_2S and pyrite/ H_2S mixtures show a distinct increase in conversion over the pure pyrite additive.

With respect to conversion to oils, however, H_2S

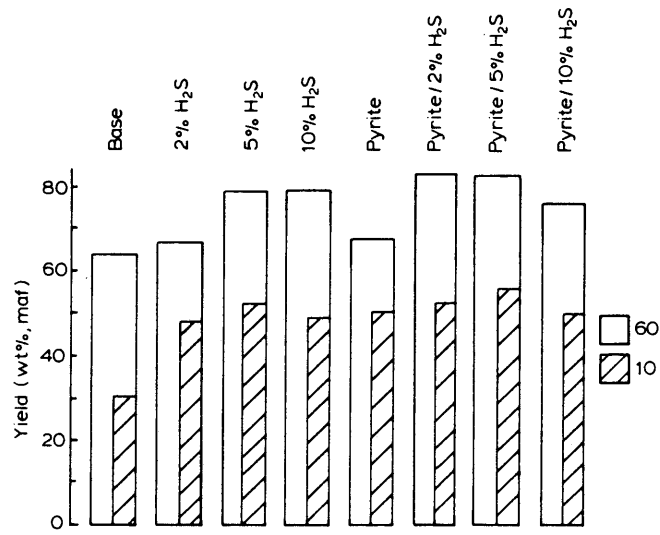


Figure 20 [56]. Conversion to THF-Soluble Materials.

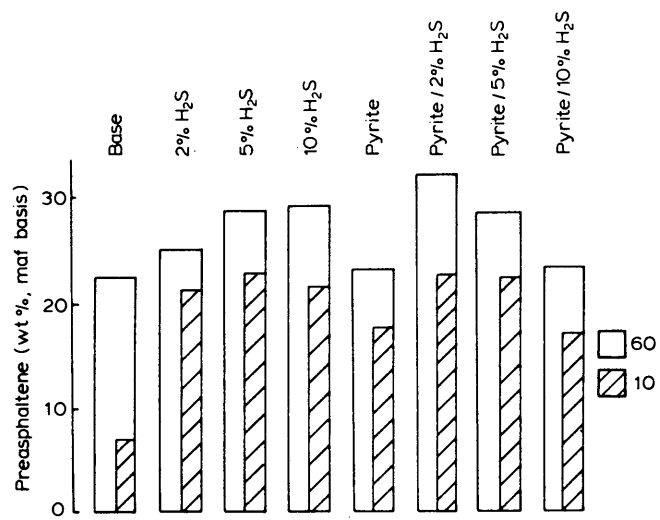


Figure 21 [56]. Oil Yield

alone showed a slight inhibiting effect at the 10 minute reaction time and little or no positive catalytic effect at the longer 60 minute reaction time. Pyrite, on the other hand, showed a definite catalytic effect at 10 minutes and a negligible effect at 60 minutes.

These results strongly indicate that both pyrite and H₂S are catalytically effective in enhancing the primary reactions of coal liquefaction. However, only pyrite or pyrite/H₂S mixtures are able to perform as catalysts for the more difficult, secondary oil-forming reactions.

The results of the present study on asphaltene hydro-processing confirms the above conclusions. Figure 22 shows conversion results using pyrite and H₂S separately as catalysts. The data was modeled by the Peel-Back method and the kinetic parameters are listed in Table 20. The two catalytic runs are referenced to the thermal run made under the same reaction conditions (400⁰C, 1500 psig).

Table 20. Pyrite and H₂S Rate Parameters

<u>RUN NO.</u>	<u>CATALYST</u>	<u>1</u>	<u>2</u>	<u>k₁(min.⁻¹)</u>	<u>k₂(min.⁻¹)</u>
10	H ₂ S	.151	.849	1.07	1.41x10 ⁻³
11	Pyrite	.195	.805	1.01	1.18x10 ⁻³

The results show that at short reaction times (<30

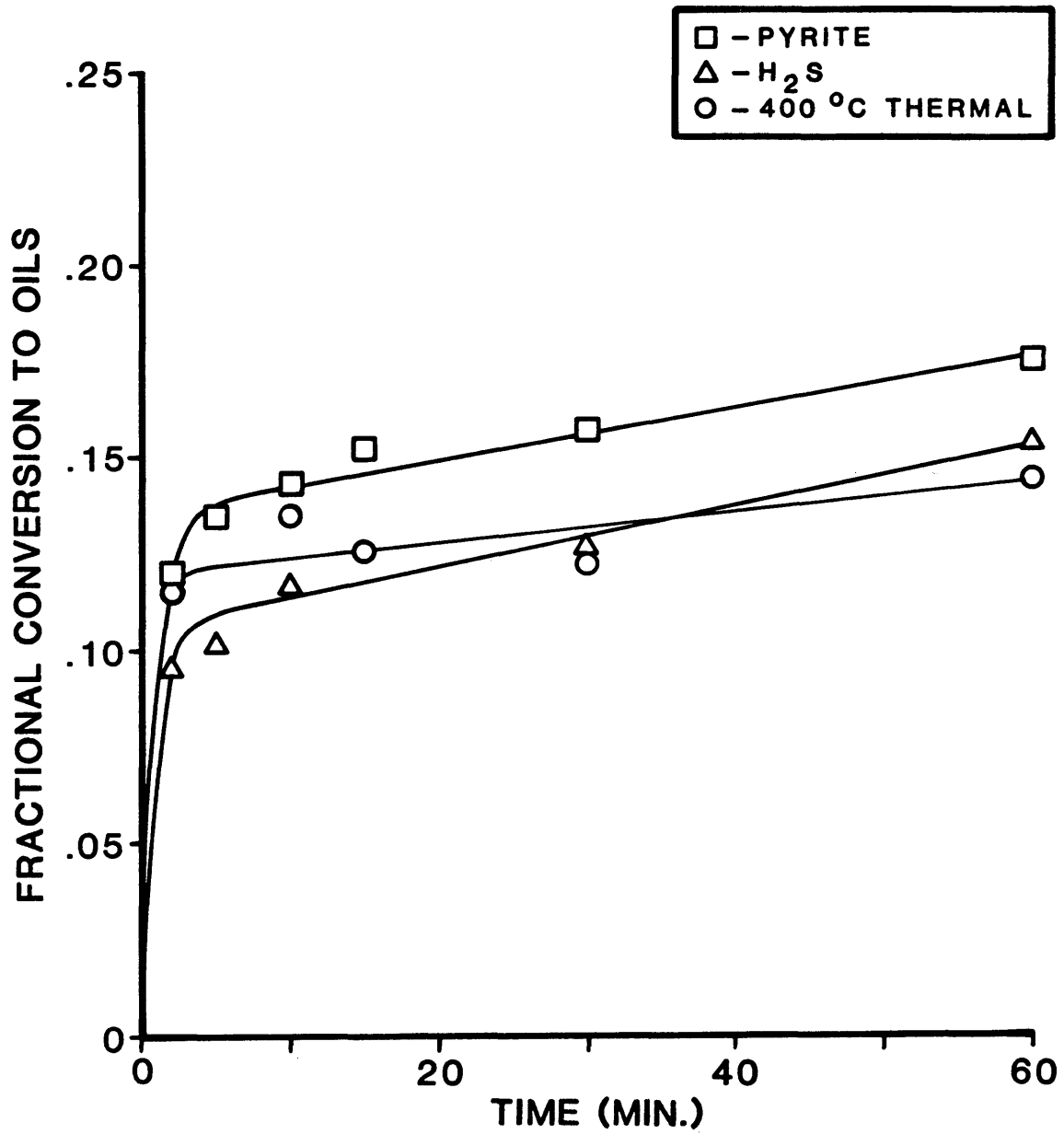


Figure 22. Conversion Results Using Pyrite and H₂S Additives.

minutes), the addition of H_2S actually retards the production of oils. At reaction times greater than 30 minutes, H_2S shows a slightly positive catalytic effect. For the run using pyrite as a catalyst, however, a positive catalytic effect is observed throughout the run indicating that, at least for asphaltene hydroprocessing, pyrite (or more accurately the pyrrhotite/ H_2S mixture) is an active catalyst while H_2S alone is, for the most part, inactive.

Phase III - Commercial Catalyst Hydroprocessing

The third phase of this study was designed to investigate the effects of various commercial catalysts on the hydroprocessing reactions of coal-derived asphaltenes. The physical and chemical properties of the four catalysts chosen for comparative study are listed in Table 12. All of the catalysts used in this study were fresh and ground to 0.074 mm. The choice of fresh catalyst was based on the assumption that comparison of the initial activity of the fresh catalyst is a good indicator of its relative steady-state activity. To test whether this assumption is actually valid, long term experimental runs would have to be made. This cannot be accomplished in the present study because of time and feedstock limitations.

The runs were carried out under identical conditions of catalyst pretreatment, time, temperature and pressure in order to allow direct analytical comparisons of catalyst

performance. Catalyst performance includes degree of conversion, relative activity of the recovered catalysts, and residual asphaltene quality. The first two of these factors are discussed here. Residual asphaltene quality will be discussed in a later section on the elemental and structural analysis of residual asphaltenes.

Reduced data for the catalytic runs are tabulated in Appendix B. Conversion results along with the corresponding kinetic models are shown in Figure 23. Also shown in Figure 23 are the results for the thermal run made under the same reaction conditions. The rate parameters for the four catalytic runs are listed in Table 21.

As is evidenced from Figure 23, the addition of a catalyst results in a greatly enhanced conversion to oils throughout the entire reaction period. The catalytic conversion at 60 minutes varies from 1.8 (HDN-30) to 2.1 (HDS-20A) times the corresponding 60 minute thermal conversion.

The HDS-20A (Co-Mo/ Al_2O_3) catalyst resulted in the greatest oil yield, followed in decreasing order by HDS-9A (Ni-Mo/ Al_2O_3), Ni-4303E (Ni-W/ Al_2O_3), and HDN-30 (Ni-Mo/ Al_2O_3). With the exception of the HDS-9A catalyst, the first 2 minutes of reaction resulted in a conversion to oils of $15.74 \pm 0.38\%$. This represents between 50 to 60 percent of the total conversion for the entire run. The remaining 40 to 50 percent of the conversion takes place

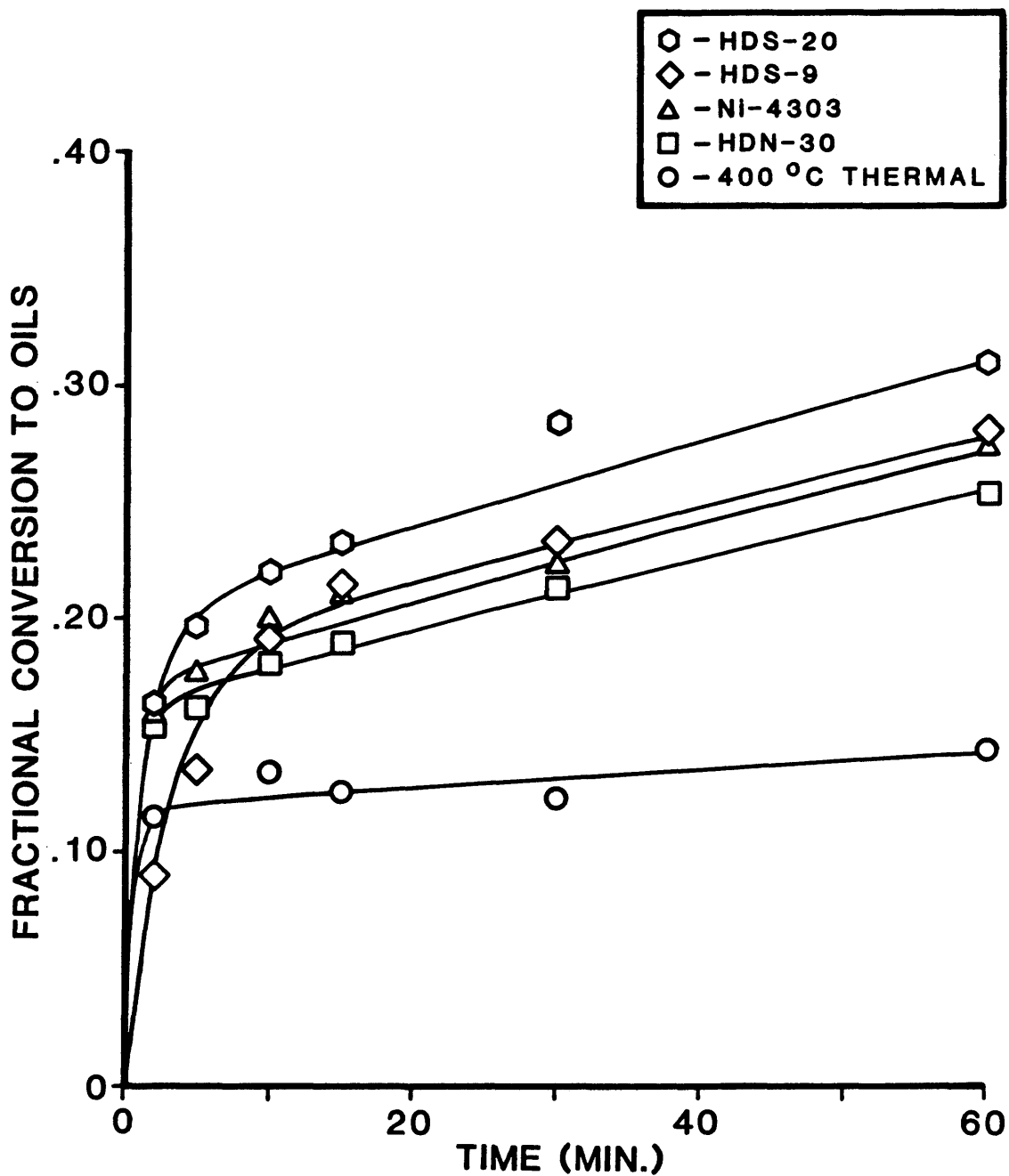


Figure 23. Conversion Results Using Commercial Hydroprocessing Catalysts.

Table 21. Commercial Catalyst
Hydroprocessing Rate Parameters

<u>RUN NO.</u>	<u>CATALYST</u>	<u>α_1</u>	<u>α_2</u>	<u>$k_1(\text{min.}^{-1})$</u>	<u>$k_2(\text{min.}^{-1})$</u>
12	HDS-20A	.287	.713	0.70	4.12×10^{-3}
13	HDS-9A	.261	.739	0.31	3.49×10^{-3}
14	HDN-30	.226	.774	1.50	3.20×10^{-3}
15	Ni-4303E	.245	.755	1.24	3.63×10^{-3}

during the subsequent 58 minutes of reaction. This latter part of the reaction appears linear due to the small values of the rate constant, k_2 .

The HDS-9A catalyst displays a much more gradual increase in the initial conversion than that observed for the other three catalysts. However, beyond the 15 minute point its behavior is similar. This indicates that with respect to the other catalysts, the HDS-9 catalyst has a lower initial rate of asphaltene conversion. Since the type of metals and the metal loading used are similar to the other catalysts it is believed that this effect is due to the physical properties of the catalyst support. In particular, the pore size distribution or the degree of metal dispersion may cause such an effect, however, further study would be required to determine the exact nature of this phenomenon.

The catalysts used in this study differed from one

another with respect to several chemical and physical properties. These include metal composition, percent metal loading, support surface area, and pore size distribution. Direct comparison of results of each catalyst is therefore difficult. However, generalizations from this work, and that of others, allows some insight into the properties of an effective asphaltene hydroprocessing catalyst.

The Co-Mo/ Al_2O_3 catalyst (HDS-20A) appeared to be more effective for liquefaction of asphaltenes than either of the Ni-Mo/ Al_2O_3 catalysts or the Ni-W/ Al_2O_3 catalyst. Since the principle mechanism for liquefaction of the initial asphaltenes is hydrogenolysis of the weaker carbon-heteroatom bonds, these results imply that the Co-Mo/ Al_2O_3 catalyst has a greater hydrogenolysis activity than either of the other catalysts. This result is consistent with work of Satterfield and Cocchetto [57] where the Co-Mo/ Al_2O_3 catalyst appeared to have a greater hydrogenolysis activity, while the Ni-Mo/ Al_2O_3 catalyst appeared to have a greater hydrogenation-dehydrogenation activity.

The surface area and pore-size distribution have decisive effects on asphaltene hydroprocessing. In order for the catalyst to remain active the pores must remain free of coke deposits so that the reactant molecules can diffuse to the active sites. For large molecules such as asphaltenes, a large macropore distribution is essential for

effective access to the interior of the pores. Pore size distributions of the macropores ($>100 \text{ \AA}$) for the fresh catalysts are listed in Appendix D.

Deactivation of the catalysts is dominated by coking and heteroatom poisoning. Table 22 lists properties of the catalysts recovered after 60 minutes of reaction. In each case the carbon buildup is approximately 7-8 percent, and the H/C ratio 1.3-1.8. The surface areas decrease from 11-48 percent of their original values. Although a rectilinear correlation between surface carbon and hydrogen concentrations with the loss of total catalyst surface area is not obtained, there are indications that the amount of carbon and hydrogen detected has a detrimental effect. The detection of nitrogen indicates the presence of nitrogen containing compounds adsorbed onto the catalyst. Such compounds have been shown to lower the catalyst activity [58]. Sulfur and oxygen compounds have not yet been distinguished from the sulfur in MoS_x or the oxygen in Al_2O_3 . However, it is reasonable to assume that adsorption of some heterocyclic compounds also contributes to lowering the catalyst activity.

Of the catalysts tested, the Ni-W/ Al_2O_3 catalyst had the largest amount of carbon deposition yet the least surface area reduction. This apparent anomaly may be due to the large average pore diameter of the Ni-W/ Al_2O_3 cata-

Table 22. Recovered Catalyst Properties

<u>CATALYST</u>	<u>INITIAL</u> <u>SURFACE AREA (m²/g)</u>	<u>RECOVERED_2</u> <u>SURFACE AREA (m²/g)</u>	<u>C (wt.%)</u>	<u>H (wt.%)</u>	<u>H/C</u>	<u>N (wt.%)</u>
HDS-20A	230	---	----	----	----	----
HDS-9A	200	134	7.66	1.16	1.82	0.54
HDN-30	160	84	7.27	1.08	1.78	0.60
Ni-4303E	152	135	8.33	0.94	1.35	0.26

lyst. With a large number of macropores, coking may occur and not block the pores completely. This leaves the rest of the pore active for reaction. The same amount of coke deposited on the entrance of a micropore, however, would completely isolate that pore from the reactants and thus remove the micropore surface from reaction. If the micropore surface area constitutes a large fraction of the total surface area, carbon deposition will have a significant effect. Therefore, it would seem that for asphaltene hydroprocessing, having a catalyst with a large pore diameter is more important than having one with a large surface area.

Phase IV - Effects of Processing Conditions

The final phase of this work was designed to determine the effects which some of the more important process conditions had upon asphaltene hydroprocessing. The following four effects were studied:

1. Catalyst Presulfiding
2. H₂S Purge from Presulfided Catalyst
3. Extended Time Run (3 Hours) and Reproducibility Test
4. Extended Time Run (3 Hours) at 425⁰C.

Catalyst Presulfiding

Run 16 was undertaken in order to study the effect of catalyst presulfiding. The HDS-9A (Ni-Mo/Al₂O₃) catalyst

was used. All reaction conditions and procedures remained the same as previously described with the exception that the catalyst was added in its oxide state and not presulfided prior to reaction. Figure 24 shows the comparison between the activities of the presulfided HDS-9A catalyst (upper curve) and the non-presulfided HDS-9A catalyst (lower curve). The substantial reduction in conversion for the non-presulfided catalyst run is likely due to overreduction of the metal oxide to the base metal. This effect, commonly known as sintering, renders the catalyst inactive. The 60 minute conversion for the non-sulfided catalyst is less than 4 percent greater than for the 400°C thermal run. It is evident, therefore, that proper presulfiding of these hydroprocessing catalysts is necessary in order to achieve their maximum activity.

H₂S Purge From Presulfided Catalyst

Run 17 was made using the HDN-30 (Ni-Mo/Al₂O₃) catalyst. The run conditions and catalyst pretreatment were identical to those previously described, with the exception that following the 3 hour presulfiding operation, the system was purged of H₂S by a flow of pure hydrogen gas at 20 cc/min. for one hour. This was intended to deplete the excess H₂S in the gas phase and enhance the hydrogen concentration. The results, depicted in Figure 25, show that the H₂S purge resulted in a decreased conversion

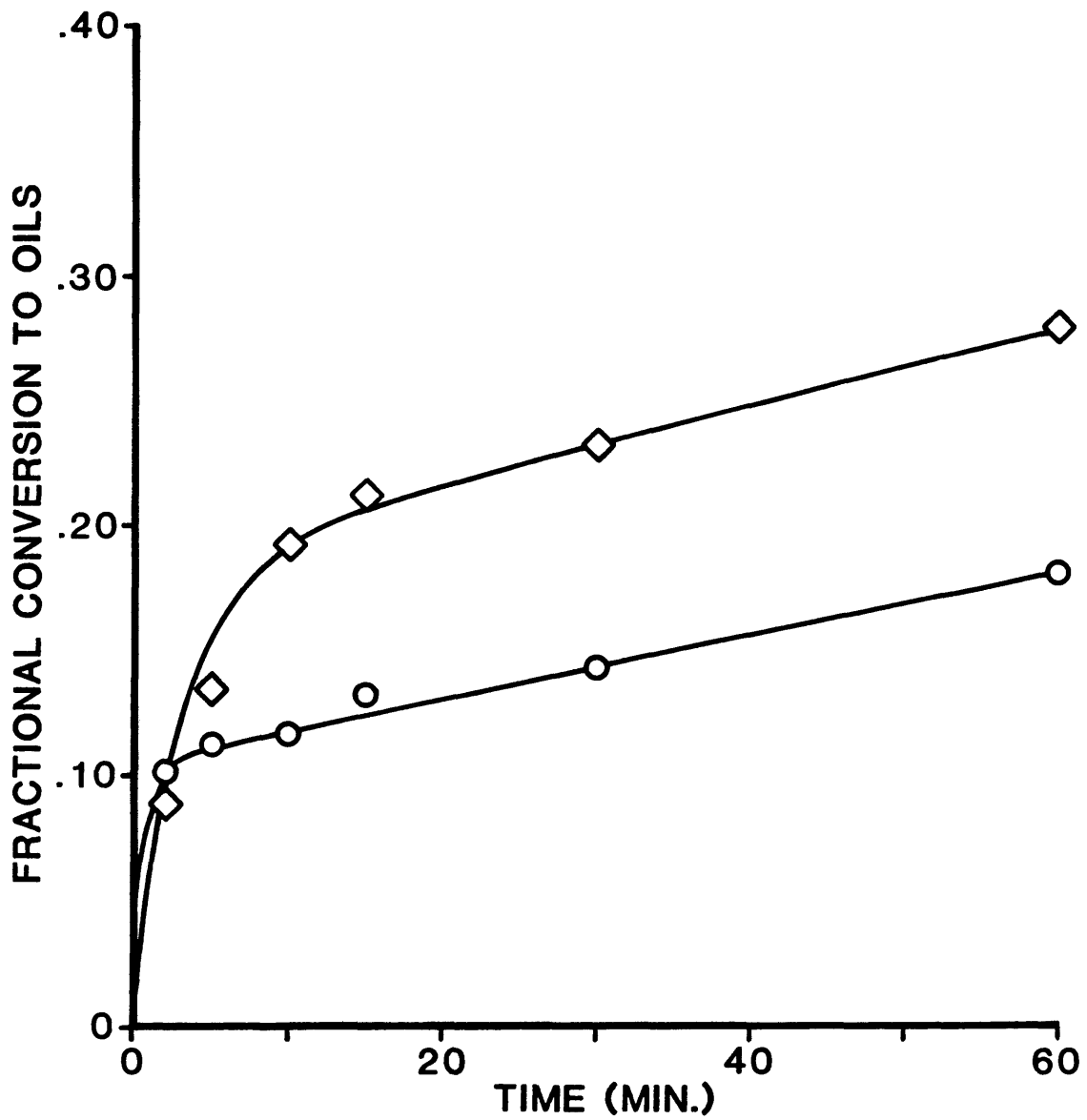


Figure 24. Effect of Presulfiding HDS-9A Catalyst on Asphaltene Conversion. Upper Curve pre-sulfided catalyst, lower curve non-presulfided catalyst.

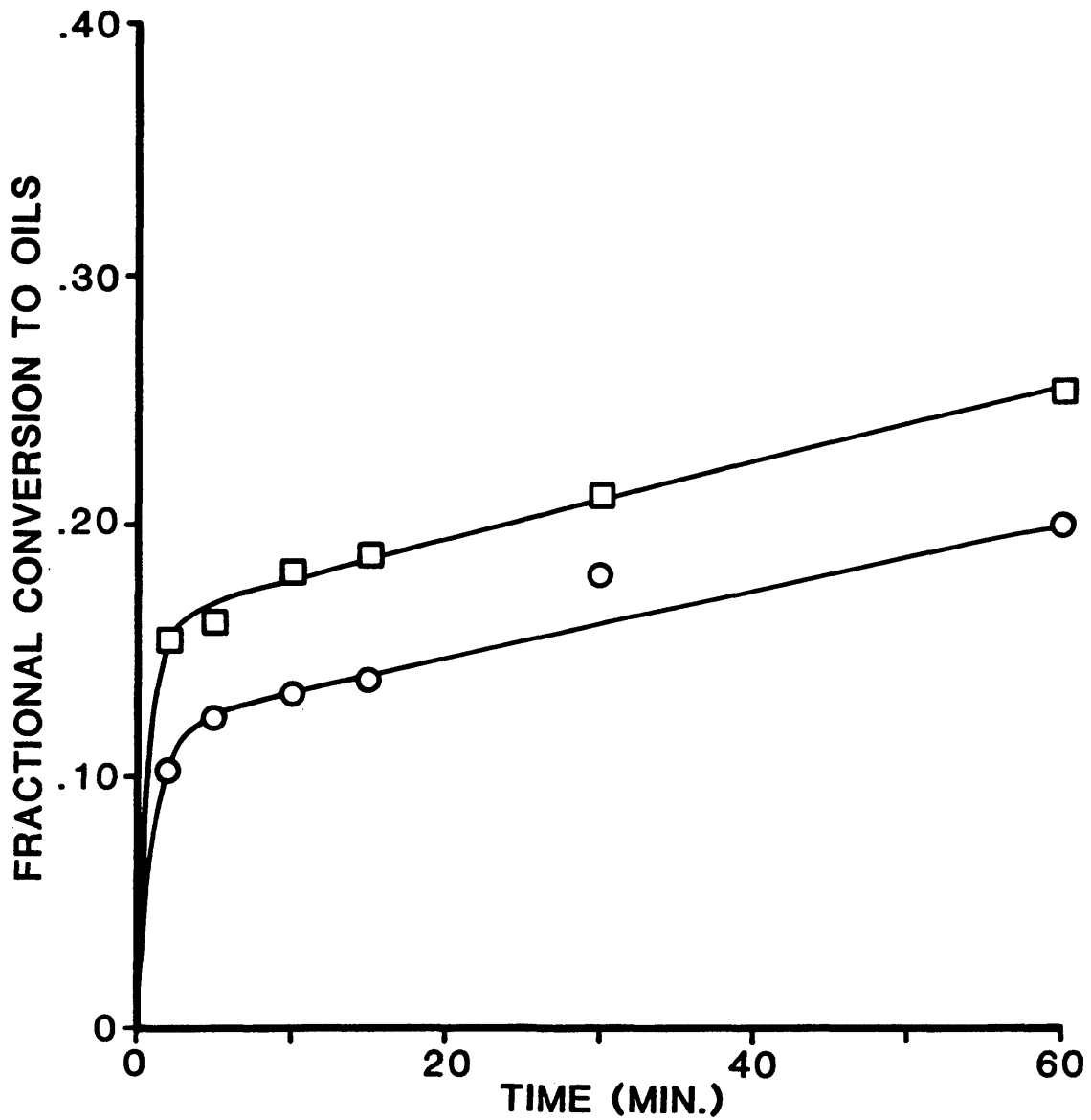


Figure 25. Activity of Presulfided HDN-30 Catalyst After H₂S Purge by H₂. Upper curve, normal run conditions; Lower curve, H₂ purge.

throughout the reaction by approximately 5 percent. This indicates that the sulfur species on the catalyst formed during presulfiding (MoS_x) is unstable. In the presence of hydrogen alone it is rapidly decomposed. This reduces the number of active sites and thus reduces the hydroprocessing activity of the catalyst.

Extended Time Run (3 Hours) and Reproducibility Test

Run 18 was the first of two 3 hour runs. It was conducted in order to observe the long-time conversion of asphaltenes as well as to test the reproducibility of the data. Figure 26 displays the combined results of runs 14 and 18. Both runs were made under identical reaction conditions using a presulfided HDN-30 catalyst. In Figure 26, run 14 is characterized by the square data points and extends up to 60 minutes. Run 18, characterized by the open circle data points, begins at 60 minutes and extends up to 180 minutes. The two most important points on Figure 26 are the two 60 minute data points. These two points, representing the conversion to oils for the two separate runs, give an indication of the reproducibility of the data and they verify the validity of the assumption of a constant volume batch reactor. The 60 minute data point of run 14 represents the final sample of the run. Prior to taking this sample approximately 12 weight percent of the initial reactor mass had been lost due to previous sam-

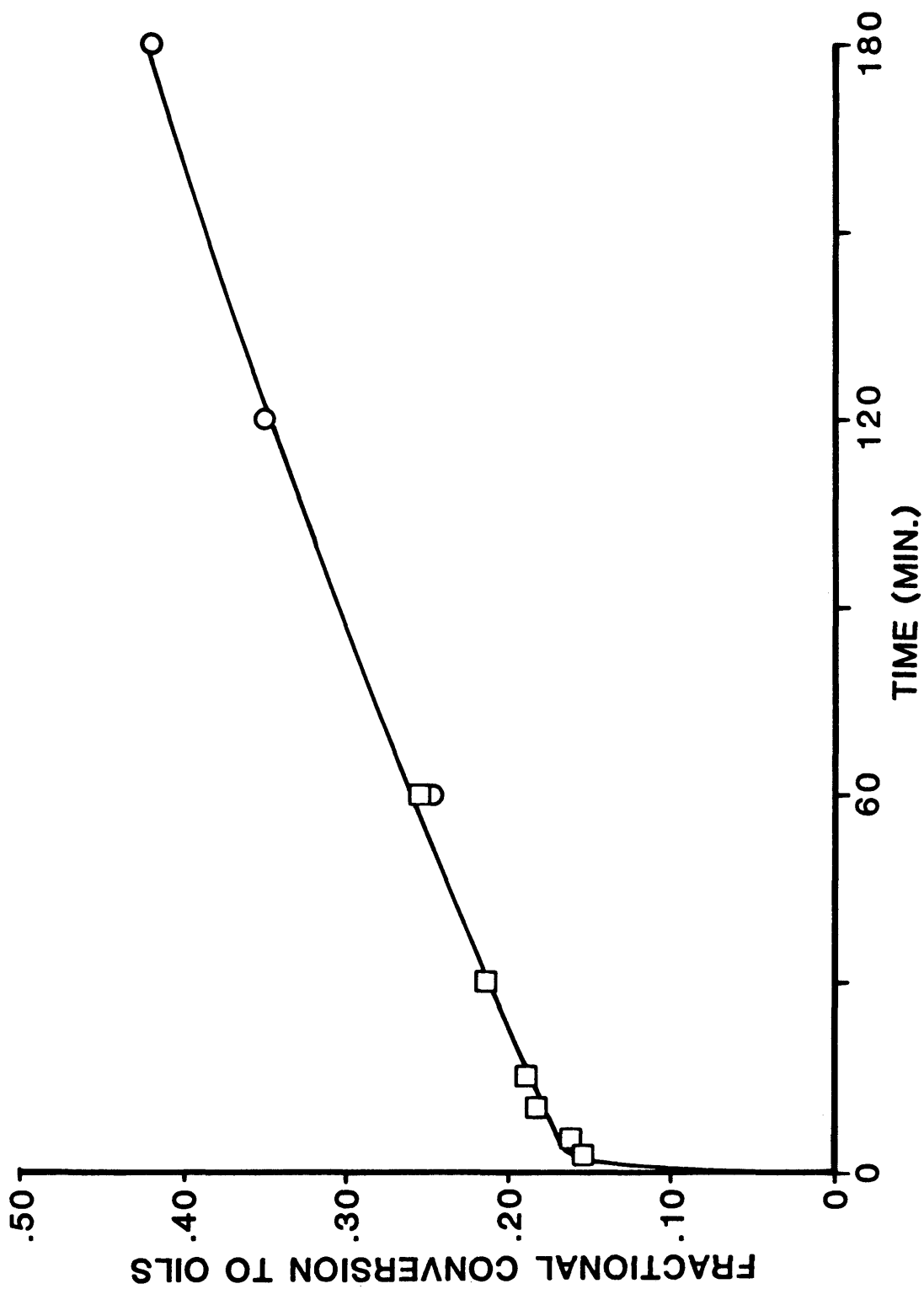


Figure 26. Fractional Conversion to Oils at 400°C Using HDN-30 Catalyst. Combined Results of Runs 14 and 18 Are Used.

pling. The 60 minute data point of run 18 represents the first sample of that run. Consequently, no previous mass loss due to sampling had occurred prior to taking this sample. The difference in conversion between the two 60 minute data points is less than 1 percent and indicates an excellent reproducibility of the data between the two runs as well as verification that the assumption of a constant volume batch reactor is valid.

The reproducibility shown here, between the two 60 minute data points, may give a misleading indication of the precision of the data from this and other runs. Although the 60 minute data points are within 1 percent of one another, they are lower than the smoothed model prediction by up to 2 percent. This same scatter is observed in several of the other runs and represents the inherent sampling error of the experiment. From this analysis it appears that the data reproducibility is within the experimental sampling error.

The continued positive slope of the conversion with respect to time in Figure 26 shows that the first-order kinetic model derived previously fits well. Although residence times of three hours and greater are not desirable in industrial reaction systems, these results indicate that a substantial conversion of asphaltene can be achieved under these conditions if the reaction time is of suffi-

cient duration.

Table 23 shows the elemental analysis of carbon, hydrogen and nitrogen on the recovered HDN-30 catalyst for run 18 after 180 minutes of reaction. These results, compared to those of run 14 for the 60 minute recovered catalyst (Table 22), shows a lower carbon content along with an increased H/C ratio. Nitrogen has increased by approximately 0.27 percent. In general, however, it does not appear that any additional significant deactivation of the catalyst has occurred.

Table 23. Elemental Analysis of HDN-30 Catalyst
After 180 Minutes of Reaction at 400°C.

<u>C (wt.%)</u>	<u>H (wt.%)</u>	<u>H/C</u>	<u>N (wt.%)</u>
6.34	1.14	2.16	0.87

Extended Time Run (3 Hours) at 425°C

The final run in this series evaluated the catalytic activity of the HDN-30 catalyst at 425°C. The catalyst was presulfided just prior to use at the previously described conditions before increasing to the reaction temperature of 425°C. Figure 27 shows the results of the asphaltene conversion under these conditions. Noticeable differences between this and previous runs are immediately apparent. First, although the jump in initial conversion (<5 minutes) is still present, it is of a significantly lower magnitude

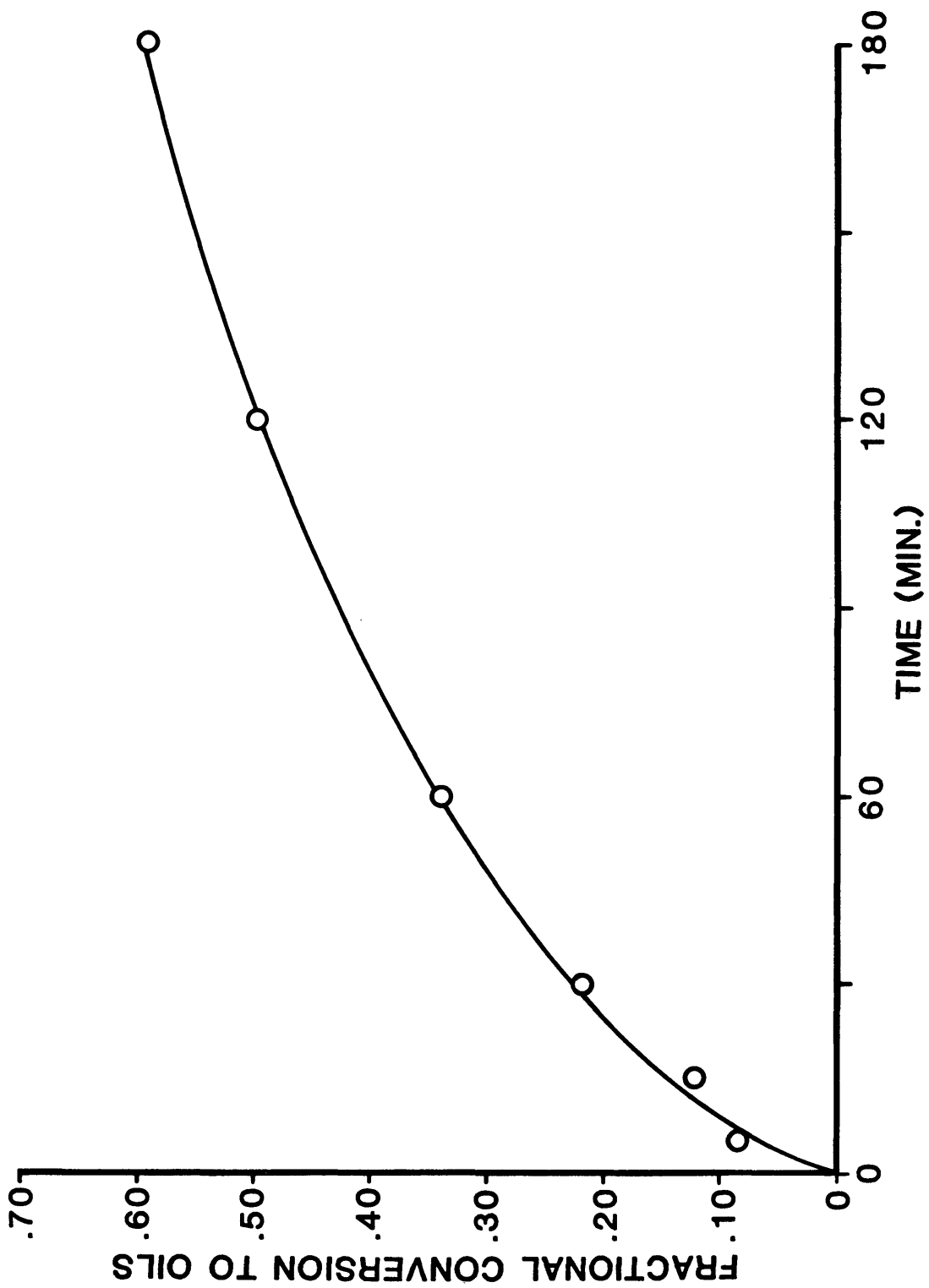


Figure 27. Fractional Conversion to Oils at 425°C Using HDN-30 Catalyst.

than for the corresponding catalytic run at 400⁰C (Figure 26). This decrease in the initial rate of conversion at the higher temperature indicates that the catalyst has suffered a moderate deactivation. Although periodic measurements of the catalyst surface were not made, this deactivation is most likely attributable to rapid coke accumulation. Beyond the initial reaction period (>15 minutes), the rate of coke accumulation decreased and the effects of the higher temperature became dominant. The higher temperature resulted in increasing the turnover frequency of the reactant asphaltenes on the accessible catalytic sites. By increasing the turnover frequency, the effect of a decreased number of active sites was diminished. The net result was an increase in the ultimate asphaltene conversion by 17% over that attained at 400⁰C.

Evidence to support the assumption of increased deactivation by coke accumulation at 425⁰C is presented in Table 24. In each case, the accumulated element (C, H, N) is of significantly greater magnitude at 425⁰C than for any of the previous catalytic runs made at 400⁰C. In particular, comparison of Table 23 (HDN-30 catalyst, 3 hours, 400⁰C) with Table 24 (HDN-30 catalyst, 3 hours, 425⁰C) shows that at 425⁰C there is a 3 percent increase in the amount of adsorbed carbon and a near doubling of the amount of adsorbed nitrogen on the catalyst after 3 hours.

Table 24. Elemental Analysis of HDN-30 Catalyst
After 180 Minutes of Reaction at 425°C

<u>C (wt.%)</u>	<u>H (wt.%)</u>	<u>H/C</u>	<u>N (wt.%)</u>
9.09	1.54	2.03	1.43

A second distinctive difference in the curve of Figure 27 is that it displays a much smoother profile throughout the reaction than for any previous run. It also appears to be approaching the limit of complete conversion ($X_A = 0.70$) in a uniform manner.

Elemental and Structural Analysis of Residual Asphaltenes

In order to obtain information on elemental and structural changes which occur to the asphaltene molecule during reaction, residual asphaltene samples were analyzed by elemental analysis, vapor pressure osmometry (VPO), ^1H nmr and ^{13}C nmr.

Elemental Analysis

Tables 25 through 27 give condensed elemental analysis results for runs 6-13. Table 25 shows, as expected, that insignificant changes occur in the H/C ratio, percent sulfur, and percent nitrogen for the thermal hydroprocessing runs. These results, along with the low extent of thermal conversion, indicate that the asphaltenes are very refractory to thermal hydroprocessing.

Table 26 compares the elemental analyses of the 400°C thermal run with the H_2S and pyrite additive catalytic

Table 25. Elemental Analysis of Residual Asphaltenes Following Thermal Hydroprocessing.

<u>RUN NO.</u>	<u>CONDITIONS</u>	<u>TIME (min.)</u>	<u>H/C</u>	<u>S</u>	<u>N</u>
-	Reprecipitated Feed Asphaltenes	--	0.849	0.09	1.88
6	21 ⁰ C	60	0.841	1.10	1.92
7	355 ⁰ C	2	0.897	0.95	1.79
		15	0.848	0.92	1.97
		60	0.842	1.01	2.01
8	375 ⁰ C	2	0.855	0.98	2.00
		15	0.855	0.99	1.99
		60	0.851	1.02	2.02
9	400 ⁰ C	2	0.850	1.03	1.96
		15	0.841	0.98	2.06
		60	0.838	0.80	2.09

Table 26. Elemental Analysis of Residual Asphaltenes Following H₂S and Pyrite Catalytic Hydroprocessing.

<u>RUN NO.</u>	<u>CONDITIONS</u>	<u>TIME (min.)</u>	<u>H/C</u>	<u>S</u>	<u>N</u>
-	Reprecipitated Feed Asphaltenes	--	0.849	1.09	1.88
9	400 ⁰ C, Thermal	2	0.850	1.03	1.96
		15	0.841	0.98	2.06
		60	0.838	0.80	2.09
10	400 ⁰ C, H ₂ S	2	0.835	1.12	2.04
		15	0.840	1.02	2.07
		60	0.847	0.95	2.11
11	400 ⁰ C, Pyrite	2	0.831	1.05	2.04
		15	0.835	0.99	2.11
		60	0.847	0.97	2.15

Table 27. Elemental Analysis of Residual Asphaltenes
Following Commercial Catalyst Hydroprocessing.

<u>RUN NO.</u>	<u>CONDITIONS</u>	<u>TIME (min.)</u>	<u>H/C</u>	<u>S</u>	<u>N</u>
-	Reprecipitated Feed Asphaltenes	--	0.849	1.09	1.88
9	400 ^o C, Thermal	2	0.850	1.03	1.96
		15	0.841	0.98	2.06
		60	0.838	0.80	2.09
12	400 ^o C, HDS-20A	2	0.853	1.07	2.03
		15	0.846	0.83	2.10
		60	0.850	0.51	2.04
13	400 ^o C, HDS-9A	2	0.841	1.01	2.05
		15	0.853	0.83	2.05
		60	0.850	0.60	2.02
14, 18	400 ^o C, HDN-30	2	0.844	1.03	2.04
		15	0.850	0.85	2.05
		60	0.875	0.52	1.88
		120	0.873	0.42	1.89
		180	0.880	0.41	1.75
15	400 ^o C, Ni-4303E	2	0.853	1.12	2.04
		15	0.863	0.80	2.09
		60	0.865	0.64	2.07

runs. Interestingly, both the H₂S and pyrite runs display similar trends, however, the changes are not greatly different from the 400°C thermal run.

The use of the commercial hydroprocessing catalysts brought about the major changes in the residual asphaltene elemental makeup. Table 27 lists the elemental analyses of the residual asphaltenes for each of the commercial catalysts used. The results illustrate that although each catalyst was approximately equally effective in removing sulfur, only the HDN-30 catalyst was effective in both removing nitrogen and increasing the H/C ratio. Figures 28 to 30 examine these results in more detail by comparing 3 important runs: the 400°C thermal run; the 400°C HDS-20A catalytic run; and the 400°C HDN-30 catalytic run. The HDS-20A catalytic run showed the greatest conversion to oils, however, it was ineffective in removing nitrogen or increasing the H/C ratio of the residual asphaltene, as is evident from Figures 29 and 30. The HDN-30 catalyst, on the other hand, had a lower overall conversion to oils, yet the results show a definite decrease in the percent nitrogen along with a concomitant increase in the H/C ratio.

Closer examination of Figures 29 and 30 show that for the HDN-30 catalytic run, the percent nitrogen remains relatively constant for the first 15 minutes of reaction. Beyond 15 minutes there is a near-linear decrease in the

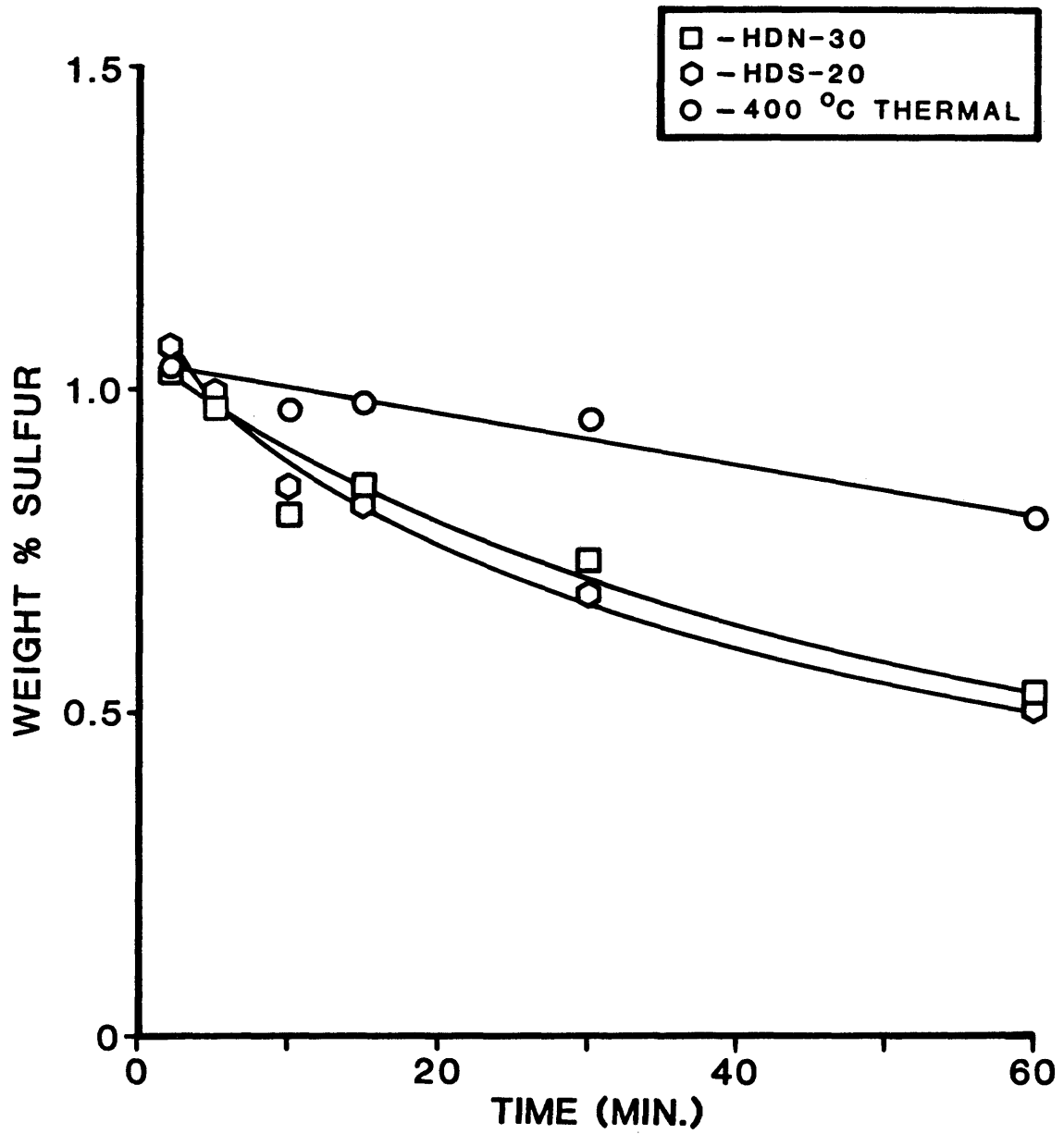


Figure 28. Percent Sulfur in Residual Asphaltenes
For 3 Run Conditions.

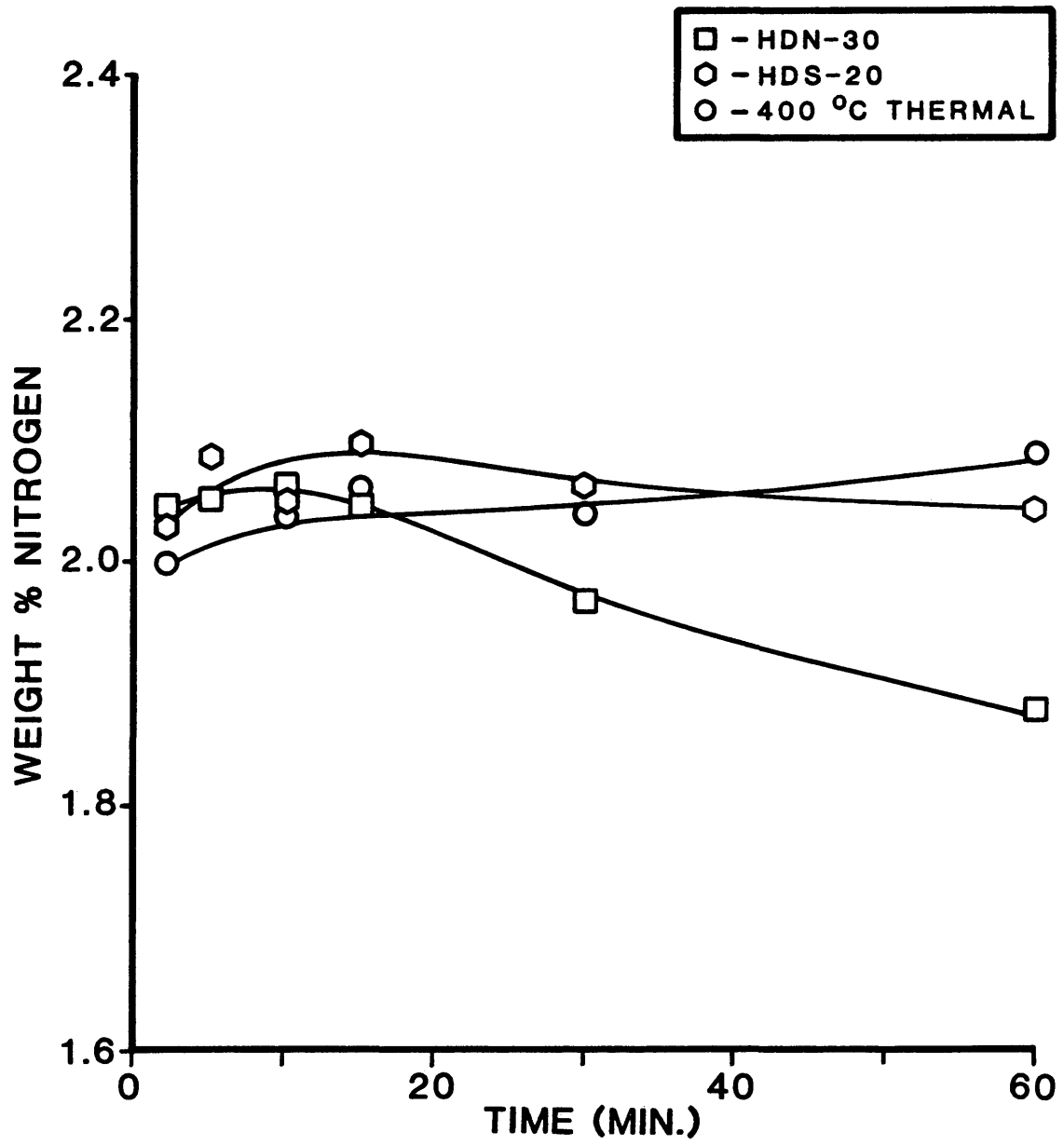


Figure 29. Percent Nitrogen in Residual Asphaltene For 3 Run Conditions.

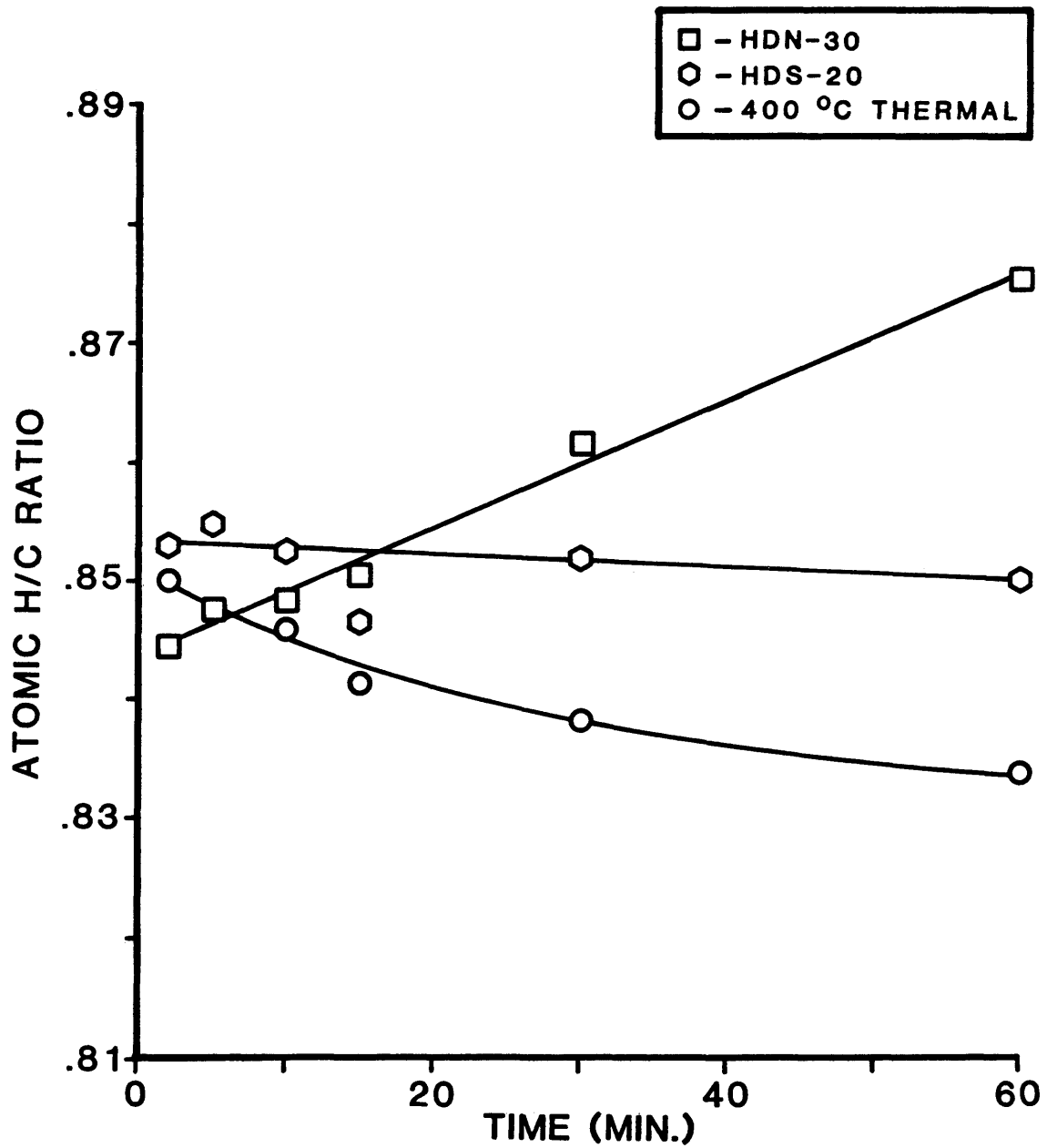
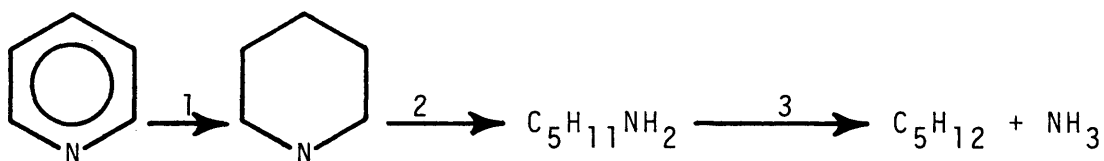


Figure 30. Atomic H/C Ratio of Residual Asphaltene For 3 Run Conditions.

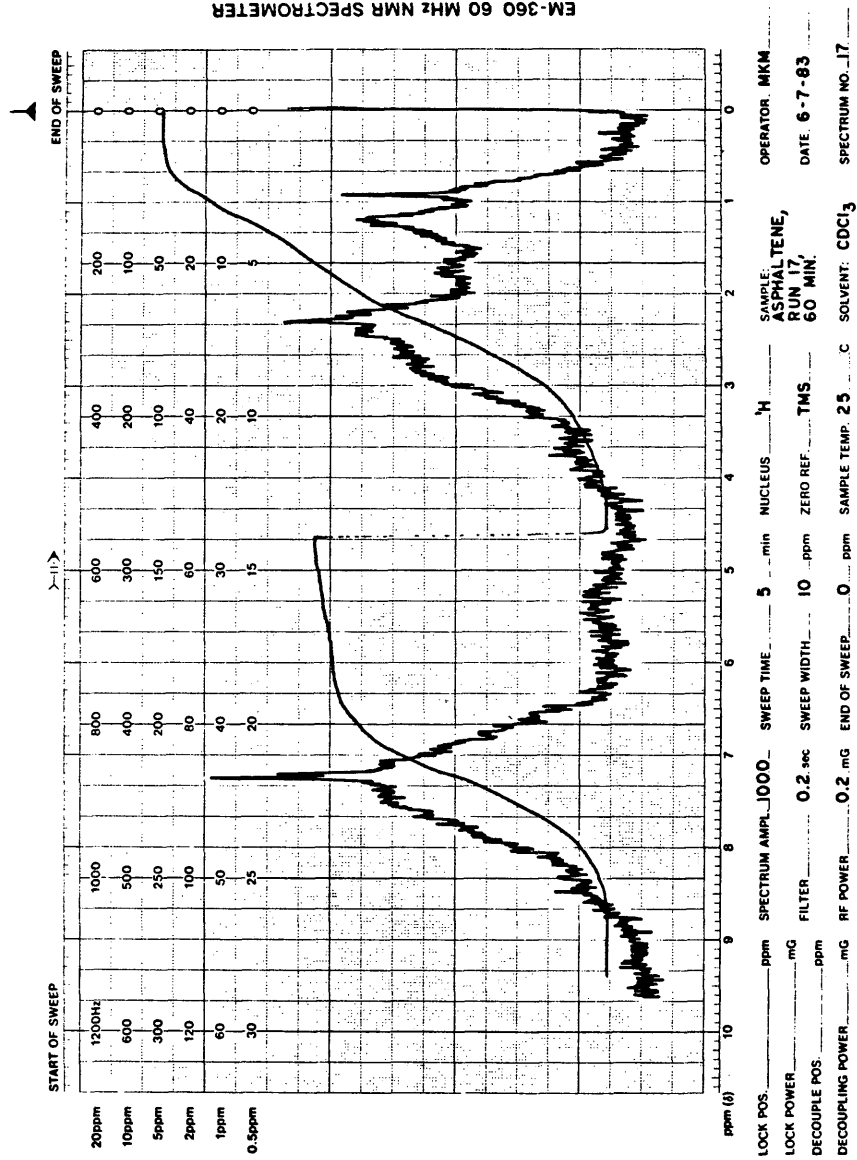
percent nitrogen. The H/C ratio, however, increases in a near-linear manner throughout the entire run. These results are consistent with the proposed mechanism for nitrogen removal from a heterocyclic system. Hydrodenitrogenation of heterocyclics such as pyridine occurs by complete hydrogenation of the ring, followed by ring opening and nitrogen removal [29].



Thus, if ring hydrogenolysis (step 2) is the rate-limiting step, as was determined by McIlvried, a delay in nitrogen removal will be observed while the H/C ratio increases continuously.

Structural Analysis

Proton and ¹³C nuclear magnetic resonance spectroscopy, along with vapor pressure osmometry, were used in this study to characterize the complex multicomponent asphaltene mixtures. Typical ¹H and ¹³C nmr spectra of the asphaltenes are shown in Figures 31 and 32. The proton spectra consists primarily of broad, featureless envelopes




 varian instrument division
 palo alto, california

PART NO. 80208-05 PRINTED IN U.S.A.

Figure 31. Typical ¹H NMR of Residual Asphaltene.

BALB09. 000 FRYE
C13 CPMAS: B-10

10NOV82



COLORADO STATE UNIVERSITY
REGIONAL NMR FACILITY
903-491-6155

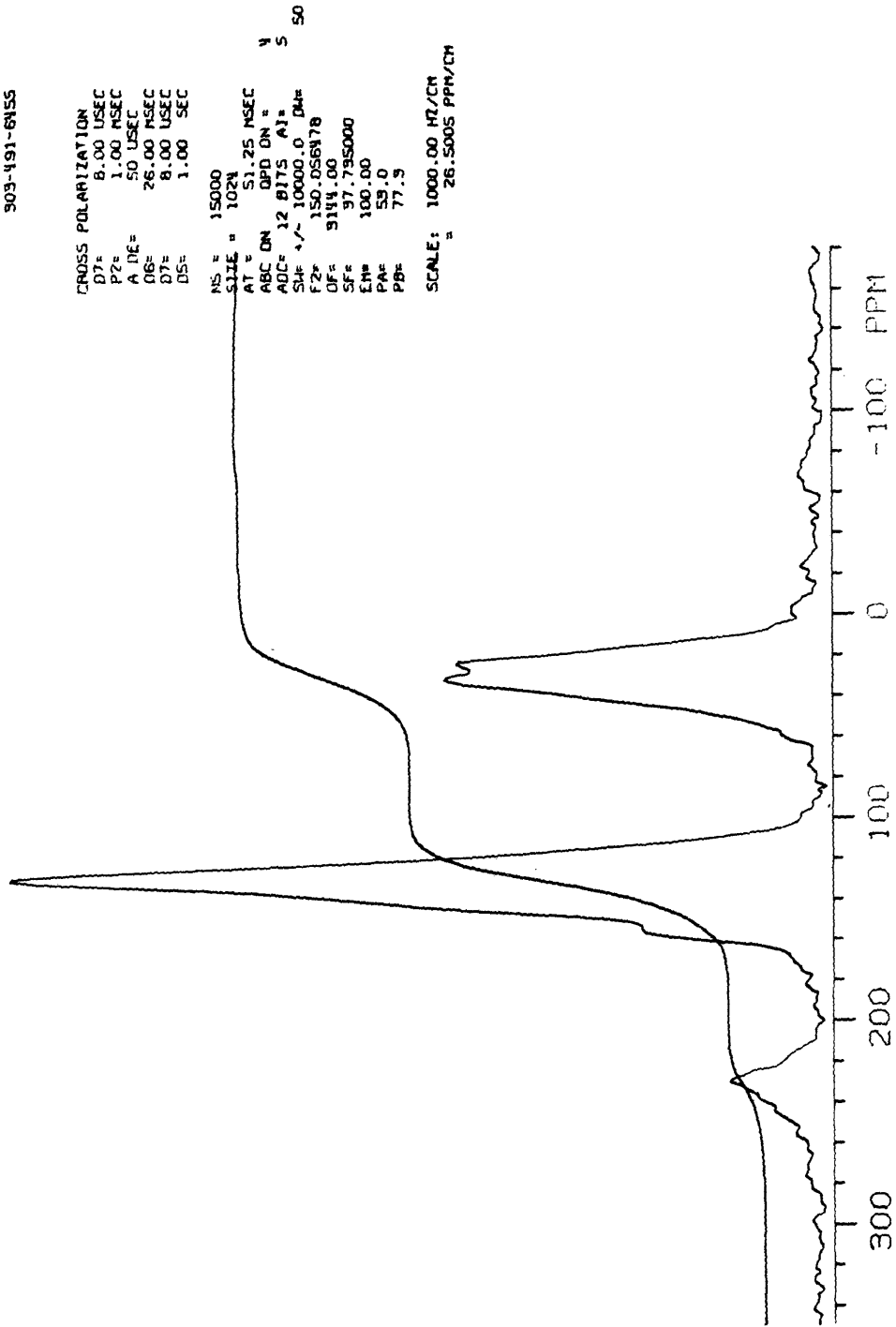


Figure 32. Typical Proton Decoupled ¹³C/PMAS NMR of Residual Asphaltene.

resulting from a large range of chemical shifts due to numerous proton environments. The basis for quantitative analysis of such spectra is dependent on the absorption bands being sufficiently separated from one another. The ^{13}C spectra, Figure 32, is more sharply resolved due to the compacted scale and the techniques of cross-polarization and magic-angle spinning (^{13}C CP/MAS).

The assignments of absorption bands for the different hydrogen and carbon types [27, 34, 39] are given in Table 28. The aromatic proton band, H_{ar} , is broad and diffuse with a sharp peak at $\delta=7.25$ ppm. This peak is due to the absorption of the methine group of chloroform in the solvent (99.8% isotopically pure CDCl_3) and is extraneous to the asphaltene spectra. The H_{ar} band also contains the phenolic protons. The H_{α} band contains those hydrogens in saturated groups α to aromatic rings. The primary absorption peak of H_{α} occurs at $\delta=2.40$ ppm. As shown in Figure 31, the base of this band is not distinctly resolved from the H_0 band. The H_0 band represents those hydrogens of methine, methylene or methyl groups β or further from an aromatic ring. This band usually shows 2 distinctive peaks imposed on a broad absorption base. The 3 primary proton absorptions in the H_0 band are: naphthenic protons, $\delta=1.58$ ppm; methylenic protons, $\delta=1.25$ ppm; and saturated methyl protons, $\delta=0.90$ ppm. A very diffuse band was sometimes

observed in the olefinic region (δ :6.00-4.50 ppm). However, due to the low intensity of this band it was not explicitly considered.

Table 28 [34]. Assignments of Proton and Carbon Bands of NMR Spectra of Asphaltenes

<u>SYMBOL</u>	<u>Range of Band Envelope δ, ppm From TMS</u>	<u>ASSIGNMENT</u>
H _{ar}	9.00 - 4.50	Aromatic protons, phenolic and olefinic protons might be included.
H _{α}	4.50 - 1.73	Hydrogen in saturated groups α to aromatic rings
H _o	1.73 - 0.00	Hydrogen in saturated groups β or further to aromatic rings.
C _{ar}	200 - 80	Aromatic carbon atoms, aromatic carbon atoms substituted by O included.
C _{al}	80 - 10.8	Saturated carbon atoms

The ^{13}C CP/MAS nmr spectra shows an absorption band centered at $\delta=230$ ppm. This is the first left spinning sideband of the aromatics. The spinning sidebands are symmetric about the absorption peak, indicating that the first right spinning sideband of the aromatics occurs within the aliphatic region. In order to correct the inte-

grated peak areas for the spinning sidebands (ssb) the ssb was measured, subtracted from the aliphatics and added twice to the aromatics. Further examination of the ^{13}C spectra shows no evidence of carbonyl resonances (δ :210-170 ppm) in the asphaltenes. The aromatic band, C_{ar} , contains a shoulder centered at 158 ppm. This is due to aromatic C-O which is primarily phenolic. Within the C_{al} band there is partial resolution of the aliphatic groups into methylenic carbons, δ =30 ppm, and methyl carbons, δ =22 ppm.

The integrated peak areas from ^1H nmr and ^{13}C nmr were used to define structural parameters by the method of Brown and Ladner [27]. The parameters and their accompanying equations are listed and defined in Table 29. Some of the equations in Table 29 are modifications of the original Brown and Ladner equations and incorporate ^{13}C nmr data where appropriate. Three assumptions are made with regard to these relations:

1. All the oxygen is directly attached to aromatic systems and is not shared between them.
2. The aromatic rings are not linked by C-C bonds, as in a polyaryl system.
3. Nitrogen and sulfur comprise a minority fraction of the materials and are not accounted for.

The necessary data for use of the equations in Table 29

Table 29. Definitions of Structural Parameters.

PARAMETER	DEFINING EQUATION	DEFINITION
1 $(H/C)_{al}$	$\frac{H}{C} \times \frac{H_a^* + H_o^*}{H} \times \frac{C}{C_{al}}$ (from $^1H_{nmr}$) (from $^{13}C_{nmr}$)	aliphatic H/C ratio
2 f_a	$\frac{C - C_{al}}{C}$	Aromaticity (determined by ^{13}C nmr)
3 f_a	$\frac{\frac{C}{H} - \frac{H_a^*}{x} - \frac{H_o^*}{y}}{\frac{C}{H}}$	Aromaticity (determined by 1H nmr)
4 $\frac{H_{aru}}{C_{ar}}$	$\frac{\frac{H_a^*}{x} + \frac{H_{ar}^*}{H} + \frac{O}{H}}{\frac{C}{H} - \frac{H_a^*}{x} - \frac{H_o^*}{y}}$	atomic hydrogen-to-carbon ratio of the hypothetical unsubstituted aromatic material
5 σ	$\frac{\frac{H_a^*}{x}}{H_{ar,OH}^* + \frac{H_a^*}{x}}$	fractional degree of substitution of the aromatic system
6 C_A	$\frac{f_a' (M) (C)}{100}$	total number of aromatic carbon atoms
7 R_s	$C_A \frac{H_{aru}}{C_{ar}}$	number of substituted aromatic ring carbons
8 n	$\frac{H_o^*}{H_a^*} + 1$	number of carbon atoms per saturated substituent
9 R_a	$C_A \frac{1 - H_{aru}/C_{ar}}{2} + 1$	number of aromatic rings

are listed in Appendices B (elemental analysis) and C (nmr data and VPO molecular weights).

The constants x and y in the Brown and Ladner equations represent the average H/C ratio on carbons α to aryl rings, and on aliphatic carbons β or further to aryl rings, respectively. There is insufficient data to determine whether x and y differ statistically. If x and y are assumed to be equal, the two constants may be combined into one. This constant, the H/C aliphatic ratio, $(H/C)_{a1}$, may be calculated from 1H and ^{13}C nmr data. Table 30 shows $(H/C)_{a1}$ ratios for runs where both 1H and ^{13}C nmr data was available. The average value of $(H/C)_{a1}$ from Table 30 is 2.02. Prior to the development of ^{13}C nmr, investigators assumed a value of $x=y=(H/C)_{a1}=2.0$. This assumption worked well in the prediction of structural parameters using the Brown and Ladner equations. The above experimental results verifies the accuracy of this assumption and indicates that the aliphatic structures are predominately methylene groups. In this thesis all calculations were made using the experimentally determined value, $x=y=(H/C)_{a1}=2.02$.

Table 30. Calculated H/C Aliphatic Ratio.

<u>RUN NO.</u>	<u>(H/C)_{a1}</u>
Feed	1.90
8	2.13
9	2.05
10	2.09
11	1.79
12	2.09
13	1.86
14	2.24

Average = 2.02

Since ^1H and ^{13}C nmr are being used in tandem to determine structural parameters of asphaltenes, it is desirable to know the relative reliability of each method. A convenient way to measure this is to compare the aromaticity values of asphaltenes as obtained by ^{13}C nmr (f_a) with those estimated from ^1H nmr using the method of Brown and Ladner (f'_a). Results of this comparison, listed in Table 31, show good agreement between the two aromaticities, with f'_a slightly lower, on the average, than f_a .

Table 31. Aromaticities of Asphaltenes as Determined
by ^{13}C NMR and ^1H NMR.

RUN NO.	Aromaticity ^a		
	f_a	f'_a	Δ^b
Feed	0.704	0.734	-0.030
8	0.752	0.739	0.013
9	0.763	0.759	0.004
10	0.758	0.750	0.008
11	0.739	0.779	-0.040
12	0.743	0.734	0.009
13	0.719	0.740	-0.021
14	0.773	0.748	0.025

^a f_a = aromaticity determined by ^{13}C nmr

f'_a = aromaticity determined by ^1H nmr

^b $\Delta = f_a - f'_a$

This relationship has been investigated by Retcofsky et al. [36] for a large number of coal derivatives. They proposed the relationship between f'_a and f_a to be

$$f'_a = 0.919f_a + 0.065$$

with a standard error of estimate of 0.027. A plot of f'_a vs. f_a is made in Figure 33 along with the above equation and its error limits. With the exception of one point, the results obtained in this thesis lie within the error limits of the above relation.

Previously described results of this thesis have shown

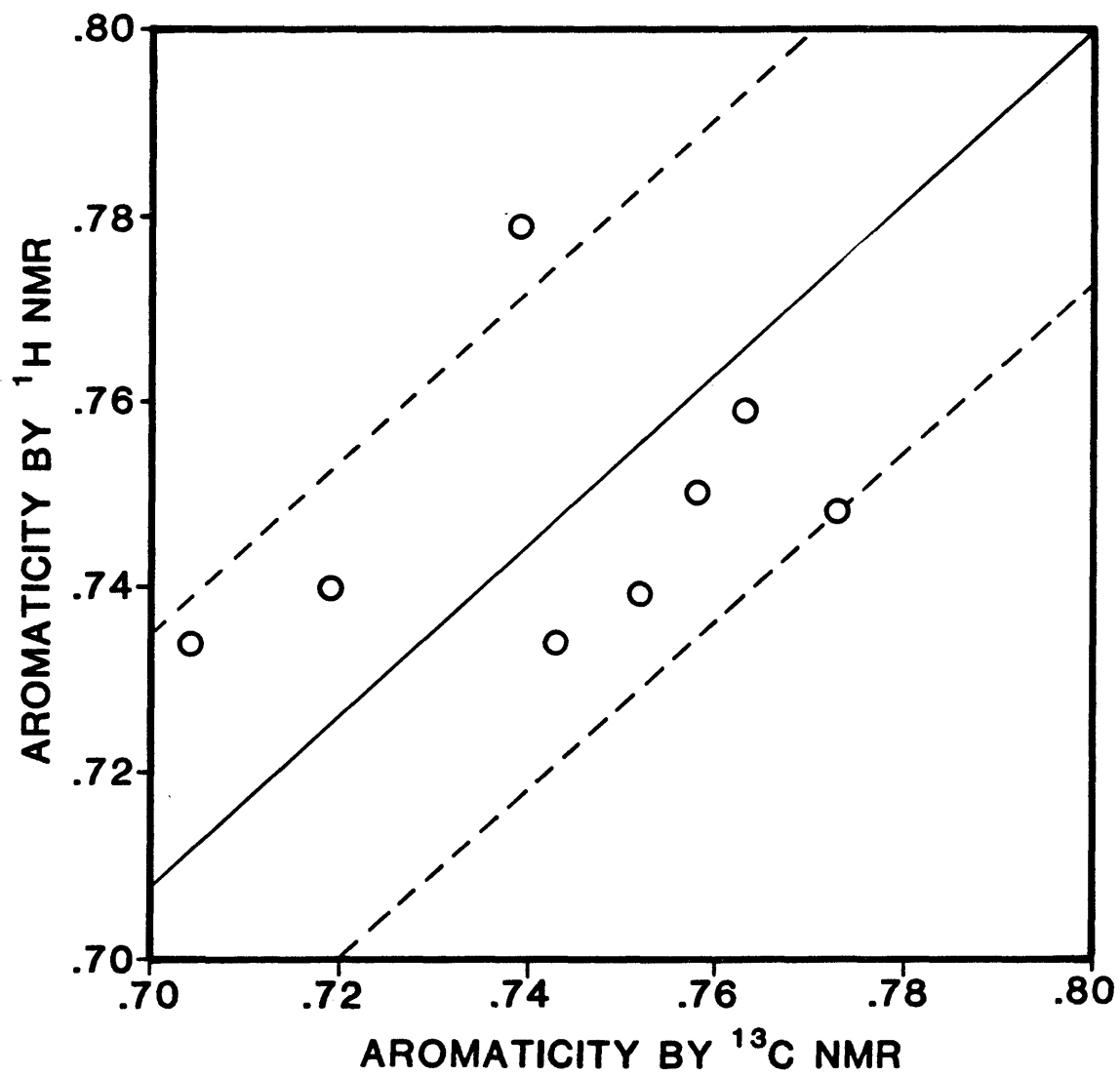


Figure 33. Comparison of Aromaticities as Determined by ^{13}C and ^1H NMR.

that for the thermal and the H₂S and pyrite additive runs the degree of conversion of the asphaltenes-to-oils was quite low. In addition, the molecular elemental makeup was only moderately altered from the reprecipitated feed asphaltenes. This indicates that, for these two phases of study, the asphaltene structural unit remained basically unchanged. Structural analysis using the equations of Brown and Ladner concurs with the above results in that most of the parameters show only moderate variation from the reprecipitated feed asphaltene. Therefore, a detailed structural analysis and comparison of results of these runs will not be made.

The major changes to the reprecipitated feed asphaltene structural unit occurred when using the commercial hydroprocessing catalysts, in particular the catalysts HDS-20A and HDN-30. These two catalysts gave the highest conversion-to-oils and the greatest heteroatom removal of the reprecipitated feed asphaltenes, respectively. It is of primary interest, therefore, to compare the structural modifications to the asphaltene molecule brought about by these two catalysts. Table 32 lists the average molecular properties of the residual asphaltenes, as determined by the modified Brown and Ladner equations, for the HDS-20A and HDN-30 catalytic runs. In addition, the properties of the reprecipitated feed asphaltenes and the 400°C thermal

Table 32. Average Molecular Properties of Asphaltenes*

RUN	REPRECIPITATED FEED ASPHALTENE	400°C, Thermal	HDS-20A (Co-Mo/Al ₂ O ₃) ¹²	HDN-30 (Ni-Mo/Al ₂ O ₃) ¹⁴
Molecular Formula	C _{39.4} H _{35.89} N _{.75} O _{2.02} S _{.18}	C _{37.85} H _{31.50} N _{.79} O _{1.71} S _{.13}	C _{37.71} H _{31.83} N _{.77} O _{1.72} S _{.08}	C _{35.26} H _{30.63} N _{.67} O _{1.98} S _{.08}
Molecular Weight	554	529	526	498
(H/C) _{al}		2.05	2.09	2.24
f _a		.763	.743	.773
f' _a	.750	.759	.734	.748
H _{aru} /C _{ar}	.736	.723	.717	.782
σ	.319	.307	.351	.307
C _A	29.61	28.75	27.71	26.30
R _S	6.95	6.38	6.97	6.31
n	1.56	1.55	1.58	1.55
R _A	4.91	4.98	4.92	3.90

* All residual asphaltenes represent 60 minute samples.

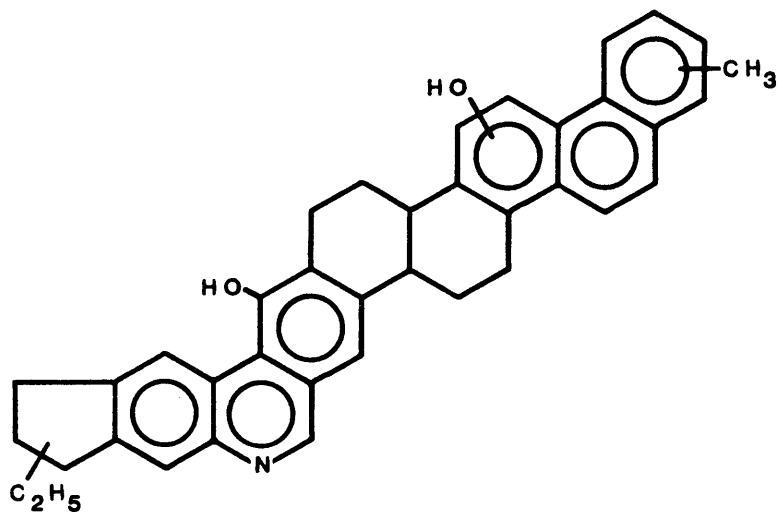
run asphaltenes are included for comparison. Examination of the results listed in Table 32 indicates that the most significant structural changes seem to have occurred to the HDN-30 processed asphaltene. The structural parameters of the HDS-20A and the 400⁰C thermal residual asphaltenes typically show values intermediate to the HDN-30 asphaltene and the reprecipitated feed asphaltene. The molecular weight of the residual asphaltenes decreases in the order Feed>400⁰C thermal>HDS-20A>HDN-30. This indicates that the molecular weight change is more a function of the degree of hydroprocessing rather than the extent of conversion. The H/C aliphatic ratio shows no observable trends, here or in Table 30. However, for the HDN-30 catalytic run, there is a significant increase in $(H/C)_{a1}$ over that of the feed. This is consistent with the observed increase in the overall H/C ratio and indicates the production of a larger alkyl group fraction. The hydrogen-to-carbon ratio of the hypothetical unsubstituted aromatic material, H_{aru}/C_{ar} , shows little change in the first three samples, however, for the HDN-30 asphaltene, results indicate that the number of cata-condensed aromatic rings decreases slightly from that of the feed. The number of aromatic carbon atoms, C_a , decreases in the order Feed>400⁰C thermal>HDS-20A>HDN-30. The number of aromatic rings, R_a , however, remains constant at 5 for the feed, 400⁰C thermal

and HDS-20A runs. For the HDN-30 processed asphaltene, R_a decreases to 4. The average number of carbon atoms per saturated substituent, n , remains nearly constant as does σ and R_s ; the fractional degree of substitution of the aromatic system and the number of substituted aromatic ring carbons, respectively.

Although there appear to be some inconsistencies in the results within a particular sample, all samples were subject to the same sources of error. Therefore, the results should be consistent between samples, thus validating the above comparison.

In summary, the asphaltene structure observed here consists of 4-5 aromatic rings with 26-30 aromatic carbon atoms. There are 9-10 non-aromatic carbon atoms (naphthenic and alkyl), 1-2 OH groups, and 0-1 heterorings per molecule. The average substituent chain length consists of 1-2 carbon atoms with 30-35 percent of the available aromatic edge atoms occupied by substituents.

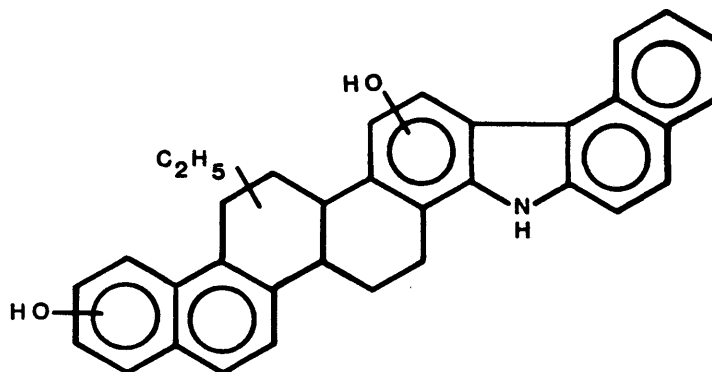
From these results a hypothetical average-asphaltene molecule may be postulated which provides a best-fit to the molecular parameters in Table 32. Figures 34 and 35 depict two possible asphaltene structures along with their structural parameters. It must be remembered that the data yields only average properties and that these proposed structures are based upon this. However, Figures 34 and 35



Molecular Formula	$C_{39} H_{35} NO_2$
Molecular Weight	549
$(H/C)_{al}$	2.0
fa	0.70
H_{aru}/C_{ar}	0.71
σ	0.45
C_a	28
R_s	9
n	1.5
R_a	6

Note: In model structures certain groups may be replaced by sulfur.

Figure 34. Hypothetical Average Asphaltene Structure I.



Molecular Formula	$C_{34} H_{29} NO_2$
Molecular Weight	483
$(H/C)_{al}$	1.75
fa	0.76
H_{aru}/C_{ar}	0.84
σ	0.45
C_A	26
R_s	10
n	1.1
R_a	5

Note: In model structure certain groups may be replaced by sulfur.

Figure 35. Hypothetical Average Asphaltene Structure II.

illustrate the types of molecules which represent the asphaltene fraction and as such may provide additional insight into the physical and chemical properties of asphaltenes.

CONCLUSIONS

The hydroprocessing of coal-derived asphaltenes, whether thermal or catalytic, resulted in conversion profiles of similar form. An initial jump in conversion, primarily due to mechanical (pressure) and thermal shock effects, occurred within the first two minutes of reaction. The subsequent reaction period involved only chemical reaction which was characterized by a very low conversion rate. The system was successfully modeled as the sum of a reactive and an unreactive asphaltene fraction, each following first-order kinetics.

The thermal hydroprocessing study showed that asphaltenes are essentially unreactive at lower temperatures and only moderately reactive at higher temperatures. The 60 minute conversions at 355^o, 375^o and 400^oC were 8.3%, 8.6% and 14.4%, respectively. There was very little change in the elemental analysis, molecular weights, and nmr determined structural parameters of the residual asphaltenes with respect to the reprecipitated feed asphaltenes. An Arrhenius plot of the rate constant of the unreactive asphaltene fraction failed to show linearity over the temperature range studied. The different activation energies of the numerous chemical compounds which form the asphaltene fraction is believed to be responsible for this non-linearity. An activation energy of 17.1 kcal/gmole was

calculated for the temperature range 375⁰ to 400⁰C. The low magnitude of this activation energy is due to the fact that only the most labile bonds are being broken.

The second phase of study, which involved H₂S and pyrite additives, showed that H₂S alone had little effect on asphaltene conversion. Pyrite, on the other hand, displayed a positive catalytic effect indicating that the pyrrhotite/H₂S mixture, which is formed in situ by the reduction of pyrite, is effective in catalyzing the more difficult secondary oil-forming reactions. However, this effect was small, and results of elemental and structural analysis, and molecular weight determinations show only minor differences between the 400⁰C thermal run and the H₂S and pyrite runs.

The use of metal-supported commercial hydroprocessing catalysts resulted in an enhanced conversion-to-oils of from 1.8 (HDN-30) to 2.1 (HDS-20A) times the corresponding 400⁰C thermal conversion. Although the HDS-20A catalyst gave the highest conversion to oils it was not the most effective catalyst for heteroatom removal. The HDN-30 catalyst had a 5 percent lower 60 minute conversion-to-oils than the HDS-20A catalyst; however, it performed as well as the HDS-20A for sulfur removal. In addition, the HDN-30 was the only commercial catalyst tested which was able to remove nitrogen and increase the atomic H/C ratio; both

desirable properties for a hydroprocessing catalyst.

The fact that the large pore HDN-30 Ni-Mo catalyst was found to be more effective for denitrogenation than either the Co-Mo or Ni-W catalysts is probably because Ni-Mo is a more active catalyst for hydrogenation. However, because of the wide range of physical and chemical properties of the catalysts used in this study it is difficult to draw any definitive conclusions on the effectiveness which a single catalyst property had. It is only possible to say that, based on overall performance, the HDN-30 catalyst was the most effective for asphaltene hydroprocessing.

Deactivation of the catalysts appeared due primarily to coke deposition. Coking occurred rapidly and corresponded to the decrease of catalyst surface area. As expected, the amount of coke laydown was greater at 425^o than at 400^oC.

It was found that catalyst presulfiding was necessary in order to bring the catalyst to its most active state; however, presulfiding conditions were not varied in order to ascertain whether or not they were optimum. Additionally, it was determined that the surface sulfur species formed during presulfiding was unstable and in order to prevent an inadvertent decrease in catalyst activity sufficient sulfur had to be present throughout the reaction.

The effect of increasing the catalytic reaction temperature to 425°C was a dramatic increase in conversion (8.6% greater at 60 minutes, 17% greater at 180 minutes). However, there was essentially no corresponding increase in the degree of heteroatom removal. Since there was also an increase in coke deposition at the elevated temperature there is an indication that more than one kind of site is operative in these hydroprocessing reactions.

Combining the results of elemental analysis, molecular weight determinations, and proton and ^{13}C nmr provided insight into the average structure of coal-derived asphaltenes. The residual asphaltenes do not show great differences in structural parameters from the reprecipitated feed asphaltenes. This result is primarily due to the fact that if any major structural modification is made to the asphaltene molecule it will not possess the same solubility characteristics and as a result will no longer be defined as an asphaltene. Therefore, molecules which remain as asphaltenes share many of the same structural characteristics. The structures depicted in Figures 34 and 35 thus provide a meaningful description of the asphaltenes in terms of their average parameters.

Finally, direct comparisons of results from this study to results from similar studies (18, 26, 44-46) are difficult to make. There typically exists significant differen-

ces between reaction variables such as asphaltene processing history, asphaltene concentration, solvent type, and catalyst type. Therefore each study must be judged on the basis of its own merit and comparisons made only where truly appropriate.

RECOMMENDATIONS FOR FURTHER STUDY

This work constitutes what may be termed as an exploratory study into the physical and chemical behavior and properties of coal-derived asphaltenes. Reaction conditions were selected primarily on the basis of the results of previous studies. However, data from some of the later runs of this investigation indicate that optimization of the processing conditions has not been attained and is still necessary for efficient asphaltene hydroprocessing. In particular, a more extensive investigation of the effects of temperature and pressure must be pursued.

In conjunction with the optimization of the processing conditions the comparative catalyst study needs to be expanded to include more of the hydroprocessing catalysts available today. A catalyst of particular interest is the Harshaw 0402T, a silica-promoted Co-Mo on alumina catalyst. As mentioned before [47] this catalyst was found to give superior performance for coal liquefaction and has been used extensively at the U.S.B.M. Synthoil pilot plant.

The quality of the oil which was produced is an area which was not investigated in this study. The ultimate goal of asphaltene hydroprocessing is to generate a high quality oil which can be upgraded for use as a liquid fuel. Therefore, it is mandatory that the oil fraction be

analyzed in terms of its physical and chemical properties so as to properly assess the desirability of expanding asphaltene hydroprocessing to an enlarged scale. Analysis of the oil fraction would necessarily center on the percent of heteroatoms, aromaticity, molecular weight and viscosity, as these properties are used to evaluate the quality of the oil and the ease with which it may be upgraded.

A final area of importance, one which was only briefly mentioned in this work, is whether or not one fraction of the asphaltene is more amenable to liquefaction than another. Further study into this area would require adopting a fractionation technique based on either chemical class (eg. SESC) or acid-base functionality. Conversion with respect to each fraction could then be followed in order to determine whether or not a specific fraction was being preferentially converted. The benefit of such a study would be to point out the particularly refractory fractions and to adopt appropriate conditions for their conversion.

REFERENCES CITED

1. Aczel, T., Williams, R.B., Chamberlain, N.F., Lumpkin, H.E., "Composition of Asphaltenes from Coal Liquids", American Chemical Society Preprints, Division of Petroleum Chemistry, Vol. 24, No. 4, p. 955-962 (Sept. 1979).
2. Long, R.B., "The Concept of Asphaltenes", American Chemical Society Preprints, Division of Petroleum Chemistry, Vol. 24, No. 4, p. 891-901 (Sept. 1979).
3. Farcasiu, M., Mitchell, T.O., Whitehurst, D.D., "The Nature and Origin of Asphaltenes in Processed Coals", First Annual Report, (AF-252), RP-410-1 to EPRI, February 1976.
4. Corbett, L.W., Petrossi, U., "Differences in Distillation and Solvent Separated Asphalt Residua", Ind. Eng. Chem. Prod. Res. Dev., Vol. 17, No. 4, p. 342-346 (1978).
5. Schweighardt, F.K., Retcofsky, H.L., Raymond, R., "Asphaltenes from Coal Liquefaction", American Chemical Society, Division of Fuel Chemistry, Vol. 21, No. 7, p. 27-32 (Sept. 1976).
6. Schultz, H., Mima, M.J., "Comparison of Methods for Determining Asphaltenes in Coal-Derived Liquid Fuels", American Chemical Society, Division of Fuel Chemistry, Vol. 23, No. 2, p. 76-78 (March 1978).
7. Schultz, H., Mima, M.J., "Comparison of Methods for the Determination of Asphaltenes, Oils and Insolubles - Part II", American Chemical Society, Division of Fuel Chemistry, Vol. 25, No. 1, p. 18-24 (March, 1980).
8. Farcasiu, M., "Fractionation and Structural Characterization of Coal Liquids", Fuel, Vol. 56, p. 9-14 (Jan. 1977).
9. Whitehurst, D.D., Mitchell, T.O., Farcasiu, M., "The Nature and Origin of Asphaltenes in Processed Coals", Final Report, (AF-1298), RP-410-1 to EPRI, December 1979.
10. Cogswell, T.E., Latham, D.R., "Chromatographic Separation of Coal Liquids", American Chemical Society, Divi-

- sion of Fuel Chemistry, Vol. 23, No. 2, p. 58-66 (March 1978).
11. Schiller, J.E. and Mathiason, D.R., "Separation Method for Coal-Derived Solids and Heavy Liquids", Analytical Chemistry, Vol. 49, No. 8, p. 1225-1228 (July 1977).
 12. Sternberg, H.W., Raymond, R., Schweighardt, F.K., "Acid-Base Structure of Coal-Derived Asphaltenes", Science, Vol. 188, p. 49-51 (April 1975).
 13. Scheppele, S.E., Benson, P.A., Greenwood, G.J., Grindstaff, Q., Aczel, T., Bieber, B., "Consequences of the Mass Spectrometric and Infrared Analysis of Oils and Asphaltenes for the Chemistry of Coal Liquefaction", American Chemical Society, Division of Petroleum Chemistry, Vol. 24, No. 4, p. 963-973 (Sept. 1979).
 14. Bockrath, B.C., and Schweighardt, F.K., "Structural Characterization of Coal-Derived Asphaltenes and its Significance to Liquefaction", American Chemical Society, Division of Petroleum Chemistry, Vol. 24, No. 4, p. 949-954 (Sept. 1979).
 15. Yen, T.F., "Structural Difference Between Petroleum and Coal-Derived Asphaltenes", American Chemical Society, Division of Petroleum Chemistry, Vol. 24, No. 4, p. 901-909 (Sept. 1979).
 16. Pelipetz, M., Kuhn, E.M., Friedman, S., Storch, H.H., "Effect of Catalysts on the Hydrogenolysis of Coal", Ind. Eng. Chem., Vol. 40, p. 1259-1264 (July 1948).
 17. Weller, S.W., Clark, E.L., Pelipetz, M.G., "Mechanism of Coal Hydrogenation", Ind. Eng. Chem., Vol. 42, p. 334-336 (Feb. 1950).
 18. Weller, S.W., Pelipetz, M.G., Friedman, S., "Kinetics of Coal Hydrogenation: Conversion of Asphalt", Ind. Eng. Chem., Vol. 43, No. 7, p. 1572-1575 (July 1951).
 19. Sternberg, H.W., Raymond, R., Akhtar, S., "Synthoil Processes and Product Analysis", American Chemical Society, Division of Petroleum Chemistry, Vol. 20, No. 3, p. 711-719 (Aug. 1975).
 20. Thomas, M.G., and Granoff, B., "Coal-Derived Product Effects on Viscosity", Fuel, Vol. 57, p. 122-123 (Feb-

bruary 1978).

21. Krzyzanowska, T., Marzec, A., "Coal Derived Group Component Effects on Viscosity", Fuel, Vol. 57, p. 804-805 (Dec. 1978).
22. Bockrath, B.C., LaCount, R.B., Noceti, R.P., "Coal-Derived Asphaltenes: Effect of Phenol Content and Molecular Weight on Viscosity of Solutions", Fuel, Vol. 59, p. 624-626 (Sept. 1980).
23. Taylor, S.R., and Li, N.C., "Nature of Hydrogen Bonding in Coal-Derived Asphaltenes", Fuel, Vol. 57, p. 117-121 (Feb. 1978).
24. Bodzek, D., Kryzyzanowski, T., Marzec, A., "Heterocompounds Present in Asphaltenes from Various Products of Coal Hydrogenation", Fuel, Vol. 58, p. 196-202 (March 1979).
25. Farcasiu, M., Mitchell, T.O., Whitehurst, D.D., "On The Chemical Nature of the Benzene Insoluble Components of Solvent Refined Coals", American Chemical Society, Division of Fuel Chemistry, Vol. 21, No. 7, p. 11-26 (Sept. 1976).
26. Bockrath, B.C., and Noceti, R.P., "Coal-Derived Asphaltenes: Relationship Between Chemical Character and Process History", Fuel Processing Technology, Vol. 2, p. 143-153 (1979).
27. Brown, J.K., and Ladner, W.R., "A Study of the Hydrogen Distribution in Coal-like Materials by High Resolution Nuclear Magnetic Resonance Spectroscopy II - A Comparison with Infrared Measurement and the Conversion to Carbon Structure", Fuel, Vol. 39, p. 87-96 (1960).
28. Bartle, K.D., Martin, T.G., Williams, D.F., "Chemical Nature of a Supercritical Gas Extract of Coal at 350°C", Fuel, Vol. 54, p. 226-235 (Oct. 1975).
29. Ladner, W.R., Martin, T.G., Snape, C.E., Bartle, K.D., "Insights into the Chemical Structure of Coal from the Nature of Extracts", American Chemical Society Preprints, Division of Fuel Chemistry, Vol. 25, No. 4, p. 67-68 (Aug. 1980).

30. Schweighardt, F.K., Retcofsky, H.L., Friedel, R.A., "Chromatographic and N.M.R. Analysis of Coal Liquefaction Products", Fuel, Vol. 55, p. 313-317 (October 1976).
31. Yoshida, R., Maekawa, Y., Ishii, T., Takeya, G., "Mechanism of High Pressure Hydrogenolysis of Hokkaido Coals (Japan). 2. Chemical Structure of Products", Fuel, Vol. 55, p. 341-345 (October 1976).
32. Dereppe, J., Moreaux, C., Castex, H., "Analysis of Asphaltenes by Carbon and Proton Nuclear Magnetic Resonance Spectroscopy", Fuel, Vol. 57, p. 435-441 (July 1978).
33. Yokoyama, S., Bodily, D.M., Wiser, W.H., "Structural Characterization of Coal-Hydrogenation Products by Proton and Carbon-13 Nuclear Magnetic Resonance", Fuel, Vol. 58, p. 162-170 (March 1979).
34. Yen, T.F., "Chemistry & Structure of Coal-Derived Asphaltenes and Preasphaltenes", FE-2031-14, U.S. Department of Energy, Interim Report.
35. Ouchi, K., Chicada, T., Itoh, H., "Pressure and Temperature Effect on the Mean Chemical Structure of Coal Hydrogenolysis Product", Fuel, Vol. 58, p. 37-42 (Jan. 1979).
36. Retcofsky, H.L., Schweighardt, F.K., Hough, M., "Determination of Aromaticities of Coal Derivatives by Nuclear Magnetic Resonance Spectrometry and the Brown-Ladner Equation", Analytical Chemistry, Vol. 49, No. 4, p. 585-588 (April 1977).
37. Schwager, I., and Yen, T.F., "Chromatographic Separation and Characterization of Coal-Derived Asphaltenes", Fuel, Vol. 58, p. 219-227 (March 1979).
38. Yen, T.F., "Chemistry and Structure of Coal-Derived Asphaltenes and Preasphaltenes", FE-2031-16, U.S. Department of Energy, Quarterly Report (Jan.-March 1980).
39. Bartle, K.D., Ladner, W.R., Martin, T.G., Snape, C.E., Williams, D.F., "Structural Analysis of Supercritical Gas Extracts of Coals", Fuel, Vol. 58, p. 413-422 (June 1979).

40. Weller, S., Pelipetz, M.G., Friedman, S., "Conversion of Anthraxylon", Industrial and Engineering Chemistry, Vol. 43, No. 7, p. 1575-1579 (July 1951).
41. Liebenberg, B.J., and Potgieter, G.J., "The Uncatalyzed Hydrogenation of Coal", Fuel, Vol. 52, p. 130-133 (April 1973).
42. Yoshida, R., Maekawa, Y., Ishii, T., Takeya, G., "Mechanism of High-Pressure Hydrogenolysis of Hokkaido Coals (Japan). 1. Simulation of Product Distributions", Fuel, Vol. 55, p. 337-340 (Oct. 1976).
43. Shalabi, M.A., Baldwin, R.M., Bain, R.L., Gary, J.H., Golden, J.O., "Noncatalytic Coal Liquefaction in a Donor Solvent. Rate of Formation of Oil, Asphaltenes, and Preasphaltenes", Industrial and Engineering Chemistry Process Design and Development, Vol. 18, No. 3, p. 474-479 (July 1979).
44. Kanda, N., Itoh, H., Yokoyama, S., Ouchi, K., "Mechanism of Hydrogenation of Coal-Derived Asphaltene", Fuel, Vol. 57, p. 676-680 (Nov. 1978).
45. Yoshida, R., Yoshida, Y., "Mechanism of High Pressure Hydrogenolysis of Hokkaido Coals (Japan) 3. Chemical Structure Changes in Coal Asphaltenes During Hydrogenolysis", Fuel Processing Technology, Vol. 6, p. 225-234 (Sept. 1982).
46. Dickey, J.H., "A Kinetic Study of the Thermal Hydrogenation of Coal-Derived Asphaltenes in Tetralin Using a Continuous Stirred Tank Reactor System", MSc. Thesis T2549, Unpublished, Arthur Lakes Library, Colorado School of Mines, Golden, Colorado (Oct. 1981).
47. Kawa, W., Friedman, S., Wu, W.R.K., Frank, L.V., Yavor-sky, P.M., "Evaluation of Catalysts for Hydrodesulfurization and Liquefaction of Coal", American Chemical Society Preprints, Division of Fuel Chemistry, Vol. 19, No. 1, p. 192-206 (April 1974).
48. Mills, G.A., "Conversion of Coals to Gasoline", Industrial and Engineering Chemistry, Vol. 61, No. 7, p. 6-17 (July 1969).

49. Furlong, M.W., "Correlation of Parent Coal Properties with a Kinetically-Defined Donor Solvent Liquefaction Reactivity", Ph.D. Thesis T2472, Arthur Lakes Library, Colorado School of Mines, Golden, Colorado (April 1981).
50. Potgieter, H.G.J., "Kinetics of Conversion of Tetralin During Hydrogenation of Coal", Fuel, Vol. 52, p. 134-137 (April 1973).
51. Hooper, R.J., Battaerd, H.A.J., Evans, D.G., "Thermal Dissociation of Tetralin Between 300 and 450°C", Fuel, Vol. 58, p. 132-138 (Feb. 1979).
52. Catalytic Inc., "Solvent Refined Coal (SRC). Process Operation of Solvent Refined Coal Pilot Plant - Quarterly Technical Progress Report for the Period January-March 1980", FE-2270-72 (Feb. 1981).
53. Eaton, W.J., "Disposable Additive Screening Study in Coal Liquefaction", M.Sc. Thesis T-2446, unpublished, Arthur Lakes Library, Colorado School of Mines, Golden, Colorado (Jan. 1981).
54. Guin, J.A., Tarrer, A.R., Prather, J.W., Johnson, D.R., and Lee, J.M., "Effects of Coal Minerals on the Hydrogenation, Desulfurization, and Solvent Extraction of Coal", Ind. Eng. Chem. Process Design and Development, Vol. 17, No. 2, p. 118-126 (April 1978).
55. Rebick, C., "H₂S Catalysis of n-Hexadecane Pyrolysis", Ind. Eng. Chem. Fundamentals, Vol. 20, No. 1, p. 54-59 (Feb. 1981).
56. Baldwin, R.M., and Vinciguerra, S., "Coal Liquefaction Catalysis - Iron Pyrite and Hydrogen Sulphide", Fuel, Vol. 62, p. 498-501 (May 1983).
57. Satterfield, C.N., and Cocchetto, J.F., "Pyridine Hydrodenitrogenation: An Equilibrium Limitation on the Formation of Piperidine Intermediate", AIChE Journal, Vol. 21, No. 6, p. 1107-1111 (Nov., 1975).
58. Holloway, P.N., and Nelson, G.C., "Deactivation Mechanisms for a Cobalt Molybdate Coal Liquefaction Catalyst", American Chemical Society Preprints, Division of Petroleum Chemistry, Vol. 22, No. 4, p. 1352-1362 (August 1977).

59. McIlvried, H.G., "Kinetics of the Hydrodenitrification of Pyridine", Ind. Eng. Chem. Process Design and Development, Vol. 10, p. 125-130 (Jan. 1971).

APPENDIX A

FEED COAL/SRC-I ANALYSIS

Feed Coal Analyses
Kentucky 9 Coal

Date, 1980	19-21 Feb
Run	201ABC MB
Mine	<u>Lafayette</u>
<u>Proximate Analysis, wt %</u>	
Moisture	1.23
Ash	9.33
Volatile Matter	31.36
Fixed Carbon	58.08
<u>Ultimate Analysis, wt %</u>	
Carbon	73.04
Hydrogen	4.39
Nitrogen	0.49
Chlorine	(a)
Sulfur	2.44
Ash	9.41
Oxygen (by difference)	10.23
<u>Dry Heating Value, Btu/lb</u>	13,311
<u>Sulfur Forms, wt %</u>	
Pyritic	0.66
Sulfate	0.01
Sulfide	<0.01
Organic	1.77
<u>Mineral Analysis, wt %</u>	
Phos. pentoxide, P ₂ O ₅	0.09
Silica, SiO ₂	59.70
Ferric Oxide, Fe ₂ O ₃	13.06
Alumina, Al ₂ O ₃	20.39
Titania, TiO ₂	1.56
Lime, CaO	1.01
Magnesia, MgO	0.80
Sulfur Trioxide, SO ₃	0.92
Potassium Oxide, K ₂ O	2.14
Sodium Oxide, Na ₂ O	0.41
Undetermined	-

(a) Chlorine data not available for Run 201ABC MB.

Typical chlorine content of Ky 9 (Lafayette) coal (SN 517.54) was 0.24 wt %.

Solvent Refined Coal Analyses
Kentucky 9 Coal

Date, 1980	19 Feb	
Run	201 MB	
Sample	K125	V110(a)
<u>Proximate Analysis, wt %</u>		
Volatile Matter	45.37	39.98
Fixed Carbon	54.37	59.18
Moisture	-0.01	0
Ash	0.26	0.84
<u>Ultimate Analysis, wt %</u>		
Carbon	87.38	86.80
Hydrogen	5.40	5.45
Nitrogen	1.30	1.34
Sulfur	1.26	1.07
Chlorine	-	-
Ash	0.26	0.43
Oxygen, by difference	4.40	4.91
Heating Value, Btu/lb	15,906	14,764
<u>Sulfur Forms, wt %</u>		
Pyritic	<0.01	-
Sulfate	<0.01	-
Sulfide	0.02	-
Organic	1.24	1.07
Fusion Point, °F	374	-
<u>Distillate</u>		
at 500°F, wt %	1.34	-
vacuum, mm Hg	0.1	-
at 600°F, wt %	6.17	-
vacuum, mm Hg	0.1	-
<u>Solvent Fractionation Analysis, wt %</u>		
Oil(b)	22.60	25.1
Asphaltene(c)	42.40	38.1
Benzene insoluble(d)	32.15	36.8
Cresol insoluble organic	2.59	-
Ash	0.26	0.43

- (a) Laboratory filtered and vacuum distilled.
 (b) Pentane soluble.
 (c) Benzene soluble, pentane insoluble.
 (d) Cresol soluble.

APPENDIX B
EXPERIMENTAL RUN RESULTS

Run Number: 6 Date: 06-01-82

Operating Conditions

Temperature: Ambient (21°C)
 Pressure: 1500 psig
 Catalyst: ----
 Solvent-to-Asphaltene Ratio: 6.14
 Total Reactant Mass: 417.37g
 % Recovery: 100
 Comments: Because of constant conversion, elemental analysis represents an average of all samples. Gas analysis unavailable.

Product Yields	Sample Time (minutes)					
	2	5	10	15	30	60
Sample Weight (g)	5.34	5.31	5.49	5.47	5.24	4.99
% Asphaltenes	66.88	67.21	67.75	68.22	67.78	66.62
% Oils ^a	2.96	2.63	2.09	1.62	2.06	3.22

^a Corrected by 30.16% Factor - See Text

Elemental Analysis of Residual Asphaltene

Carbon (wt. %) 85.36
 Hydrogen 6.05
 Nitrogen 1.92
 Sulfur 1.10
 Oxygen^b 5.57
^b Oxygen determined by difference

Gas Analysis (mole %)

H ₂	CO	CO ₂	CH ₄	C ₂ H ₄	C ₂ H ₆	C ₃ H ₆	C ₃ H ₈	H ₂ S
----------------	----	-----------------	-----------------	-------------------------------	-------------------------------	-------------------------------	-------------------------------	------------------

Run Number: 7

Date: 06-30-82

T-2857

Operating Conditions

Temperature: 355°C
 Pressure: 1500 psig
 Catalyst: ----
 Solvent-to-Asphaltene Ratio: 6.03
 Total Reactant Mass: 414.10g
 % Recovery: 99.3
 Comments:

Product Yields	Sample Time (minutes)					
	2	5	10	15	30	60
Sample Weight (g)	4.74	4.94	4.87	4.79	5.18	4.94
% Asphaltenes	63.54	62.78	62.57	62.67	63.35	61.49
% Oils ^a	6.30	7.06	7.27	7.17	6.49	8.35

^a Corrected by 30.16% Factor - See Text

Elemental Analysis of Residual Asphaltene

Carbon (wt. %)	85.50	85.75	85.29	85.05	85.55	85.68
Hydrogen	6.39	6.42	6.04	6.01	6.34	6.01
Nitrogen	1.97	1.81	1.95	1.97	1.89	2.01
Sulfur	0.95	0.97	1.04	0.92	0.94	1.01
Oxygen ^b	5.37	5.05	5.68	6.05	5.28	5.29

^b Oxygen determined by difference

Gas Analysis (mole %)

H ₂	CO	CO ₂	CH ₄	C ₂ H ₄	C ₂ H ₆	C ₃ H ₆	C ₃ H ₈	H ₂ S
99.90	.024	.035	.028	--	.011	--	.002	--

147

Run Number: 8
Date: 06-12-82

Operating Conditions

Temperature: 375°C
 Pressure: 1500 psig
 Catalyst: ----
 Solvent-to-Asphaltene Ratio: 6.02
 Total Reactant Mass: 415.65g
 % Recovery: 99.7
 Comments:

Product Yields	Sample Time (minutes)					
	2	5	10	15	30	60
Sample Weight (g)	4.94	4.63	5.17	4.99	5.01	4.94
% Asphaltenes	64.05	61.87	62.76	61.83	62.00	61.28
% Oils ^a	5.79	7.97	7.08	8.01	7.84	8.56

^a Corrected by 30.16% Factor - See Text

Elemental Analysis of Residual Asphaltene

Carbon (wt. %)	85.63	85.66	85.80	85.85	85.73	85.83
Hydrogen	6.10	6.02	6.04	6.12	6.07	6.09
Nitrogen	2.00	2.00	2.01	1.99	2.02	2.02
Sulfur	0.98	1.02	1.05	0.99	1.11	1.02
Oxygen ^b	5.29	5.30	5.10	5.05	5.07	5.04

^b Oxygen determined by difference

Gas Analysis (mole %)

H ₂	CO	CO ₂	CH ₄	C ₂ H ₄	C ₂ H ₆	C ₃ H ₆	C ₃ H ₈	H ₂ S
----------------	----	-----------------	-----------------	-------------------------------	-------------------------------	-------------------------------	-------------------------------	------------------

Run Number: 9 Date: 06-22-82

Operating Conditions

Temperature: 400°C
 Pressure: 1500 psig
 Catalyst: ----
 Solvent-to-Asphaltene Ratio: 6.08
 Total Reactant Mass: 414.14g
 % Recovery: 96.8
 Comments:

Product Yields	Sample Time (minutes)					
	2	5	10	15	30	60
Sample Weight (g)	4.66	---	4.37	4.86	4.98	4.50
% Asphaltenes	58.35	---	56.32	57.27	57.68	55.41
% Oils ^a	11.49	---	13.52	12.57	12.16	14.43

^a Corrected by 30.16% Factor - See Text

Elemental Analysis of Residual Asphaltene

Carbon (wt. %)	85.66	85.86	86.06	85.93	85.65
Hydrogen	6.07	6.05	6.03	6.00	5.95
Nitrogen	2.00	2.04	2.06	2.04	2.09
Sulfur	1.03	0.96	0.98	0.96	0.80
Oxygen ^b	5.28	5.09	4.87	5.40	5.18

^b Oxygen determined by difference

Gas Analysis (mole %)

H ₂	CO	CO ₂	CH ₄	C ₂ H ₄	C ₂ H ₆	C ₃ H ₆	C ₃ H ₈	H ₂ S
99.300	.095	.034	.280	.048	.224	.004	.015	---

Run Number: 10 Date: 07-13-82

Operating Conditions

Temperature: 400°C
 Pressure: 1500 psig
 Catalyst: H₂S
 Solvent-to-Asphaltene Ratio: 6.09
 Total Reactant Mass: 414.28g
 % Recovery: 99.4
 Comments:

Product Yields	Sample Time (minutes)					
	2	5	10	15	30	60
Sample Weight (g)	4.75	4.91	4.58	5.27	5.16	4.84
% Asphaltenes	60.34	59.72	58.08	57.24	57.28	54.44
% Oils ^a	9.50	10.12	11.76	12.60	12.56	15.40

^a Corrected by 30.16% Factor - See Text

Elemental Analysis of Residual Asphaltene

Carbon (wt. %)	85.08	85.12	85.07	84.86	85.06	85.72
Hydrogen	5.92	5.94	5.94	5.94	6.00	6.05
Nitrogen	2.04	2.10	2.07	2.07	2.10	2.11
Sulfur ^b	1.12	1.01	1.06	1.02	0.96	0.95
Oxygen ^b	5.84	5.83	5.86	6.11	5.88	5.17

^b Oxygen determined by difference

Gas Analysis (mole %)

H ₂	CO	CO ₂	CH ₄	C ₂ H ₄	C ₂ H ₆	C ₃ H ₆	C ₃ H ₈	H ₂ S
98.18	.077	.047	.303	.006	.084	.007	.024	1.271

Run Number: 11 Date: 07-28-82

Operating Conditions

Temperature: 400°C
 Pressure: 1500 psig
 Catalyst: Pyrite, 5 wt. %
 Solvent-to-Asphaltene Ratio: 6.08
 Total Reactant Mass: 418.20g
 % Recovery: 99.7
 Comments:

Product Yields	Sample Time (minutes)					
	2	5	10	15	30	60
Sample Weight (g)	5.14	5.11	5.09	5.03	5.30	4.85
% Asphaltenes	57.86	56.39	55.51	54.58	54.13	52.35
% Oils ^a	11.98	13.45	14.33	15.26	15.71	17.49

^a Corrected by 30.16% Factor - See Text

Elemental Analysis of Residual Asphaltene

Carbon (wt. %)	85.96	86.23	86.04	86.41	86.03	85.55
Hydrogen	5.95	6.01	6.01	6.01	5.95	6.04
Nitrogen	2.04	2.08	2.07	2.11	2.12	2.15
Sulfur	1.05	1.06	0.95	0.99	0.80	0.97
Oxygen ^b	5.00	4.62	4.93	4.48	5.10	5.29

^b Oxygen determined by difference

Gas Analysis (mole %)

H ₂	CO	CO ₂	CH ₄	C ₂ H ₄	C ₂ H ₆	C ₃ H ₆	C ₃ H ₈	H ₂ S
98.659	.076	.092	.354	--	.110	.009	.034	.666

Run Number: 12 Date: 08-25-82

Operating Conditions

Temperature: 400°C
 Pressure: 1500 psig
 Catalyst: HDS-20A, 5 wt. %
 Solvent-to-Asphaltene Ratio: 6.13
 Total Reactant Mass: 416.55g
 % Recovery: 98.7
 Comments: Catalyst presulfided in 10% H₂S/H₂ gas mixture for 3 hours prior to reaction.

Product Yields	Sample Time (minutes)					
	2	5	10	15	30	60
Sample Weight (g)	4.62	4.01	4.11	4.47	3.64	4.09
% Asphaltenes	54.28	50.30	47.87	46.46	41.11	38.93
% Oils ^a	15.56	19.54	21.97	23.38	28.73	30.91

^a Corrected by 30.16% Factor - See Text

Elemental Analysis of Residual Asphaltene

Carbon (wt. %)	85.40	85.86	85.60	86.76	86.16	86.12
Hydrogen	6.07	6.12	6.08	6.12	6.12	6.10
Nitrogen	2.03	2.09	2.05	2.10	2.06	2.04
Sulfur ^b	1.07	0.99	0.84	0.83	0.69	0.51
Oxygen ^b	5.43	4.94	5.43	4.19	4.97	5.23

^b Oxygen determined by difference

Gas Analysis (mole %)

H ₂	CO	CO ₂	CH ₄	C ₂ H ₄	C ₂ H ₆	C ₃ H ₆	C ₃ H ₈	H ₂ S
96.495	.065	.058	.482	--	.264	.003	.127	2.459

Run Number: 13 Date: 09-07-82

Operating Conditions

Temperature: 400°C
 Pressure: 1500 psig
 Catalyst: HDS-9A, 5 wt. %
 Solvent-to-Asphaltene Ratio: 6.02
 Total Reactant Mass: 424.08g
 % Recovery: 98
 Comments: Catalyst presulfided in 10% H₂S/H₂ gas mixture for 3 hours prior to reaction.

Product Yields	Sample Time (minutes)					
	2	5	10	15	30	60
Sample Weight (g)	4.30	5.11	4.35	3.73	5.09	4.32
% Asphaltenes	60.90	56.35	50.53	48.50	46.53	41.79
% Oils ^a	8.94	13.49	19.31	21.34	23.31	28.05

^a Corrected by 30.16% Factor - See Text

Elemental Analysis of Residual Asphaltene

Carbon (wt. %)	85.50	85.66	85.15	85.70	86.15	86.57
Hydrogen	5.99	6.00	6.05	6.09	6.11	6.13
Nitrogen	2.05	2.07	2.08	2.05	2.04	2.02
Sulfur	1.01	0.97	0.81	0.83	0.69	0.60
Oxygen ^b	5.45	5.30	5.91	5.33	5.01	4.68

^b Oxygen determined by difference

Gas Analysis (mole %)

H ₂	CO	CO ₂	CH ₄	C ₂ H ₄	C ₂ H ₆	C ₃ H ₆	C ₃ H ₈	H ₂ S
92.467	.088	.084	.517	--	.336	--	.169	6.056

Run Number: 14 Date: 09-14-82

Operating Conditions

Temperature: 400°C
 Pressure: 1500 psig
 Catalyst: HDN-30, 5 wt. %
 Solvent-to-Asphaltene Ratio: 5.96
 Total Reactant Mass: 417.33g
 % Recovery: 99.9
 Comments: Catalyst presulfided in 10% H₂S/H₂ gas mixture for 3 hours prior to reaction.

Product Yields	Sample Time (minutes)					
	2	5	10	15	30	60
Sample Weight (g)	4.58	4.58	4.76	4.58	4.85	4.70
% Asphaltenes	54.47	53.85	51.55	50.87	48.49	44.56
% Oils ^a	15.37	15.99	18.29	18.97	21.35	25.28

^a Corrected by 30.16% Factor - See Text

Elemental Analysis of Residual Asphaltene

Carbon (wt. %)	85.87	86.00	86.04	86.26	86.45	85.04
Hydrogen	6.04	6.08	6.08	6.11	6.21	6.20
Nitrogen	2.04	2.05	2.06	2.05	1.97	1.88
Sulfur ^b	1.03	0.98	0.80	0.85	0.74	0.52
Oxygen ^b	5.02	4.89	5.02	4.73	4.63	6.36

^b Oxygen determined by difference

Gas Analysis (mole %)

H ₂	CO	CO ₂	CH ₄	C ₂ H ₄	C ₂ H ₆	C ₃ H ₆	C ₃ H ₈	H ₂ S
93.361	.094	.078	.534	--	.324	.004	.150	5.425

Run Number: 15 Date: 09-18-82

Operating Conditions

Temperature: 400°C
 Pressure: 1500 psig
 Catalyst: Ni-4303E, 5 wt. %
 Solvent-to-Asphaltene Ratio: 6.10
 Total Reactant Mass: 416.71g
 % Recovery: 99.3
 Comments: Catalyst presulfided in 10% H₂S/H₂ gas mixture for 3 hours prior to reaction.

Product Yields	Sample Time (minutes)					
	2	5	10	15	30	60
Sample Weight (g)	4.63	4.82	4.84	4.29	5.03	4.37
% Asphaltenes	53.72	52.37	50.07	48.32	47.49	42.35
% Oils ^a	16.12	17.47	19.77	21.52	22.35	27.49

^a Corrected by 30.16% Factor - See Text

Elemental Analysis of Residual Asphaltene

Carbon (wt. %)	84.94	85.00	85.48	86.10	86.34	86.59
Hydrogen	6.04	6.06	6.15	6.19	6.22	6.24
Nitrogen	2.04	2.06	2.07	2.09	2.07	2.07
Sulfur	1.12	0.70	0.88	0.80	0.69	0.64
Oxygen ^b	5.86	6.18	5.42	4.82	4.68	4.46

^b Oxygen determined by difference

Gas Analysis (mole %)

H ₂	CO	CO ₂	CH ₄	C ₂ H ₄	C ₂ H ₆	C ₃ H ₆	C ₃ H ₈	H ₂ S
98.392	.063	.041	.387	--	.113	--	.064	0.899

Run Number: 16 Date: 10-16-82

Operating Conditions

Temperature: 400°C
 Pressure: 1500 psig
 Catalyst: HDS-9A, 5 wt.%
 Solvent-to-Asphaltene Ratio: 6.03
 Total Reactant Mass: 416.97g
 % Recovery: 98.7

Comments: Catalyst was not presulfided prior to reaction.

Product Yields	Sample Time (minutes)					
	2	5	10	15	30	60
Sample Weight (g)	4.53	3.88	4.86	4.25	4.35	4.64
% Asphaltenes	49.67	58.51	58.24	56.47	55.65	51.77
% Oils ^a	10.17	11.33	11.60	13.37	14.19	18.07

^a Corrected by 30.16% Factor - See Text

Elemental Analysis of Residual Asphaltene

Carbon (wt. %)	85.15	85.57	85.61	85.33	85.81	85.86
Hydrogen	6.00	6.02	6.11	6.05	6.06	6.05
Nitrogen	1.98	2.04	2.01	2.03	2.05	2.08
Sulfur	0.90	0.98	0.95	0.93	0.91	0.88
Oxygen ^b	5.97	5.39	5.32	5.66	5.17	5.13

^b Oxygen determined by difference

Gas Analysis (mole %)

H ₂	CO	CO ₂	CH ₄	C ₂ H ₄	C ₂ H ₆	C ₃ H ₆	C ₃ H ₈	H ₂ S
----------------	----	-----------------	-----------------	-------------------------------	-------------------------------	-------------------------------	-------------------------------	------------------

Run Number: 17 Date: 10-23-82

Operating Conditions

Temperature: 400°C
 Pressure: 1500 psig
 Catalyst: HDN-30, 5 wt. %
 Solvent-to-Asphaltene Ratio: 5.96
 Total Reactant Mass: 416.43g
 % Recovery: 99.0
 Comments: Catalyst initially presulfided in 10% H₂S/H₂ gas mixture for 3 hours prior to reaction. H₂S then purged from reactor by flow of pure H₂ at 20 cc/sec for 1 hour.

Product Yields	Sample Time (minutes)					
	2	5	10	15	30	60
Sample Weight (g)	5.07	4.96	4.77	5.33	5.22	5.26
% Asphaltenes	59.53	57.57	56.46	56.13	51.54	49.65
% Oil ^a	10.31	12.27	13.38	13.71	18.30	20.19

^a Corrected by 30.16% Factor - See Text

Elemental Analysis of Residual Asphaltene

Carbon (wt. %)	86.04	85.77	85.93	86.13	86.06	86.14
Hydrogen	6.15	6.14	6.16	6.18	6.21	6.16
Nitrogen	1.99	1.98	2.01	2.00	1.99	1.97
Sulfur	0.98	0.83	0.73	0.70	0.56	0.47
Oxygen ^b	4.84	5.28	5.17	4.99	5.18	5.26

^b Oxygen determined by difference

Gas Analysis (mole %)

H ₂	CO	CO ₂	CH ₄	C ₂ H ₄	C ₂ H ₆	C ₃ H ₆	C ₃ H ₈	H ₂ S
93.731	.093	.116	.472	--	.257	.003	.108	.417

Run Number: 18 Date: 10-30-82

Operating Conditions

Temperature: 400°C
 Pressure: 1500 psig
 Catalyst: HDN-30, 5 wt. %
 Solvent-to-Asphaltene Ratio: 6.07
 Total Reactant Mass: 416.22g
 % Recovery: 99.0
 Comments: 3 hour run using same reaction conditions as run #14. Catalyst presul-
 fided in 10% H₂S/H₂ gas mixture for 3 hours prior to reaction.

Product Yields	60	120	180
Sample Weight (g)	5.22	5.05	5.37
% Asphaltenes	45.37	34.56	27.66
% Oils ^a	24.47	35.28	42.18

^a Corrected by 30.16% Factor - See Text

Elemental Analysis of Residual Asphaltene

Carbon (wt. %)	85.69	86.72	86.04
Hydrogen	6.32	6.31	6.31
Nitrogen	1.86	1.89	1.75
Sulfur	0.51	0.42	0.41
Oxygen ^b	5.62	4.66	5.49

^b Oxygen determined by difference

Gas Analysis (mole %)

H ₂	CO	CO ₂	CH ₄	C ₂ H ₄	C ₂ H ₆	C ₃ H ₆	C ₃ H ₈	H ₂ S
89.920	.102	.083	1.16	--	.635	.002	.283	5.937

Run Number: 19 Date: 11-21-82

Operating Conditions

Temperature: 425°C
 Pressure: 1500 psig
 Catalyst: HDN-30, 5 wt. %
 Solvent-to-Asphaltene Ratio: 6.09
 Total Reactant Mass: 417.51g
 % Recovery: 97.8
 Comments: 3 hour run at 425°C using HDN-30 catalyst. Catalyst presulfided in 10% H₂S/H₂ gas mixture for 3 hours prior to reaction.

Product Yields	Sample Time (minutes)				
	5	15	30	60	180
Sample Weight (g)	4.86	5.03	4.40	4.92	5.00
% Asphaltenes	61.23	57.72	48.03	35.94	20.07
% Oils ^a	8.61	12.12	21.81	33.90	49.77

^a Corrected by 30.16% Factor - See Text

Elemental Analysis of Residual Asphaltene

Carbon (wt. %)	85.39	85.67	86.06	86.98	86.82	88.71
Hydrogen	6.11	6.12	6.08	6.08	5.79	5.74
Nitrogen	2.00	2.00	2.01	1.95	1.84	1.73
Sulfur ^b	1.06	0.95	0.75	0.53	0.47	0.38
Oxygen	5.44	5.26	5.10	4.46	5.08	3.44

^b Oxygen determined by difference

Gas Analysis (mole %)

H ₂	CO	CO ₂	CH ₄	C ₂ H ₄	C ₂ H ₆	C ₃ H ₆	C ₃ H ₈	H ₂ S
----------------	----	-----------------	-----------------	-------------------------------	-------------------------------	-------------------------------	-------------------------------	------------------

APPENDIX C

ASPHALTENE STRUCTURAL RESULTS

Run Number	7	8
Conditions	Reprecipitated Feed Asphaltene	355°C Thermal, 60 Minutes
Molecular Formula	$C_{39.4}H_{35.89}N_{.75}O_{2.02}S_{.18}$	$C_{38.16}H_{32.26}N_{.77}O_{1.68}S_{.17}$
Molecular Weight	554	534
H_{ar}^*	0.404	0.434
H_a^*	0.382	0.355
H_o^*	0.214	0.211
C_{ar}^*	---	0.669
C_{al}^*	---	0.331
		0.752
		0.248

Run Number	9	10	11
Conditions	400°C Thermal 60 Minutes	400°C, H ₂ S Additive 60 Minutes	400°C, Pyrite Additive 60 Minutes
Molecular Formula	C _{37.85} H _{31.50} N _{0.79} O _{1.71} S _{0.13}	C _{36.68} H _{32.77} H _{0.82} O _{1.76} S _{0.16}	C _{36.11} H _{30.38} N _{0.79} O _{1.68} S _{0.15}
Molecular Weight	529	546	507
H _{ar} *	0.419	0.403	0.474
H _a *	0.375	0.493	0.358
H _o *	0.206	0.104	0.168
C _{ar} *	0.763	0.758	0.752
C _{al} *	0.237	0.242	0.248

Run Number	12	13	14
Conditions	400°C, HDS-20A Catalyst 60 Minutes	400°C, HDS-9A Catalyst 60 Minutes	400°C, HDN-30 Catalyst 60 Minutes
Molecular Formula	C _{37.71} H _{31.83} N _{0.77} O _{1.72} S _{0.08}	C _{38.06} H _{32.11} N _{0.76} O _{1.54} S _{0.10}	C _{35.26} H _{30.63} N _{0.67} O _{1.98} S _{0.08}
Molecular Weight	526	528	498
H _{ar} *	0.367	0.383	0.419
H _a *	0.401	0.415	0.375
H _o *	0.232	0.202	0.206
C _{ar} *	0.743	0.719	0.773
C _{al} *	0.257	0.281	0.227

Run Number	15	16	17
Conditions	400°C, Ni-4303E Catalyst 60 Minutes	400°C, HDS-9A Catalyst non-sulfided, 60 min. sample	400°C, HDN-30 Catalyst H ₂ S purged, 60 min. sample
Molecular Formula	C _{34.10} H _{29.28} N _{.70} O _{1.32} S _{.09}	C _{39.60} H _{33.25} N _{.82} O _{1.78} S _{.15}	C _{36.58} H _{31.17} N _{.72} O _{1.68} S _{.07}
Molecular Weight	521	526	510
H _{ar} *	0.390	0.450	0.398
H _a *	0.396	0.366	0.390
H _o *	0.214	0.183	0.212
C _{ar} *	---	---	---
C _{al} *	---	---	---

Run Number	18	19
Conditions	400°C, HDN-30 Catalyst 120 Minutes	425°C, HDN-30 Catalyst 60 Minutes
Molecular Formula	---	---
Molecular Weight	---	---
H _{ar} *	0.352	0.405
H _o *	0.426	0.389
H _o *	0.222	0.206
C _{ar} *	---	---
C _{al} *	---	---

NOTES

1. $H_i^* = \frac{H_i}{\sum H}$
2. $C_i^* = \frac{C_i}{\sum C}$
3. Molecular weights determined by VPO in pyridine at 80°C.
4. H_i determined by ¹H nmr.
5. C_i determined by ¹³C CP/MAS nmr.

APPENDIX D
CATALYST PROPERTIES

Fresh Catalyst Properties*

CATALYST	METAL COMPOSITION (WT%)	SUPPORT	SURFACE AREA (m ² /g)	PORE VOLUME (cc/g)	PORE DIAMETER (A)
AMERICAN CYANAMID AERO HDS-20A	16.2% MoO ₃ 5.0% CoO	Al ₂ O ₃	230	0.70	122
AMERICAN CYANAMID AERO HDS-9A	18.4% MoO ₃ 3.1% NiO	Al ₂ O ₃	200	0.65	130
AMERICAN CYANAMID HDN-30	20.5% MoO ₃ 5.0% NiO	Al ₂ O ₃	160	0.59	148
HARSHAW Ni-4303E	19.0% W ₂ O ₃ 6.0% NiO	Al ₂ O ₃	152	0.62	163

* 0.074 mm catalyst particles

POROSITY DETERMINATION

SUPERPRESSURE
FORM
Cat. No. B-7135 A

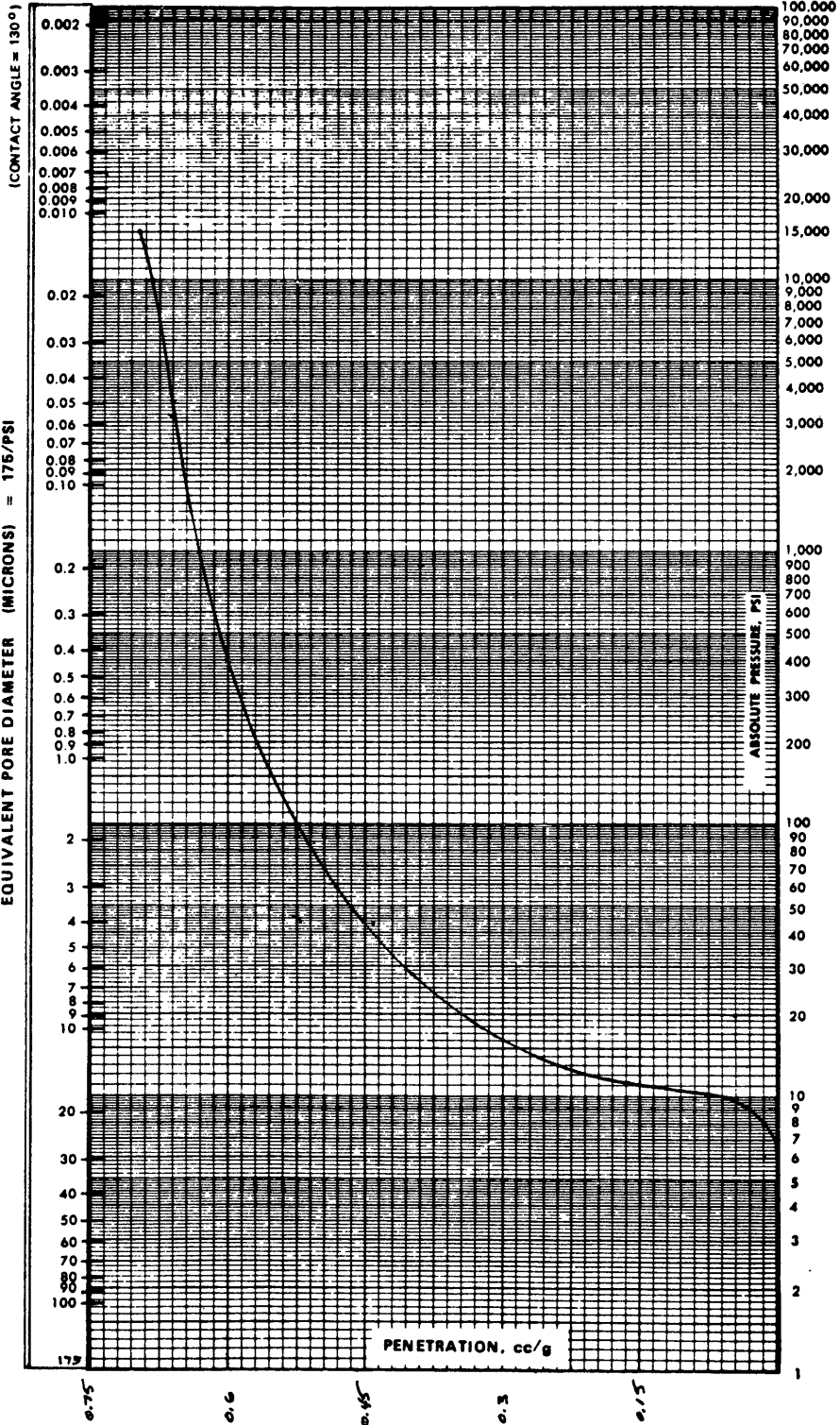
SAMPLE HDS-20A

SAMPLE WEIGHT 0.2472 grams

DATE 11-3-82 ORDER No. 92674

Por. Volume @ 15000 psia = 0.70 cc/g

EQUIVALENT PORE DIAMETER (MICRONS) = 175/PSI



POROSIITY DETERMINATION

SUPERPRESSURE
FORM
Cat. No. 5-7135 A

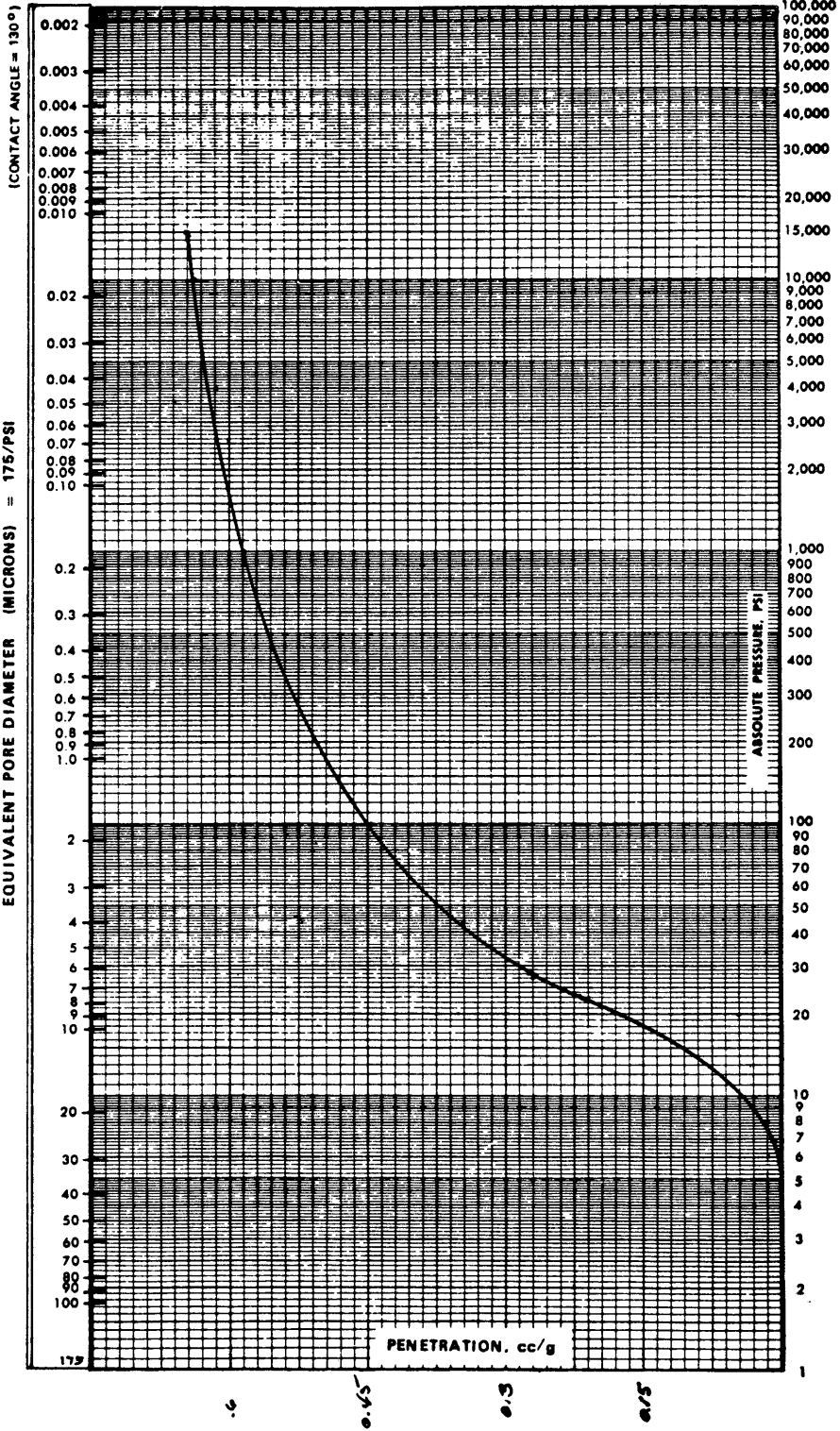
SAMPLE AD5-9A

SAMPLE WEIGHT 0.2550 grams

DATE 11-2-82 ORDER No. 92674

Pen Volume @ 15,000 psia = 0.65 cc/g

EQUIVALENT PORE DIAMETER (MICRONS) = 1775/PSI



POROSITY DETERMINATION

SUPERPRESSURE
FORM
Cat. No. B-7135 A

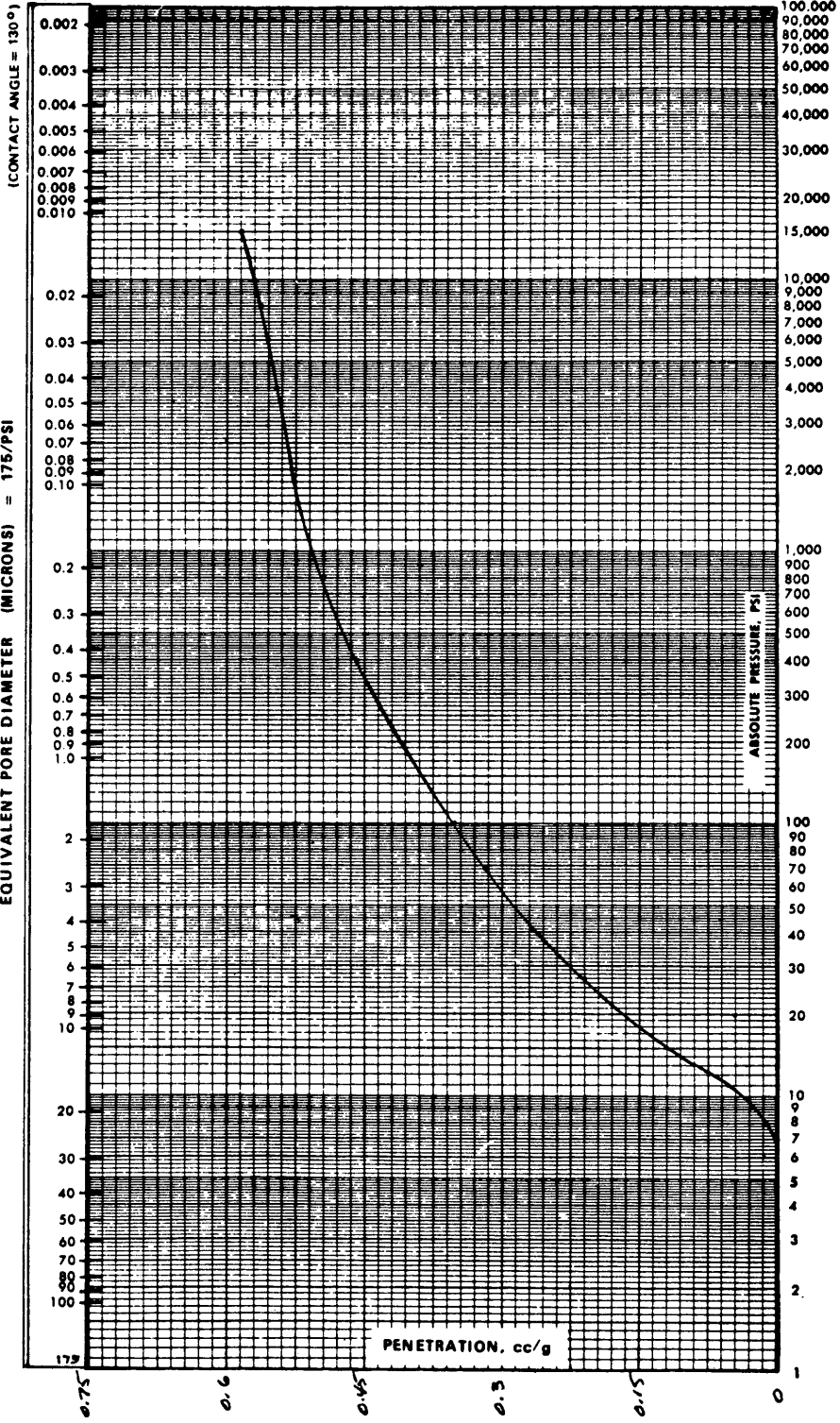
SAMPLE ADJ-30

SAMPLE WEIGHT 0.2487 grams

DATE 11-5-82 ORDER No. 92674

Pore Volume @ 15,000 PSI = 0.59 cc/g

EQUIVALENT PORE DIAMETER (MICRONS) = 175/PSI



POROSITY DETERMINATION

SUPERPRESSURE
FORM
Cat. No. 5-7135 A

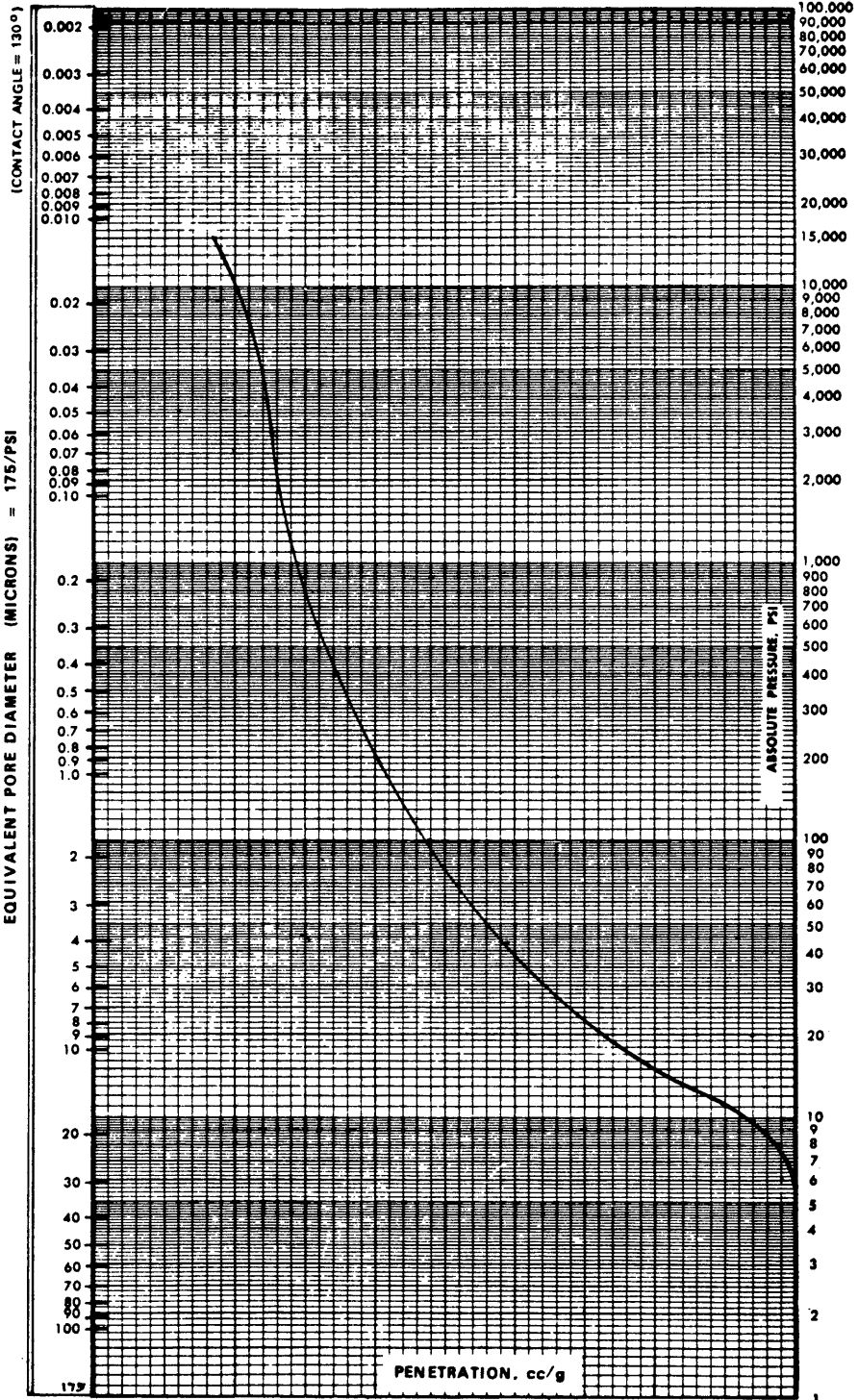
SAMPLE Al 803 E

SAMPLE WEIGHT 0.2465 grams

DATE 11-2-82 ORDER No. 92674

Pore volume @ 15,000 psia = 0.62 cc/g

EQUIVALENT PORE DIAMETER (MICRONS) = 175/PSI



.6
54.
3
.5

APPENDIX E
SAMPLE CALCULATIONS

SAMPLE CALCULATIONS

The following pages show sample calculations for the material balance and conversion-to-oils from run 17. The Peel-Back method calculations are presented using run 11 as an example.

I. Material Balance

Total Mass In:

Asphaltene	60.06g	
Tetralin (injected)	75.17g	
Tetralin (in reactor)	278.16g	
Catalyst	<u>3.04g</u>	
	416.45g	Total

Total Mass Recovered:

Uncharged Slurry	1.73g	
Uninjected Slurry	1.97g	
Reactor	305.39g	
Slop	29.23g	
Wash	10.61g	
Samples	59.86g	
Tetralin Recovered from Knock-Out Vessel	<u>3.25g</u>	
	412.04g	Total

Mass Lost = 4.39g

% Recovery = 98.95%

II. Conversion to Oils

A. Prepared Slurry

Asphaltene	=	60.06g
Tetralin	=	75.15g
Injection Solvent-to-Feed Ratio	=	1.25
X Asphaltene	=	0.44
X Tetralin	=	0.56

B. Uncharged Mass

Total Uncharged Mass = 1.73g
 Uncharged Asphaltene = 0.77g
 Uncharged Tetralin = 0.96g

C. Uninjected Mass

Total Uninjected Mass = 1.97g
 Uninjected Asphaltene = 0.87g
 Uninjected Tetralin = 1.10g

D. Tetralin Recovered During Purge

Total Tetralin Recovered = 3.25g

E. Total Mass in Reactor

Asphaltenes: $60.06 - 0.77 - 0.87 = 58.42\text{g}$
 Tetralin: $278.16 + 75.17 - 0.96 - 1.10 - 3.25 = 348.02\text{g}$
 Reactor Solvent-to-Feed Ratio: 5.96
 $X_{\text{Asphaltene}} = 0.14$
 $X_{\text{Tetralin}} = 0.86$

F. Conversion

<u>TIME</u>	<u>UNCORRECTED (%)</u>	<u>CORRECTED (%)*</u>
0	30.16	0.00
2	40.47	10.31
5	42.43	12.27
10	43.87	13.71
15	43.54	13.38
30	48.46	18.30
60	51.07	20.91

* Corrected by 30.16% Factor

III. Peel-Back Model Calculations

A. Conversion Data

<u>TIME</u>	<u>X_a</u>	<u>$(.7 - X_a) / .7$</u>
0	0.0	1.0
2	0.1198	0.8289
5	0.1345	0.8079
10	0.1433	0.7953
15	0.1526	0.7820
30	0.1571	0.7756
60	0.1749	0.7501

B. Slow Reaction Equation

$$\alpha_2(t) = -9.47 \times 10^{-4}t + 0.8049$$

$$t_{\frac{1}{2},2} = 425.1 \text{ min.}$$

$$k_2 = \frac{\ln 2}{t_{\frac{1}{2},2}} = 1.631 \times 10^{-3} \text{ min.}^{-1}$$

C. Isolation of Fast Reaction

<u>TIME</u>	<u>(.7-X)/.7</u>	<u>RESPONSE FUNCTION</u>	<u>Δ</u>
0	1.0	0.8049	0.1951
2	0.8289	0.8030	0.0259

D. Fast Reaction Equation

$$\alpha_1(t) = -0.0846t + 0.1951$$

$$t_{\frac{1}{2},1} = 1.15 \text{ min.}$$

$$k_1 = 0.601 \text{ min.}^{-1}$$

E. Kinetic Model

$$X_A = 0.7[1 - 0.1951e^{-.601t} - 0.8049e^{-1.631 \times 10^{-3}t}]$$